

UCSF

UC San Francisco Electronic Theses and Dissertations

Title

Role of MGE- and CGE-derived Interneuron Subtypes in Transplant-induced Cortical Plasticity

Permalink

<https://escholarship.org/uc/item/4kz9m0f9>

Author

Tang, Yunshuo

Publication Date

2015

Peer reviewed|Thesis/dissertation

Role of MGE- and CGE-derived Interneuron Subtypes in Transplant-
Induced Cortical Plasticity

by

Yunshuo Tang

DISSERTATION

Submitted in partial satisfaction of the requirements for the degree of

DOCTOR OF PHILOSOPHY

in

Biomedical Sciences

in the

GRADUATE DIVISION

of the

UNIVERSITY OF CALIFORNIA, SAN FRANCISCO

Copyright 2015

by

Yunshuo Tang

To my parents, Weizhong Tang and Mangli Zhang

Acknowledgements

I want to express my most sincere gratitude to my thesis advisor, Arturo Alvarez-Buylla, for the opportunity to work in his laboratory and learn under his guidance. Throughout my time in his lab, Arturo has continuously provided me with generous support and gentle encouragement. His high scientific standard has challenged me to be meticulous yet innovative. Arturo has instilled in me the belief that one should never do science to fit a predetermined hypothesis, but to faithfully describe and embrace nature as it is. Arturo has taught me that success in science requires not only diligence and technical competency, but also passion, scientific curiosity, open-mindedness, and appreciation for the beauty of biology. I will always look up to Arturo as my role model when I continue my scientific adventure.

My graduate school experience has been immensely enriched by the past and present members of the Alvarez-Buylla Lab. In particular, I want to thank Young-Goo Han for supervising me during my rotation and Derek Southwell for teaching me micro-dissection and cell transplantation. Ricardo Romero, Jose Rodriguez, Cristina Guinto, Thuhien Nguyen, and Joseph Elspend provided excellent technical as well as administrative support. Mercedes Paredes collaborated with me on freezing and culturing MGE cells. Gabriella Herrera worked with me to characterize the early migratory behaviors of transplanted MGE cells. Shawn Sorrells, Cheuk ka Tong, Robert Lindquist, Shinya Ohata, Kirsten Obernier, and Luis Fuentealba provided helpful discussions and a supportive and collegial environment.

I also want to thank my collaborators, Michael Stryker and Sebastian Espinosa, along with the rest of the Stryker Lab, for an exciting and productive collaboration. Sebastian performed the intrinsic imaging and molecular deprivation experiments and analysis of imaging data (Chapter 3 and 4). Michael provided ample guidance and scientific insight that was invaluable to the project and my scientific education.

I have greatly benefited from the scientists and technical experts in many other labs. John Rubenstein resided on my thesis committee and offered many advices. I thank Sunil Gandhi for kindly providing the PV-cre mice and Corey Harewell for teaching me perfusion techniques. I thank Jiadong Chen and Cory Nicolas for the opportunity to collaborate on transplantation of interneurons derived from human ES cells, and Yu Fu and Megumi Kaneko for the chance to collaborate on their study of inhibitory circuitry in adult ocular dominance plasticity. Finally, I thank Daniel Vogt for technical advices.

I thank my previous mentors, Laurence Tecott and Miles Berger, for introducing me to the fascinating world of biomedical research. They offered me the opportunity to work independently, and their clinically oriented research sparked my interest in becoming a physician scientist, a career path I never knew existed before. My experience in the Tecott Lab has truly been life-changing.

Last but not least, I am forever grateful to my parents, Weizhong Tang and Mangli Zhang, for teaching me the values of honesty, humility, and hard work. They have made great sacrifices to provide me with the best education, and have supported me unconditionally on my decision to pursue science and medicine.

The texts and figures of Chapter 2 and Chapter 3 are a reprint of the material as it appears in: Tang Y, Stryker MP, Alvarez-Buylla A, Espinosa JS. (2014). Cortical plasticity induced by parvalbumin and somatostatin expressing interneurons. *Proc Natl Acad Sci U S A* 111(51):18339-44. doi: 10.1073/pnas.1421844112.

This research has been funded by the National Institutes of Health, the California Institute for Regenerative Medicine, and the Biomedical Sciences Graduate Program and the Medical Scientist Training Program of the University of California, San Francisco.

Abstract

Role of MGE- and CGE-derived Interneuron Subtypes in Transplant-Induced Cortical Plasticity

by

Yunshuo Tang

Cortical GABAergic interneurons have been shown to play a pivotal role in ocular dominance plasticity (ODP) during the developmental critical period. GABAergic interneurons are extremely diverse, and currently it is unclear which interneuron subtypes contribute to critical period plasticity. The majority of cortical GABAergic interneurons originate from the medial and caudal ganglionic eminences (MGE and CGE, respectively). Transplanted into the visual cortex of postnatal animals, MGE-derived interneuron precursors can disperse, mature, integrate into local visual cortical circuit, and open a second window of critical-period-like plasticity. Because transplanted MGE precursor cells differentiate primarily into parvalbumin-expressing (PV^+) and somatostatin-expressing (SST^+) cells, we genetically ablated PV^+ or SST^+ cells in the transplants and tested whether the remaining cells can induce plasticity in the recipients. Surprisingly, removing PV^+ cells did not prevent MGE transplants from inducing plasticity, despite strong evidence linking PV^+ interneurons to critical period plasticity. Depleting SST^+ cells did not abolish transplant-induced plasticity, either, but removing both PV^+ and SST^+ cells eliminated plasticity. Our results show that SST^+ interneurons, which are abundant and powerful inhibitors in the visual cortex but have scarcely been studied in the context of ODP, are as competent as PV^+ interneurons in mediating plasticity.

To investigate the contribution of other interneuron subtypes to critical period plasticity, we transplanted CGE-derived interneuron precursors into postnatal recipients. Cells from CGE transplants migrated into the visual cortex as efficiently as MGE-derived interneurons. CGE-derived precursor cells did not differentiate into PV⁺ or SST⁺ cells, but instead generated interneurons expressing diverse subtype markers such as reelin, calretinin, and vasoactive intestinal peptide. Despite successful engraftment and efficient migration, CGE-derived interneurons failed to induce plasticity. Our results demonstrate that transplanted interneuron precursors from both MGE and CGE migrate vigorously in the postnatal cortex and differentiate into a diverse panel of cortical interneuron subtypes. However, only PV⁺ and SST⁺ interneurons derived from the MGE can modify host neural circuits and reintroduce juvenile-like plasticity into the adult cortex. These findings provide important insights into the functional application of interneuron subtypes. Such information will be crucial in investigating the mechanisms of critical period plasticity and devising effective strategies of transplant therapy.

Table of Contents

Title	i
Copyright	ii
Dedication	iii
Acknowledgments	iv
Abstract	vi
Table of Contents	viii
List of Tables	xii
List of Figures	xiii
List of Abbreviations	xvii
Chapter 1. Introduction	1
<u>Section 1: Overview</u>	1
<u>Section 2: Generation of cortical inhibitory interneurons</u>	3
Diversity of interneurons	4
Origin of cortical interneurons	5
Migration of interneurons into the cerebral cortex	7
Function of interneurons in normal and diseased brain	8
<u>Section 3: Transplantation of interneuron precursors</u>	9

<u>Section 4: Interneuron and ocular dominance plasticity</u>	10
Chapter 2: Materials and Methods	21
<u>Section 1: Animals</u>	21
<u>Section 2: Cell preparation and transplantation</u>	23
Donor tissue preparation	23
Cell Transplantation	24
<u>Section 3: Immunohistochemistry</u>	24
<u>Section 4: Optical imaging of intrinsic signal</u>	25
Image acquisition and quantification	26
Optical imaging of intrinsic signal	26
Analysis of optical imaging data	27
<u>Section 5: Statistical analysis</u>	27
Chapter 3: Role of Parvalbumin- and Somatostatin-expressing Interneurons in Transplant-induced Cortical Plasticity	28
<u>Section 1: Introduction</u>	28
<u>Section 2: Results</u>	30
Unsuccessful Purification of PV+ and SST+ neuroblasts from dissected MGE cells	30
Genetic ablation of PV+ and SST+ interneurons in MGE transplants	31

Optical imaging of intrinsic signals to detect plasticity in recipients of R26-DTA and dead MGE cells	33
MGE transplants depleted of PV+ cells or SST+ cells, but not of both, induced ODP in recipients	34
Plasticity induced by MGE transplants recapitulated key features of critical period plasticity	36
<u>Section 3: Discussion</u>	37
Chapter 4: Migration, Differentiation, and Induction of Cortical Plasticity by Transplanted CGE Cells	58
<u>Section 1: Introduction</u>	58
<u>Section 2: Results</u>	60
Dissection and transplantation of the dorsal CGE	60
Transplanted CGE cells migrate extensively in the cortex and show a specific pattern of layer occupation	60
Transplanted CGE cells differentiate into interneurons expressing diverse cellular markers	61
Reelin ⁺ cells are found in both MGE and CGE transplants, but differ in marker co-expression and layer distribution	62
CGE transplants induce ocular dominance plasticity only in the presence of MGE-derived PV ⁺ and SST ⁺ cells	63
<u>Section 3: Discussion</u>	64

Chapter 5: Conclusions	85
Chapter 6: References	90
Appendix	110
UCSF Library Release	120

List of Tables

Chapter 2 Materials and Methods

Table 1. Mouse strains and descriptions	21
Table 2. Antibodies	25

List of Figures

Chapter 1 Introduction

Figure 1. Diversity of cortical GABAergic interneurons	13
Figure 2. Transcriptional regulation of interneuron subtype development	15
Figure 3. Tangential and radial migration of cortical interneurons	16
Figure 4. Cell sources and potential applications of interneuron transplantation	17
Figure 5. Ocular dominance plasticity of the mouse binocular visual cortex	19
Figure 6. GABAergic inhibition and ocular dominance plasticity	20

Chapter 3 Role of Parvalbumin- and Somatostatin-expressing Interneurons in Transplant-induced Cortical Plasticity

Figure 1. Lack of GFP expression in the MGE of Gin and G42 embryos at E13.5	41
Figure 2. Transplanted P0 cortical cells have poor survival and migration	42
Figure 3. Genetic strategy of ablating PV ⁺ and SST ⁺ cells using Cre-induced expression of DTA	43
Figure 4. MGE Transplantation and optical imaging of visual responses	44

Figure 5. Cre-induced expression of DTA ablates PV⁺ and SST⁺ cells along with their layer-specific projections 46

Figure 6. Depletions of PV⁺ and SST⁺ cells are efficient and do not affect the absolute population size of each other in the transplant 48

Figure 7. PV-depleted and SST-depleted transplants consist of low percentages of PV⁺ and SST⁺ cells, respectively, throughout development 49

Figure 8. Efficient depletions of PV⁺ and SST⁺ cells cause reciprocal increase in the percentage of each other in the transplant 50

Figure 9. Marker expression of the surviving cells in PV-SST-depleted transplants 51

Figure 10. Ocular dominance plasticity is induced by *R26-DTA* transplants, but not dead MGE cells 52

Figure 11. MGE transplants depleted in PV⁺ or SST⁺ cells, both not both, are capable of inducing plasticity 53

Figure 12. Change in ODI is similar among *R26-DTA*, PV-depleted, and SST-depleted transplants 54

Figure 13. Magnitude of plasticity induced by MGE transplants is not related to the density of total GFP⁺ cells, PV⁺ cells, or SST⁺ cells 55

Figure 14. Critical period-like characteristics of transplant-induced plasticity 56

Figure 15. Depression of contralateral responses is not correlated with the density of total GFP⁺ cells, PV⁺ cells, or SST⁺ cells 57

Chapter 4 Migration, Differentiation, and Induction of Cortical Plasticity by Transplanted CGE Cells

Figure 1. Dissection and transplantation of dorsal CGE	70
Figure 2. Extensive migration of transplanted CGE cells	71
Figure 3. Occupation of layer 1 by cell bodies of CGE but not MGE cells	72
Figure 4. Population of superficial layers by transplanted CGE and MGE cells	73
Figure 5. Transplanted CGE cells differentiate into many classes of interneurons	74
Figure 6. Quantification of interneuron marker expression in transplanted CGE and MGE cells	76
Figure 7. Almost all PV ⁺ and SST ⁺ cells in CGE transplants are Nkx2.1 ⁺ and likely MGE in origin	77
Figure 8. MGE- and CGE-derived reelin ⁺ cells have distinct neurochemical marker profiles ...	79
Figure 9. CGE-derived reelin ⁺ cells migrate into layer 1 of the cortex of transplant recipients ..	80
Figure 10. Indistinguishable ocular dominance plasticity mediated by transplanted CGE and MGE cells	81
Figure 11. Density of PV ⁺ and SST ⁺ cells in R26-DTA CGE and PV-SST-depleted CGE transplants	82
Figure 12. CGE transplants depleted of PV ⁺ and SST ⁺ cells fail to induce plasticity	84

Appendix

Figure A1. Transplantation of previously frozen MGE cells	110
Figure A2. Transplanted frozen MGE cells express markers of mature interneurons	112
Figure A3. Migration of transplanted tdTomato ⁺ MGE cells in the host cortex	113
Figure A4. Tangential and radial migration of transplanted MGE cells	115
Figure A5. Transplanted interneurons do not express calbindin	116
Figure A6. Transplantation of MGE cells cultured for 4 days in vitro	117
Figure A7. Expression of subtype markers by MGE cells cultured for 4 days in vitro	118
Figure A8. Transplantation of MGE cells cultured for 6 days in vitro shows poor survival	119

List of Abbreviations

5-hydroxytryptamine receptor 3A	5-HT _{3A} R
apoE4	apolipoprotein E4
BDNF	brain derived neurotrophic factor
CB	calbindin
CR	calretinin
CCK	cholecystokinin
CGE	caudal ganglionic eminence
COUP-TF	COUP transcription factor
Cxcl	chemokine (C-X-C motif) ligand
Cxcr	chemokine (C-X-C motif) receptor
Dlx	distal-less
DTA	diphtheria toxin alpha subunit
E	embryonic day
Efna	ephrin A
FACS	fluorescence activated cell sorting
GABA	gamma-aminobutyric acid
GAD	glutamic acid decarboxylase
GDNF	glial derived neurotrophic factor
GFAP	glial fibrillary acidic protein
GFP	green fluorescent protein
HGF	hepatocyte growth factor
IGF-1	insulin-like growth factor 1
IRES	internal ribosome entry site
LGE	lateral ganglionic eminence

Lhx	LIM homeobox protein
MGE	medial ganglionic eminence
Nkx2.1	NK2 homeobox 1
NPY	neuropeptide Y
Nrg1	neuregulin-1
NT4	neurotrophin-4
ODI	ocular dominance index
ODP	ocular dominance plasticity
Otx2	orthodenticle homolog 2
P	postnatal day
PBS	phosphate buffered saline
PNN	perineuronal nets
POA	preoptic area
PSA-NCAM	polysialylated neural cell adhesion molecule
PV	parvalbumin
Sox	SRY (sex determining region Y)-box
SSRI	selective serotonin reuptake inhibitor
SST	somatostatin
TBS	Tris-buffered saline
VIP	vasoactive intestinal peptide

Introduction

Section 1: Overview

The brain is a highly organized and complex structure which governs voluntary actions such as speech, movements, thoughts, emotions, and sensory perceptions, as well as involuntary functions such as breathing, temperature regulation, and secretion of hormones. The brain also has a protracted development that continues into and even beyond early adulthood, which allows life experience to shape the millions of intricately connected neuronal networks formed by billions of cells and trillions of synaptic connections. During this prolonged development, many parts of the brain are vulnerable to damages, which can lead to debilitating diseases including cerebral palsy, epilepsy, and schizophrenia. Throughout a person's lifetime, the brain is susceptible to trauma, stroke, or age-related neurodegenerative diseases, all of which lead to significant morbidity for the patients and financial burdens on their families and the society. These diseases all affect the health of neurons and neural networks. Current treatments with pharmacological agents cannot replenish lost cells; nor can they rebuild disrupted network connections. As such, it becomes imperative to develop alternative therapeutic strategies that can both generate new cells and rewire synaptic connections.

In the late 1990s, our laboratory discovered a group of cells that are capable of both. They are precursors of inhibitory cortical interneurons derived from an embryonic neurogenic

zone, the medial ganglionic eminence (MGE). The MGE generates the majority of interneurons in the mouse cortex, where they provide inhibitory control of neural networks and coordinate neural activity. Transplanted into the cerebral cortex of older animals, MGE-derived interneuron precursors survive, migrate, and integrate into host neural circuits (Wichterle et al., 1999; Alvarez-Dolado et al., 2006). Subsequent investigation revealed that these cells alter the inhibitory circuits in host cortex to increase inhibition, suppress seizures, and can open a second period of heightened ocular dominance plasticity (Baraban et al., 2009; Southwell et al., 2010; Hunt et al., 2013). Thus, MGE-derived interneuron precursor cells seem to be capable of replacing lost neurons and modify inhibitory neural networks, the two crucial functions required to effectively treat a variety of developmental and degenerative diseases of the brain.

However, MGE-derived interneurons are far from homogenous. They are a mixture of inhibitory cells that differ widely in morphology, cellular marker expression, membrane properties, firing frequency, and synaptic targeting. Currently, we do not have a comprehensive understanding of how each group of interneurons specifically contributes to the observed impact MGE transplants exert on host cortex. Also unclear is whether cortical interneurons from other neurogenic zones, such as the caudal ganglionic eminence (CGE), display similar behaviors and hold similar therapeutic promises as their MGE-derived counterparts. These are fundamental questions to be answered in order to gain a comprehensive understanding of the developmental and functional diversity of cortical inhibitory interneurons.

In my thesis research, I investigated the contribution of different interneuron subpopulations to cortical plasticity induced by transplanted interneuron precursors. I examined cells derived from the two major sources of cortical interneurons, MGE and CGE. Using transplantation and intrinsic signal imaging of visually evoked neural responses, my experiments investigated the major subtypes of cortical interneurons for 1) their ability to disperse and differentiate in a postnatal brain environment, and 2) their contribution in

transplant-induced ocular dominance plasticity. In Chapter 3, I first describe the development of a genetic method of ablating the interneuron subtype of interest using Cre-induced expression of an intracellular toxin. Then, in collaboration with the Stryker Lab, I tested whether PV⁺ and SST⁺ interneurons are required for MGE transplants to induce plasticity. Surprisingly, transplants depleted of either PV⁺ or SST⁺ cells still induced plasticity, but simultaneous ablation of both subtypes abolished plasticity. These findings demonstrate that, despite strong evidences of PV⁺ interneurons being the responsible cell type in the induction of critical period plasticity (Fagiolini et al., 2004; Sugiyama et al., 2008; Kuhlman et al., 2013), these cells are not necessary for transplanted MGE interneurons to mediate juvenile-like plasticity in the recipient brain. Furthermore, we determined that transplant-induced plasticity recapitulates the depression of contralateral response, which is characteristic of critical period ocular dominance plasticity.

In Chapter 4, I explored transplantation of CGE interneuron precursor cells. Similar to MGE precursor cells, CGE-derived interneuron precursors migrate widely within the host cortex and mature into interneurons known to originate in the CGE during development. Although we determined that transplantation of dissected CGE cells induced ocular dominance plasticity, these transplants contained a small population of MGE-derived PV⁺ and SST⁺ cells. Upon depletion of these MGE-derived cells, the remaining CGE-born interneurons could no longer mediate plasticity. These experiments define PV⁺ and SST⁺ interneurons as the key interneuron subtypes in the induction of plasticity when transplanted into the postnatal cortex.

Section 2: Generation of cortical inhibitory interneurons

The cerebral cortex is the outer layer of densely packed cells of the mammalian brain. It is organized into six layers, each with a unique composition of neurons and distinctive patterns

of connectivity (Shipp, 2007). Among the neurons that reside in the cerebral cortex, the majority are excitatory neurons that are pyramidal in shape and release glutamate to depolarize their downstream synaptic targets. But about 20% of cortical neurons release gamma-aminobutyric acid (GABA) to hyperpolarize their synaptic targets and inhibit their neural activity (Markram et al., 2004; Tamamaki et al., 2003). These cells are first described as “short axon cells” by Ramón y Cajal, because in contrast to the far-reaching projections pyramidal cells send throughout the brain, GABAergic inhibitory neurons make short axons that project to nearby targets, usually within the cortex (Ramón y Cajal, 1894; 1901). Now commonly referred to as “interneurons”, these small and round cells provide inhibitory signals that modulate the activities of excitatory neurons. They are an essential component of cortical neural circuits that maintain the excitatory-inhibitory balance and integrity of cortical neural networks (Roux and Buzsáki, 2015).

Diversity of interneurons

Cortical GABAergic interneurons display great diversity in cellular marker expression, localization of synapses on post-synaptic targets, and electrophysiological properties (Figure 1). While all GABAergic interneurons synthesize GABA, individual subtypes can be distinguished by their expression of several secreted peptides including somatostatin (SST), reelin, neuropeptide Y (NPY), vasoactive intestinal peptide (VIP), cholecystokinin (CCK), and intracellular calcium binding proteins such as parvalbumin (PV), calbindin (CB), and calretinin (CR. Markram et al., 2004; Gonchar et al., 2008). Expression of some markers partially overlaps, especially among SST, CB, CR, and NPY; on the other hand, expression of PV is not known to significantly overlap with other subtype markers (Wonders and Anderson, 2006; Gonchar et al., 2008).

Some correlation exists between neurochemically defined subtypes of interneurons and the subcellular compartment of post-synaptic neurons these cells target (Markram et al., 2004;

Roux and Buzsáki, 2015). PV⁺ and CCK⁺ basket cells densely innervate the soma and proximal dendrites to exert powerful influence over the membrane potential of target cells. Another class of PV⁺ cells, the chandelier cells, prefers to make synaptic contact with the initial segment of axons, thereby strongly influencing the final output of their target neurons (Freund and Katona, 2007). In contrast, most other interneuron subtypes project onto the distal dendrites of target cells. Their inhibitory signals become integrated as part of the local dendritic input that influence the neuron's decision to fire action potentials (Spratling, 2003).

Cortical GABAergic interneurons can also be classified by their firing patterns. Fast-spiking PV⁺ basket cells, for example, are able to fire at extremely high frequencies and do not show frequency adaptation after prolonged depolarization. Others such as bipolar, bi-tufted, neurogliaform, and SST⁺ Martinotti cells show a variety of slower and less uniform firing patterns, including regular firing with frequency adaptation, irregular firing of single or groups of spikes, or bursts of rapid firing followed by periods of relative inactivity (Makram et al., 2004; Wonders and Anderson, 2006; Rudy et al., 2011).

Origin of cortical interneurons

Unlike pyramidal neurons which are born within the developing cortex, GABAergic interneurons originate from three regions in the subpallial germinal zone, the medial ganglionic eminence (MGE), the caudal ganglionic eminence (CGE), and the preoptic area (POA) (Anderson et al., 1997; Nery et al., 2002; Gelman et al., 2011). The MGE and CGE together produce 90% of cortical interneurons and almost all interneuron subtypes (Gelman et al., 2011; Rudy et al., 2011). In mice, the majority of interneurons are born between embryonic days (E) 12 – 16, although some chandelier cells are produced as late as E17, after the bulk of germinal zones have disappeared (Wonders and Anderson, 2006; Taniguchi et al., 2013).

Over the past decade, analysis of null mutants and genetic fate mapping has identified several key transcriptional factors directing neurogenesis and subtype specification in these germinal regions. Two of the distal-less homeobox genes, *Dlx1* and *Dlx2*, are essential for interneuron genesis (Anderson et al., 1997; Cobos et al., 2005; Xu et al., 2005). In the MGE, expression of the transcription factor *Nkx2.1* maintains MGE identity and represses lateral ganglionic eminence (LGE) identity of neural progenitors (Sussel et al., 1999). *Nkx2.1* and its downstream targets *Lhx6*, *Lhx8*, and *Sox6* are necessary for the production and maturation of PV^+ and SST^+ interneurons, which are the main interneuron subtypes derived from the MGE and the two main populations of interneuron in the cortex (Corbin et al., 2003; Du et al., 2008; Gelman and Marin, 2010; Flandin et al., 2011; Rudy et al., 2011). Null mutants of these transcription factors show significant reductions of interneurons in the cortex and epileptic seizures (Sussel et al., 1999; Butt et al., 2008; Batista-Brito et al., 2009). In addition, the PV^+ subtype also requires *Dlx5* and *Dlx6* to properly migrate and functionally mature (Wang et al., 2010).

Most transcription factors expressed in the CGE are also found in MGE, LGE, or both (Nery et al., 2002; Xu et al., 2004; Butt et al., 2005; Wonders and Anderson, 2006). Unlike MGE-born interneurons, cells from the CGE depend on the expression of COUP-TFI and COUP-TFII for specification and migration (Kanatani et al., 2008; Gelman and Marin, 2010; Lodato et al., 2011). All CGE-derived interneurons express the serotonin 5-hydroxytryptamine 3A receptor ($5-HT_{3A}R$), which distinguishes them from other cortical interneurons. In addition to $5-HT_{3A}R$, interneurons that originate from the CGE also express a wide array of subtype markers including VIP, NPY, CCK, reelin, and CR, but not PV or SST. (Lee et al., 2010; Miyoshi et al., 2010; Rudy et al., 2011). Except for CCK^+ basket cells that synapse onto the soma of postsynaptic cells, all CGE-derived interneurons target the dendrites of their synaptic targets (Markram et al., 2004; Miyoshi et al., 2010). VIP^+ cells target other GABAergic interneurons and

cause disinhibition through the inhibition of inhibitory interneurons (Pi et al., 2013; Pfeffer et al., 2013). Therefore, CGE and MGE give rise to interneurons with distinct neurochemical and electrophysiological properties (Figure 2).

Migration of interneurons into the cerebral cortex

After becoming postmitotic neuroblasts, young interneurons from both MGE and CGE migrate long distances from their subpallial birthplaces to populate the cortex (Anderson et al., 2001; Yozu et al., 2005). The leading process of migrating interneurons continuously forms and retracts branches and determines the orientation and direction of migration (Martini et al., 2009). During this journey, numerous chemoattractants and chemorepellents guide these cells away from the ventral telencephalon and towards the cortical plate (Figure 3). MGE-born interneurons are first led away from the germinal zones by extracellular repellents Slit1 and EfnA5, while intracellular expression of COUP-TFII directs CGE-derived interneurons towards the caudal cortex (Wichterle et al., 2003; Yozu et al., 2005; Zimmer et al., 2008; Kanatani et al., 2008). The striatum also repels migrating interneurons destined for the cortex through its expression of class III semaphorins (Marín et al., 2001). Once out of the ventral telencephalon, the tangential migration towards the cortex is facilitated by multiple factors such as brain- and glial-derived neurotrophic factor (BDNF and GDNF, respectively), hepatocyte growth factor (HGF), neurotrophin-4 (NT4), neuregulin-1 (Nrg1), and GABA (Powell et al., 2001; Polleux et al., 2002; Flames et al., 2004; Pozas and Ibáñez, 2005; Inada et al., 2011).

Upon reaching the developing cortex, interneurons are organized into two migrating streams: a superficial stream through the marginal zone, and a deep stream through the subventricular zone (Wichterle et al., 2001). The extracellular environment around these streams facilitates interneuron migration through Cxcl12 and its receptors Cxcr4 and Cxcr7 (Li et al., 2008; Wang et al., 2011). After completing tangential migration, interneurons migrate

radially on the apical fibers of cortical radial glia cells to reach their final destination within the cortical layers. The switch from tangential to radial migration and the radial movements along the radial glial fibers require adhesive contacts provided by gap junctions, specifically connexin-43 and connexin-26 (Elias et al., 2007; Elias et al., 2010).

Function of interneurons in normal and diseased brain

During early development, GABA is depolarizing due to high intracellular chloride concentration in young neurons (Li et al., 2002). GABAergic signaling regulates proliferation, migration, synaptogenesis, and maturation of both inhibitory and excitatory neurons (LoTurco et al., 1995; Behar et al., 1996; Owens and Kriegstein, 2002; Manent et al., 2005; Ben-Ari, 2006; Cancedda et al., 2007; Wang and Kriegstein, 2008; Inada et al., 2011; Wu et al., 2012). Dysfunctions of GABAergic signaling and defective GABAergic interneuron development have been implicated in neurodevelopment disorders. For example, increased interneuron production and enhanced GABAergic inhibition have been described in a mouse model of Down syndrome (Mitra et al., 2012). In models of Dravet syndrome, deletion of sodium channel *Nv1.1* leads to hypoexcitability of cortical interneurons and severe epilepsy (Bender et al., 2012; Tai et al., 2014). Decreased cortical GABAergic inhibition has also been observed in patients and animal models of schizophrenia and autism spectrum disorder (Blatt et al., 2001; McCauley et al., 2004; Gonzalez-Burgos and Lewis, 2008; Liu et al., 2009; Spencer, 2009; Volk et al., 2012).

In the adult cortex, GABAergic interneurons maintain the excitation-inhibition balance of cortical neural circuits and provide feedback control to excitatory networks. Interconnected GABAergic interneurons synchronize the firing of pyramidal neurons that propagate through the entire cortex as network oscillations of various frequencies. Cortical PV⁺ and SST⁺ interneurons participate in both gamma oscillation (30-80Hz), which is implicated in memory processing and attention, and theta oscillation (5-15Hz), which contributes to sensorimotor integration (Tallon-

Baudry and Bertrand, 1999; Fries et al., 2001; Bland and Oddie, 2001; Blatow et al., 2003; Whittington and Traub, 2003; Buzsáki and Wang, 2012; Li et al., 2013). Disruption of GABAergic inhibition in the adult cortex can cause epilepsy, anxiety, sleep disruption, and migraine (Bhalla et al., 2011; Martinowich et al., 2011; Möhler, 2012; Coppola and Schoenen, 2012). In the aging brain, damage to cortical and hippocampal GABAergic interneurons is a common pathological feature of many neurodegenerative diseases (Koliatsos et al., 2006; Palop and Mucke, 2010; Verret et al., 2012; Lanoue et al., 2013). In particular, recent studies have identified cortical SST⁺ interneurons as early targets of Alzheimer's disease (Burgos-Ramos et al., 2008; Saiz-Sanchez et al., 2014).

Section 3: Transplantation of interneuron precursors

Over fifteen years ago, our laboratory discovered that interneuron precursors isolated from the MGE possess remarkable capacities to disperse in a heterotopic environment. They can migrate to and within the cortex whether they are transplanted isochronically into another MGE, or heterochronically into the postnatal cortex (Wichterle et al., 1999; Wichterle et al., 2001). The majority of transplanted MGE precursor cells differentiate into GABAergic interneurons that express the appropriate cellular markers of mature MGE-born interneurons (Alvarez-Dolado et al., 2006; Southwell et al., 2010). Electrophysiological experiments show that these cells functionally integrate into the host neural circuits, receiving input from host neurons while also forming inhibitory synapses onto host cells (Alvarez-Dolado et al., 2006; Baraban et al., 2008). Intriguingly, compared to synapses formed by endogenous interneurons, inhibitory synapses made by transplanted interneurons are almost three times as numerous, but each synapse is only one-third as strong (Southwell et al., 2010). Therefore, each transplanted cell generates the same total inhibitory output as an endogenous interneuron, but the output is

distributed over more synapses and potentially more target neurons. Overall, transplanted MGE precursor cells increase cortical inhibition, seen as increased frequency of spontaneous inhibitory post-synaptic currents in host pyramidal cells (Alvarez-Dolado et al., 2006; Baraban et al., 2008).

Because of their unique ability to survive, disperse, mature, and functionally integrate into the host brain, MGE-derived interneuron precursors have been extensively tested as therapeutic agents in cell therapy. Indeed, MGE transplantation has shown promises in treating neurological diseases. When transplanted into the cortex and hippocampus of mouse models of congenital and injury-induced epilepsy, MGE-derived interneurons are able to survive in the abnormal brain environment and reduce seizure frequency by 85-90% (Baraban et al., 2008; Hunt et al., 2013). In a rat model of Parkinson's disease, MGE cells transplanted into the striatum also integrate and ameliorate the motor symptoms of Parkinson's disease (Martínez-Cerdeño et al., 2010). In an apolipoprotein E4 (apoE4) model of Alzheimer's disease, MGE cells, remarkably, are able to develop normally in the toxic environment of aged and symptomatic apoE4 mice and improve their memory performance (Tong et al., 2014). Perhaps most surprisingly, even when transplanted into the spinal cord, a foreign environment endogenous where cortical interneurons never go to, MGE precursor cells can survive and ameliorate injury-induced neuropathic pain (Bráz et al., 2012). Therefore, transplanted interneurons can effectively modify brain function in normal and diseased brain.

Section 4: Interneuron and ocular dominance plasticity

The mammalian brain is highly plastic during early development. Many regions of the cerebral cortex exhibit temporally restricted periods of critical period plasticity. In the mouse visual cortex, neurons that are stimulated by visual input from both eyes usually prefer the

contralateral eye, a phenomenon called ocular dominance. During the critical period, these binocular neurons can rapidly shift their responses away from the dominant eye if that eye becomes visually deprived. This ocular dominance plasticity (ODP) is a conserved feature of many binocular mammals including mouse, cat, monkey and human (Wiesel and Hubel, 1963; Awaya et al., 1973; Hubel et al., 1977; Gordon and Stryker, 1996). Studies of the mouse visual cortex have shown that GABAergic signaling plays an essential role in critical period ODP, which normally occurs during postnatal days 19-32 (Gordon and Stryker, 1996). An elevated level of GABAergic inhibition is required to open the critical period, as null mutants of the synaptic glutamic acid decarboxylase (GAD65) fail to open the critical period. However, critical period ODP can be initiated in these mice during and even after the critical period by infusion of GABA_A receptor agonists (benzodiazepines) (Hensch et al., 1998; Fagiolini and Hensch, 2000). In fact, increasing GABAergic inhibition is sufficient to precipitate an episode of precocious ODP before the actual critical period (Fagiolini and Hensch, 2000). Overexpression of BDNF, which promotes interneuron maturation, also accelerates ODP in young mice (Hanover et al., 1999; Huang et al., 1999). Therefore, the increased levels of inhibition likely reflect greater inhibitory output of mature GABAergic interneurons.

Further investigation identified specific GABAergic circuits and cell types whose maturation is needed for critical period ODP to commence. Mutants of several GABA_A receptor subunits revealed that $\alpha 1$, but not $\alpha 2$ or $\alpha 3$ subunits are necessary for GABA_A receptor agonist diazepam to induce precocious ODP in pre-critical period mice (Fagiolini et al., 2004). The GABA_A receptor $\alpha 1$ subunits are enriched at perisomatic GABAergic synapses, alluding to the role of perisomatic inhibition in critical period ODP (Klausberger et al., 2002). Indeed, several additional lines of evidence support a crucial role for the main type of perisomatic-innervating interneurons, the PV⁺ basket cells, in critical period. Maturation of PV⁺ interneurons coincides with the opening of the critical period (Chattopadhyaya et al., 2004). PV⁺ interneurons

development also requires the transcription factor *Otx2*, which can also induce precocious ODP and accelerate PV⁺ cell maturation when infused into pre-critical period mice (Sugiyama et al., 2008). Disruption of perineuronal nets (PNN), which are special extracellular matrix structures formed around mature PV⁺ interneurons, also causes persistent ODP (Miyata et al., 2012). Finally, PV⁺ interneurons change their firing pattern in response to visual deprivation during the critical period, and recapitulation of this activity pattern can reactivate critical-period-like ODP in adult mice (Kuhlman et al., 2013).

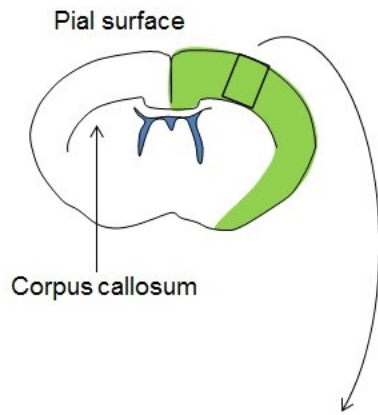
After the critical period has closed, some plasticity lingers in the adult cortex. Adult forms of plasticity are slower and less pronounced, and disinhibition, rather than increased inhibition, seems to mediate adult plasticity (van Versendaal et al., 2012). This is consistent with adult plasticity being dominated by disinhibition of the non-deprived eye, while critical period plasticity is mediated mainly by depression of the deprived eye (Sato and Stryker, 2008). Adult ODP can be enhanced by manipulations that are not known to affect critical period ODP, such as environmental enrichment and administration of a selective serotonin reuptake inhibitor (SSRI) (Sale et al., 2007; Maya Vetencourt et al., 2008). Therefore, adult and critical period plasticity probably arise from different mechanisms and may even be mediated by different neural circuits.

A recent collaboration between our laboratory and the Stryker Lab has demonstrated that transplantation of MGE-derived interneuron precursors can induce a second period of heightened ODP in the mouse visual cortex (Southwell et al., 2010). Interestingly, the timing of transplant-induced ODP is not determined by the age of the host neurons, but the age of the transplanted interneurons. The transplanted cells follow their intrinsically timed developmental program and modify cortical neural circuits when they reach the same cellular age as that of endogenous interneurons during the critical period. These findings illustrate the powerful influence interneurons exert on neural circuits and the crucial role they play in cortical plasticity.

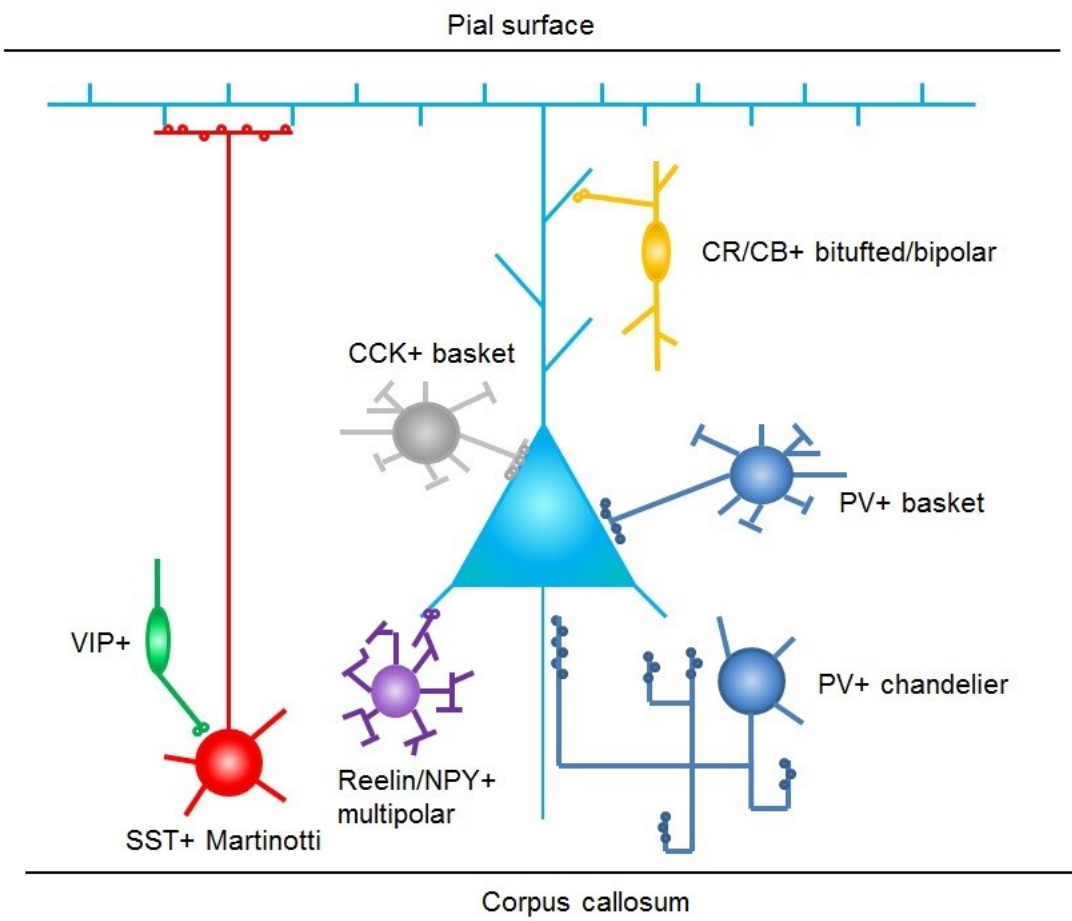
Figure 1. Diversity of cortical GABAergic interneurons.

A. A coronal section of the adult mouse brain at the level of somatosensory cortex. The left cerebral cortex in this section is highlighted in green. The pial surface and the corpus callosum are labeled for orientation of the rectangular insert, which depicts **B. B.** Schematic representation of a pyramidal cell (light blue), and the major subtypes of cortical interneurons (red, Martinotti cells; dark blue, basket and chandelier cells; grey, CCK⁺ basket cells; gold, CR⁺ cells; green, VIP⁺ cells; and purple, reelin⁺ cells). These interneurons exhibit diverse morphologies, marker expressions, firing patterns, and preferred subcellular compartments that they synapse onto.

A



B



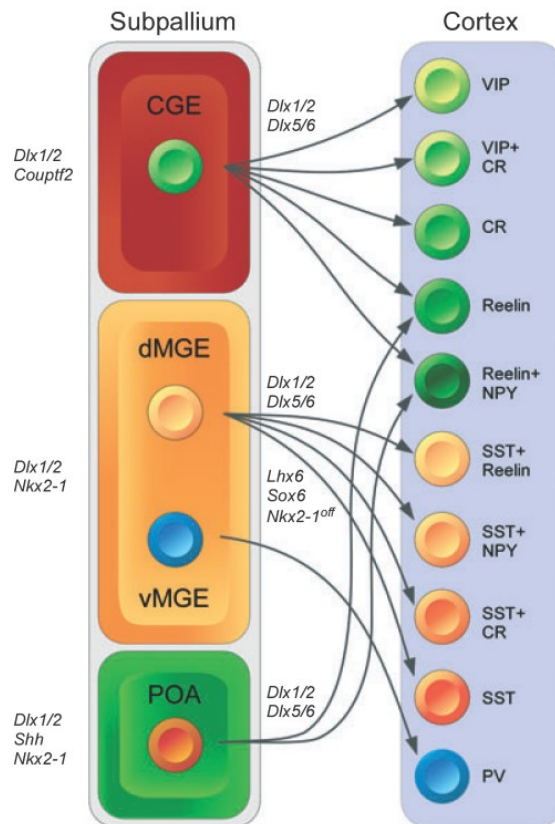


Figure 2. Transcriptional regulation of interneuron subtype development.

Distinct cortical interneuron subtypes originate from the caudal ganglionic eminence (CGE), dorsal medial ganglionic eminence (dMGE), ventral medial ganglionic eminence (vMGE), and preoptic area (POA). Progenitor cells in the ganglionic eminences express transcription factors such as *Dlx1/2*, *Nkx2.1*, and *Couptf2* that help to maintain region-specific progenitor identity. Expression of other transcription factors such as *Dlx5/6* and *Lhx6* promote the survival and differentiation of intermediate progenitors into diverse interneuron subtypes (arrows). Image adapted from Gelman and Marín, 2010.

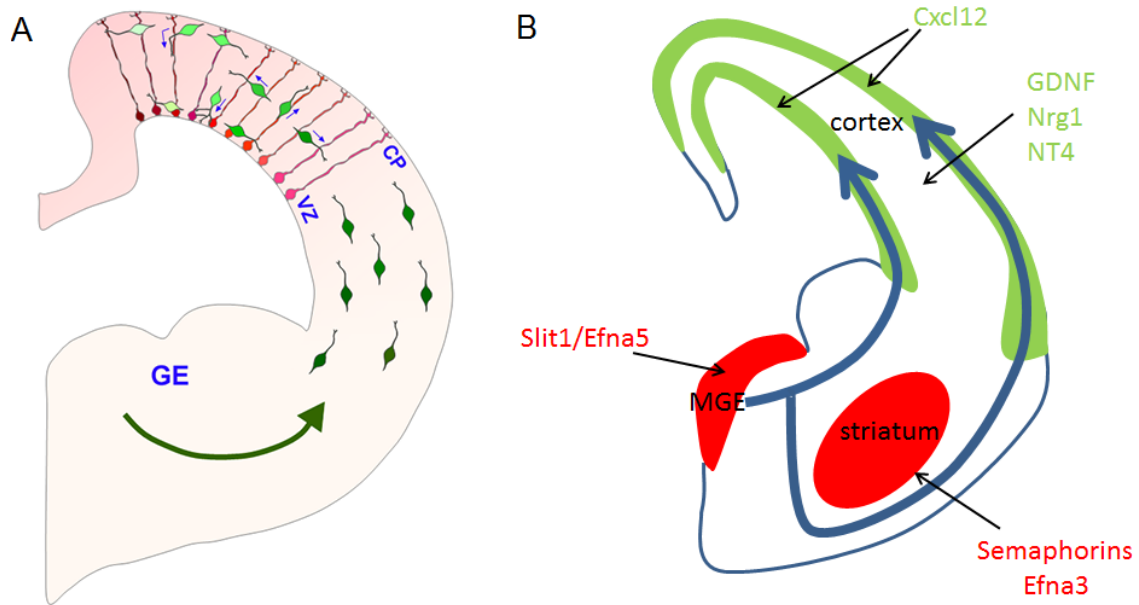
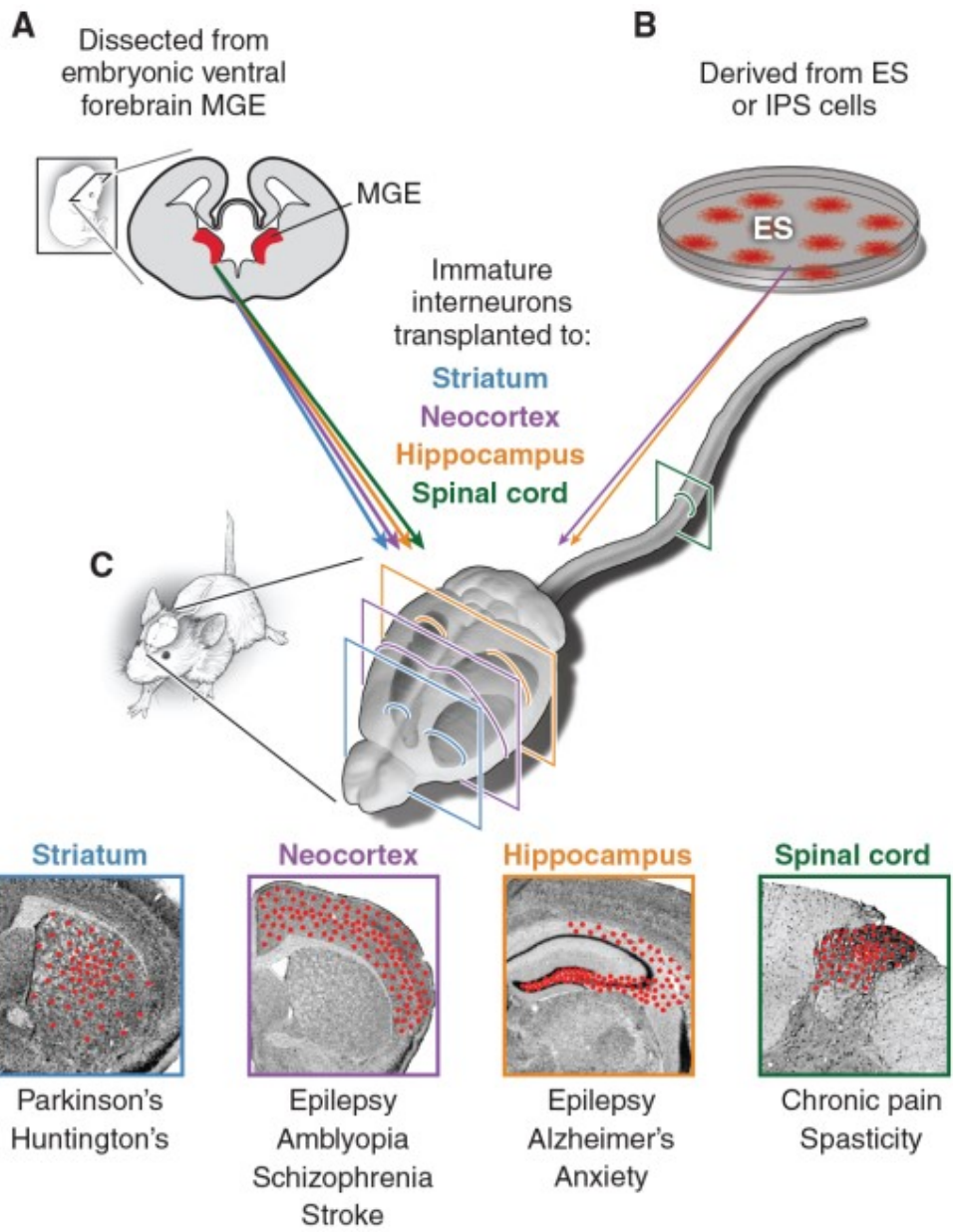


Figure 3. Tangential and radial migration of cortical interneurons.

A. Interneurons generated in the subpallial ganglionic eminences (GE) migrate tangentially to reach the cortical plate (CP). At the end of their tangential migration, interneurons climb the apical fibers of radial glia in the cortical ventricular zone (VZ) to populate all layers of the cortex. Image adapted from Yokota et al., 2007. **B.** A schematic representation of a coronal section of one hemisphere of the E13.5 forebrain. During migration, non-diffusible chemorepellents such as Slit1, semaphorins, and Efna3/5 (red) in the MGE and basal ganglial structures make subpallium less permissive to migration than cortex. Chemoattractants (green) facilitate interneuron migration into and inside the cortical plates. In particular, the expression of Cxcl12 in the marginal zone and the VZ/SVZ encourages interneurons to organize into a superficial and a deep migratory stream. Blue arrows indicate directions of interneuron migration.

Figure 4. Cell sources and potential applications of interneuron transplantation.

A. Dissected mouse MGE cells can be transplanted into postnatal mouse brain, where they migrate, differentiate, and integrate into the host neural circuits. **B.** Alternatively, human embryonic stem (ES) cells and induced pluripotent stem (IPS) cells can also be differentiated into interneuron-like cells (Liu et al., 2013), which can be subsequently transplanted into immunosuppressed animal models. **C.** Depending on the site of transplantation, interneurons have been shown to ameliorate epilepsy (Baraban et al., 2009; Hunt et al., 2013), Parkinson's disease (Martínez-Cerdeño et al., 2010), Alzheimer's disease (Tong et al., 2014), and chronic pain (Bráz et al., 2012). These cells may hold potential to therapeutically modify other neurological diseases, such as Huntington's disease, amblyopia, schizophrenia, stroke, anxiety, and spasticity. Images adapted from Southwell et al., 2014.



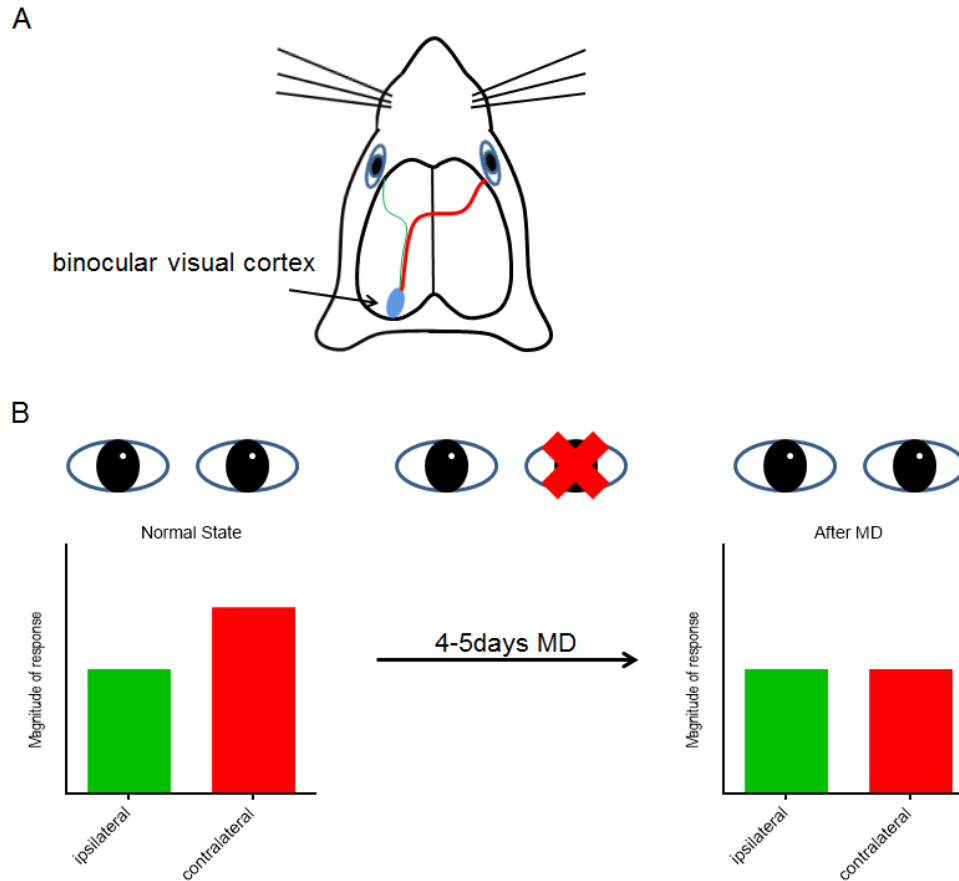


Figure 5. Ocular dominance plasticity of the mouse binocular visual cortex.

A. In the mouse visual system, the binocular region (blue) of the visual cortex receives strong input from the contralateral eye (red line), as well as a small input from the ipsilateral eye (green line). **B.** In the unperturbed animal, the binocular visual cortex has a contralateral ocular dominance, where the cortical responses to visual stimuli from the contralateral eye (red bar) are stronger compared to responses to the ipsilateral eye (green bar). A brief (4-5 days) monocular deprivation (MD) of the contralateral eye during the critical period elicits plasticity that produces a significant weakening of cortical response to the deprived eye and diminished contralateral ocular dominance.

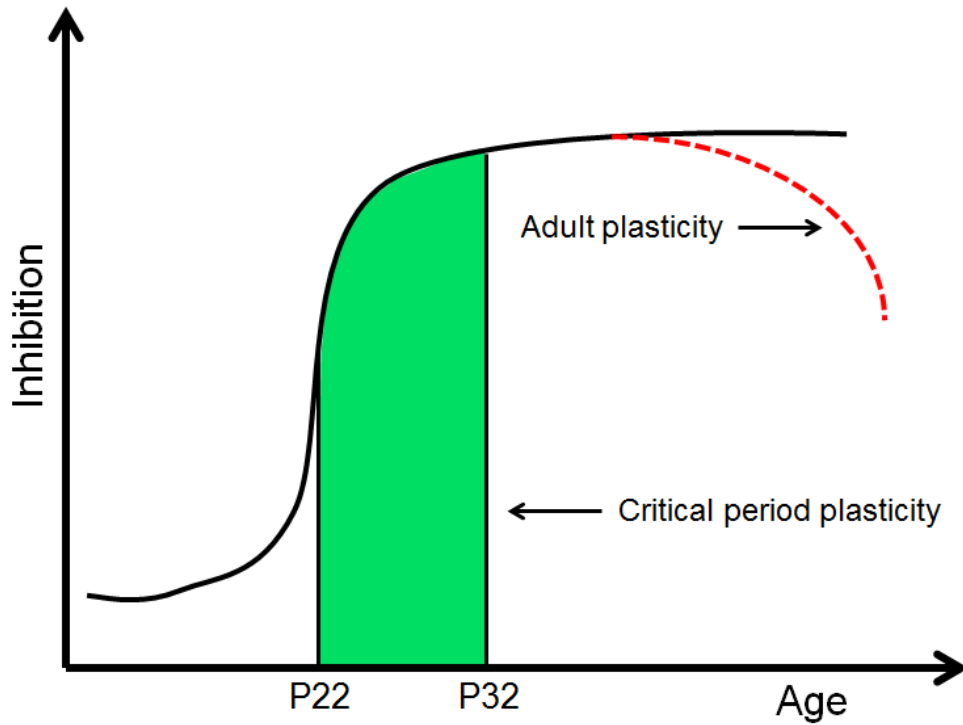


Figure 6. GABAergic inhibition and ocular dominance plasticity.

In the mouse visual cortex, the critical period occurs between postnatal days (P) 22 – 32 (green area). This period corresponds with increased GABAergic inhibition, which is required to open the critical period. During the critical period, brief (4-5 days) monocular deprivation elicits ocular dominance plasticity mediated by strong inhibition of response to the deprived eye. After the closure of the critical period, elevated levels of inhibition are maintained during adulthood. In contrast to critical period plasticity, plasticity in the fully mature cortex is elicited by a decrease in GABAergic inhibition (red dashed line). Adult plasticity requires longer (>7 days) deprivation is mediated by disinhibition of neural response to the non-deprived eye.

Materials and Methods

Section 1: Animals

Mouse (*Mus musculus*) was the only animal species used. All mice were housed in the Laboratory Animal Resource Center and treated according to the guidelines established by the Institutional Animal Care and Use Committee. Strains used are detailed in Table 1.

Table 1. Mouse Strain information.

Strain	Full Name	Description	Source	Reference
C57Bl/6J	C57Bl/6J	Inbred wild-type strain used as breeders and recipients of cell transplantation.	Jackson Labs	N/A
PV-cre	B6; 129P2-Pvalb ^{tm1(cre)Arbr} /J	Knock-in of <i>IRE5</i> and <i>Cre</i> into the 3' untranslated region of the endogenous <i>PV</i> locus. Maintained as double homozygotes of <i>PV-cre</i> and <i>Ai14</i> on C57Bl/6J background.	Jackson Labs	Hippenmeyer <i>et al.</i> , 2005.
SST-cre	Sst ^{tm2.1(cre)Zjh} /J	Knock-in of <i>IRE5</i> and <i>Cre</i> into the 3' untranslated region of the endogenous <i>SST</i> locus. Maintained as	Jackson Labs	Taniguchi <i>et al.</i> , 2011.

		double homozygotes of <i>SST-cre</i> and <i>Ai14</i> on C57Bl/6J background.		
Nkx2.1-cre	C57Bl/6J ^{Tg(Nkx2-1-cre)2Sand} /J	Transgenic insertion of the Nkx2.1 gene with <i>Cre</i> replacing part of exon 2. Maintained as heterozygotes on C57Bl/6J background.	Jackson Labs	Xu <i>et al.</i> , 2008.
Gad2-cre	Gad2 ^{tm2(cre)Zjh} /J	Knock-in of <i>IRES</i> and <i>Cre</i> into the 3' untranslated region of the endogenous glutamic acid decarboxylase 2 (<i>Gad2</i>) locus. Maintained as double homozygotes of <i>Gad2-cre</i> and <i>Ai14</i> on C57Bl/6J background.	Jackson Labs	Taniguchi <i>et al.</i> , 2011.
R26-DTA	Gt(ROSA)26Sor ^{tm1(DTA)Jpmb} /J	Knock-in of CAG promoter, <i>loxP</i> -flanked GFP and stop cassette, and DTA into the <i>Rosa26</i> locus. Maintained as homozygotes on CD-1 background.	Jackson Labs	Ivanova <i>et al.</i> , 2005.
Ai14	B6.Cg-Gt(ROSA)26Sor ^{tm14(CAG-tdTomato)Hze} /J	Knock-in of CAG promoter, <i>loxP</i> -flanked stop cassette, and <i>tdTomato</i> into the <i>Rosa26</i> locus. Maintained as double homozygotes in <i>PV-cre</i> , <i>SST-cre</i> , or <i>Gad2-cre</i> on C57Bl/6J background.	Jackson Labs	Madisen <i>et al.</i> , 2010.
Actin-GFP	C57Bl/6 ^{Tg(CAG-EGFP)10sb} /J	Transgenic mice constitutively expressing <i>EGFP</i> from a CAG promoter in all cells. Maintained as	Jackson Labs	Okabe <i>et al.</i> , 1997.

		homozygotes on C57Bl/6J background.		
A-DTA	B6;129-Gt(ROSA)26Sor ^{tm1(DTA)Mrc} /J	Knock-in of CAG promoter, <i>loxP</i> -flanked stop cassette, and attenuated <i>DTA</i> into the <i>Rosa26</i> locus. Maintained as homozygotes on mixed C57Bl/6J and 129 background.	Jackson Labs	Wu <i>et al.</i> , 2006.
L-DTA	B6.129P2-Gt(ROSA)26Sor ^{tm1(DTA)Lky} /J	Knock-in of CAG promoter, <i>loxP</i> -flanked stop cassette, and <i>DTA</i> into the <i>Rosa26</i> locus. Maintained as homozygotes on C57Bl/6J background.	Jackson Labs	Voehringer <i>et al.</i> , 2008.
G42	CB6 ^{Tg(Gad1-EGFP)G42Zjh} /J	Transgenic mice expressing <i>EGFP</i> constitutively in a subset of parvalbumin interneurons. Maintained as heterozygotes on CB6F1/J background.	Jackson Labs	Chattopadhyaya <i>et al.</i> , 2004.
Gin	FVB ^{Tg(GadGFP)45704Swn} /J	Transgenic mice <i>EGFP</i> constitutively in a subset of somatostatin interneurons. Maintained as homozygotes on FVB background.	Jackson Labs	Oliva <i>et al.</i> , 2000.

Section 2: Cell preparation and transplantation

Donor tissue preparation

Mice were mated and plugs were checked daily. The time when the semen plug was detected was considered to be embryonic day 0.5. At embryonic day 13.5-15.5, pregnant female mice were euthanized by isoflurane overdose followed by cervical dislocation, and embryos were dissected out from the uterus. The ventricular and subventricular zones of the MGE or the dorsal CGE were dissected from the embryos and dissociated into single cells via repeated pipetting in Leibovitz's L-15 medium containing 100 IU/ml DNase I (Roche). Cells were then concentrated by centrifugation at 600 *g* for 3 minutes.

Cell Transplantation

P7 C57Bl/6J recipients were anesthetized using hypothermia until pedal reflex disappeared and were then placed on a stereotaxic injection platform. The concentrated cells (~100,000 cells per μ l) were loaded into beveled Drummond glass micropipette (Drummond Scientific) that was positioned at 30 degrees from vertical. Two injections were placed into the caudal left cortex with the following coordinates: 1) anterior-posterior (A-P) 7 mm, medial-lateral (M-L) 3.5 mm; 2) A-P 6.5 mm, M-L 3.2 mm. Zero for A-P and M-L was defined as the inner corner of the eye, and midpoint between two eyes, respectively. The depth of both injections was 1.3 mm from the surface of the skin. After injections, recipients were placed on a heating pad until they became warm and active. Mice were subsequently returned to their mothers until weaning age (P21).

Section 3: Immunohistochemistry

Embryonic mouse brains were drop fixed in 4% formaldehyde overnight, cryoprotected in 30% sucrose, and imbedded in OCT (Tissue-Tek). The brains were then cut using a cryostat (Leica). Postnatal brains were collected by first perfusing the animals with 4% formaldehyde in

phosphate buffered saline (PBS). The brains were then removed, postfixed for 30 minutes (for detection of VIP) or 2 hours (for detection of all other antigens) in 4% formaldehyde, and cryoprotected in 30% sucrose. 30 μ m coronal sections were cut using a sliding microtome (Leica & Physitemp Instruments). Free floating sections were blocked for 1 hour at room temperature in blocking solution (Tris buffered saline (TBS), 10% normal donkey serum, and 1% Tween-100), and incubated at 4 degrees centigrade overnight in primary antibodies. After washing in TBS and 1% Tween-100 three times, 15 minutes each, sections were incubated in blocking solution with the appropriate Alexa secondary antibodies at 1:1000 (Life Technologies). After 1 hour of incubation with secondary antibodies at room temperature, sections were washed in PBS 3 times, 10 minutes each, mounted on glass slides, and coverslipped.

Table 2. Primary antibodies.

Antigen	Host	Dilution	Source
GFP	Chicken (polyclonal)	1:1000	Aves
PV	Mouse (monoclonal)	1:1000	Sigma
SST	Rabbit (polyclonal)	1:300	Swant
SST	Goat (polyclonal)	1:200	Santa Cruz
Calbindin	Rabbit (polyclonal)	1:1000	Millipore
Calretinin	Rabbit (polyclonal)	1:1000	Millipore
NPY	Rabbit (polyclonal)	1:1000	Abcam
Reelin	Rabbit (polyclonal)	1:1000	Abcam
VIP	Rabbit (polyclonal)	1:1000	Immunostar
Sp8	Goat (polyclonal)	1:500	Santa Cruz
CoupTF II	Rabbit (polyclonal)	1:200	R&D Systems
GFAP	Mouse (polyclonal)	1:1000	Millipore
CD68	Rat (polyclonal)	1:1000	ABD serotec
Iba1	Rabbit (polyclonal)	1:1000	Wako
Satb2	Mouse	1:500	Abcam
Ctip2	Rat (polyclonal)	1:500	Abcam

Section 4: Optical imaging of intrinsic signal

Image acquisition and quantification

Images of the binocular visual cortex, demarcated by the Dil injections, were captured using the Zeiss Axiovert-200 microscope (Zeiss), AxioCam Mrm (Zeiss), and Neurolucida (MBF). GFP⁺ cells were counted in every sixth section (180 μ m apart). Cell density was computed by counting all GFP⁺ cells within the binocular visual cortex and dividing by the area of binocular visual cortex delineated by the Dil injections.

Optical imaging of intrinsic signal

Surgical preparation, optical imaging, and analysis of intrinsic signals were performed as previously described (Gandhi et al., 2008; Kaneko et al., 2014). Briefly, 2-3 days before imaging, mice were anesthetized using 2.5% isoflurane in oxygen and the skull over the left visual cortex was exposed and protected with a layer of nitrocellulose (New-Skin, MedTech Products). A custom stainless steel head plate was attached to the skull with dental acrylic. Mice were then given 5 mg/kg of carprofen subcutaneously for post-operative analgesia. On the day of baseline imaging, mice were anesthetized with 0.7% isoflurane in oxygen, supplemented with a single intraperitoneal injection of 2-5 mg/kg chlorprothixene, and placed on a heating pad that maintained the body temperature at 37.5 °C through a rectal thermo probe feedback. The head plate was secured in a stereotaxic frame and the imaging window directly above the binocular visual cortex was covered with agarose and topped with a coverslip to provide a flat imaging surface. The eyes were protected with a thin coat of silicone oil. Black-and-white contrast-modulated stochastic noise movie was presented to the binocular visual field (-5° to +15° azimuth) at 25 cm in from of the mice. The movie was presented for 5 min per session, 4-5 times alternatively to each eye, for a total of 20-30 min each eye. During the imaging sessions, 610 nm light reflected by the visual cortex was gathered using a Dalsa 1M30 CCD camera (Dalsa) focused at 550 μ m beneath the surface of the brain. At the end of the last imaging

session, the boundaries of the binocular cortex were determined by overlapping the response maps of optical imaging with images of surface blood vessels, and were marked thin tungsten wire coated with Dil (Invitrogen).

Analysis of optical imaging data

A map of visual response data was extracted from the raw optical imaging data using a custom Fourier analysis program (Kalatsky and Stryker, 2003). The average amplitude of signal within the region corresponding to the binocular visual cortex was taken to represent the strength of visual response. Ocular dominance index (ODI) was computed as the average of $(C - I)/(C + I)$ at each pixel within the binocular response region, where C is the response to contralateral visual stimulation and I is the response to ipsilateral stimulation.

Section 5: Statistical analysis

Rank sum test was performed to compare ODIs at baseline and 4-5 days MD for each mouse to determine the significance of differences. Kruskal-Wallis test with adjusted *P* values was performed to determine significance of differences in ODI, ocular dominance shift (defined as baseline ODI – post MD ODI), rostral-caudal distribution of transplanted cells and the degree of plasticity, and amplitude of ocular response among experimental groups. Linear regression was performed to determine the dependency of magnitude of plasticity or amplitude of visual response on density of total transplanted cells, transplanted PV⁺ cells, or transplanted SST⁺ cells. All statistical analysis was performed using Prism 5 (Graphpad).

Role of Parvalbumin- and Somatostatin-expressing Interneurons in Transplant-induced Cortical Plasticity

Section 1: Introduction

Brain plasticity is the dynamic modification and rearrangement of neural networks. Critical periods of heightened, activity-dependent plasticity shape the early development of many cortical areas. In the mouse binocular visual cortex, this critical period of plasticity occurs between P22 to P32, with a peak at around P28 (Gordon and Stryker, 1996). During the critical period, deprivation of vision in one eye causes rapid changes in cortical responses: the binocular visual area becomes less responsive to the deprived eye. GABAergic inhibition has been shown to play an important role in this ocular dominance plasticity (ODP). Administering the GABA receptor agonist diazepam to pre-critical-period mice is able to trigger the precocious opening of ODP (Hensch et al., 1998). On the other hand, knockout mice lacking the synaptic GABA synthase GAD65 fail to open the critical period (Fagiolini and Hensch, 2000). These findings suggest that GABAergic interneurons and their inhibitory output play a pivotal role in the induction of critical period ODP.

The majority of GABAergic interneurons in the neocortex are derived from the MGE (Anderson et al., 1997; Wichterle et al., 2001; Pleasure et al., 2000; Wonders and Anderson, 2013). Transplantation of MGE-derived inhibitory neuronal precursors into the visual cortex of

postnatal mice has been shown to induce a second window of plasticity (Southwell et al., 2010). The transplanted interneurons, consisting primarily of parvalbumin-expressing (PV⁺) and somatostatin-expressing (SST⁺) cells, disperse, mature, and integrate into local visual cortical circuit (Wichterle et al., 1999; Alvarez-Dolado et al., 2006; Hunter et al., 2013). Current research predominantly focuses on PV⁺ interneurons, with ample, albeit indirect, evidences links these cells to the opening of critical period ODP (Sugiyama et al., 2008; Miyata et al., 2012; Kuhlman et al., 2013). In these studies, disrupting peri-neuronal nests or mimicking the electrophysiological activity patterns of young PV⁺ cells was sufficient to reintroduce ODP after the closure of the endogenous critical period, indicating that immature PV⁺ interneurons may play a key role in driving ODP.

In contrast to the comprehensive body of work on PV⁺ interneurons, few studies have been conducted on SST⁺ interneurons in the context of ODP despite their abundance in the visual cortex and their powerful influence on the apical dendrites of pyramidal cells (Spratling and Johnson, 2003; Gonchar et al., 2007). To investigate the contribution of these two distinct interneuron subtypes to ODP, I took advantage of MGE transplantation and grafted cells in which PV⁺ cells, SST⁺ cells, or both were genetically ablated. In collaboration with the Stryker Lab, we tested whether these transplants induced a second critical period in the recipients. Here I present findings demonstrating that removing either PV⁺ or SST⁺ cells did not hinder the ability of MGE transplants to induce ODP, but removing both eliminated the plasticity. These results demonstrate that PV⁺ cells do not play an exclusive role in ODP; SST⁺ cells can also drive plasticity and reshape neural circuits when the majority of PV⁺ cells are eliminated. Furthermore, examination of the characteristics of ODP induced by MGE transplants revealed that it resembled plasticity in the normal critical period and differed from plasticity observed in older animals in its magnitude, sensitivity to brief MD, and in the weakening of response to the

deprived eye. These findings reveal specific cortical GABAergic inhibitory cell types that mediate plasticity.

Section 2: Results

Unsuccessful Purification of PV⁺ and SST⁺ neuroblasts from dissected MGE cells

Logically, the best approach to determining the function of PV⁺ and SST⁺ subtypes of interneuron in transplant-induced cortical plasticity is transplantation of pure populations of PV⁺ or SST⁺ cells. However, interneuron progenitors and precursors in the MGE do not readily express PV or SST: In situ hybridization fails to detect RNA of either in the mouse MGE at E13.5 (Alan Brain Atlas). This precluded the possibility of FACS using PV and SST immunostaining. Next, I tested two transgenic mouse lines of Gad67-GFP, G42 and Gin. Due to insertion site effects, G42 and Gin mice express GFP only in a subset of PV⁺ and SST⁺ interneurons, respectively. The expression of GFP in these lines precedes the expression of PV or SST, and can be detected as early as the first postnatal week (Oliva et al., 2000; Chattopadhyaya et al., 2004). When I performed immunostaining for GFP in these lines at E13.5, I found no GFP⁺ cell in the MGE of either line of mice, although GFP⁺ cells were observed in the globus pallidus, ventral septum, and medial forebrain bundle of the G42 brain (Figure 1). A FACS of MGE cells pooled from several E13.5 G42 embryos collected fewer than 1000 GFP⁺ cells, several magnitude lower than the number reported to induce plasticity (Southwell et al., 2010).

After I have determined that purification of MGE cells was not practical, I transplanted dissociated cortical cells from P0 actin-GFP embryos to assess whether inhibitory neuroblasts, already exited from the MGE, could survive and disperse in the host cortex after transplantation.

Since G42 and Gin mice express GFP in interneurons neonatally, if cortical interneurons migrate and integrate after transplantation, I could circumvent the lack of GFP expression in the MGE by transplanting purified GFP⁺ cortical cells from neonatal G42 and Gin mice. At 30 DAT, only a few surviving cells were found in and near the injection site. Neither the number of cells nor the extent of dispersion was comparable to that of MGE transplants (Figure 2). In conclusion, the current genetic tools do not allow for isolation of PV⁺ or SST⁺ cells from the MGE in sufficient quantities. An alternative was needed.

Genetic ablation of PV⁺ and SST⁺ interneurons in MGE transplants

Once I have determined that it's not practical to transplant of purified subgroups of interneurons, I turned to methods to ablate interneurons in a subtype-specific manner and investigate the contribution of these cells to plasticity through their absence. I developed a genetic strategy to selectively deplete PV⁺ or SST⁺ interneurons from MGE transplants through the use of *PV-cre* and *SST-cre* donor mice. In these mice, the *IRES-Cre* element is knocked into the 3' untranslated region of the PV and SST loci (Hippenmeyer et al., 2005; Taniguchi et al., 2011). This configuration allows the Cre recombinase to be expressed under the control of the endogenous PV and SST promoters without disrupting the genes themselves. When I examined the MGE at E14, no expression of a fluorescent reporter was detected in *PV-cre* or *SST-cre* mice, again precluding the possibility of sorting pure populations of PV⁺ or SST⁺ cells by fluorescence for transplantation. Therefore I elected to eliminate PV⁺ populations, SST⁺ populations, or both populations, after transplantation and then study their effects on transplant-induced plasticity. I crossed *PV-cre* and *SST-cre* mice to transgenic mice harboring a Cre-inducible allele of Diphtheria toxin alpha subunit (*R26-DTA*) to achieve targeted depletion of PV- and SST-expressing cells, respectively (Figure 3). DTA is a potent intracellular toxin that induces programmed cell death within 48 hours of expression by blocking protein synthesis (Choe et al. 1992). The *R26-DTA* mice also express GFP ubiquitously, permitting the

visualization of transplanted cells (Ivanova et al., 2005). *PV-cre;R26-DTA* (PV-depleted) and *SST-cre;R26-DTA* (SST-depleted) mice didn't survive beyond the perinatal period, but E13.5 embryos from both crosses were of normal size and gross appearance.

Next I transplanted MGE cells from PV-depleted, SST-depleted, and *PV-cre;SST-cre;R26-DTA* (PV-SST-depleted) embryos into cortical regions near the binocular visual cortex of P7 C57Bl/6J recipients (Figure 4). *R26-DTA* cells (without any Cre allele) and freeze-thaw-killed MGE cells were also transplanted as positive and negative controls, respectively. The surviving donor GFP⁺ cells in PV-depleted, SST-depleted, and PV-SST-depleted transplants migrated and integrated into visual cortex similarly to control *R26-DTA* MGE donor cells (Figure 5). Immunohistochemistry for PV and SST revealed that by 40 days after transplantation (DAT), the vast majority of PV⁺ cells had been eliminated from PV-depleted, and SST⁺ cells from SST-depleted transplants, while the simultaneous expression of both Cre alleles depleted both PV⁺ and SST⁺ populations (Figure 6). Examination of PV-depleted and SST-depleted transplants at earlier ages revealed that the Cre-expressing population was significantly decreased by 21 DAT for PV⁺ cells (the earliest age when PV is detectable by immunohistochemistry) and by 14 DAT for SST⁺ cells (Figure 7). Because PV⁺ and SST⁺ cells account for the majority of MGE-derived interneurons (Wonders and Anderson, 2006; Gelman and Marin, 2010), depletion of one population led to a statistically significant increase in the percentage of total transplant of the other (PV-depleted: 52.11% SST⁺, *R26-DTA*: 38.22% SST⁺, Mann-Whitney test, $P < 0.05$. SST-depleted: 49.58% PV⁺, *R26-DTA*: 35.71% PV⁺, Mann-Whitney test, $P < 0.01$. Figure 8). However, the densities (per mm²) of SST⁺ cells in PV-depleted and PV⁺ cells in SST-depleted transplants were similar to those in control *R26-DTA* transplant recipients, indicating that DTA-mediated cell death of one population did not affect the survival or induce a compensatory increase of the non-Cre-expressing population (Figure 6). In PV-SST-depleted transplants, where the densities of both PV⁺ and SST⁺ cells were very low, the remaining cells expressed

interneuron markers such as calretinin, calbindin, and reelin, indicating that they differentiated normally despite the death of the majority of transplanted cells (Figure 9). These findings show that selectively ablating PV⁺ or SST⁺ cells by DTA efficiently eliminated the target population without affecting the survival or migration of the remaining cells.

Optical imaging of intrinsic signals to detect plasticity in recipients of *R26-DTA* and dead MGE cells

After characterizing the subtype-depleted MGE transplants, in collaboration with Sebastian Espinosa, a postdoctoral fellow from the Stryker Lab, I examined whether these transplants could induce a second critical period of plasticity. Using intrinsic signal optical imaging, we first tested recipients of control *R26-DTA* and freeze-thaw-killed MGE cells for plasticity at 33-35 DAT, when the transplanted cells were at an equivalent age of P26-P28 and display the greatest ability to induce plasticity (Southwell et al., 2010). The purpose of these experiments was to establish that the *R26-DTA* allele and expression of GFP from the *Rosa26* locus do not affect the transplants' ability to induce plasticity or alter the baseline ocular dominance index of the recipients. Neuronal response to visual stimuli was measured using optical imaging, a non-invasive and repeatable technique developed by the Stryker Lab that measures neuronal activity via hemodynamic changes in local microcirculation (Kalatsky and Stryker, 2003). The animal was presented with periodic stimuli that generate robust responses at a frequency distinct from other episodic hemodynamic changes such as heart beat and respiration, while a camera gathered 610 nm light reflected off the binocular zone of the primary visual cortex through intact skull. The stimuli were presented to one eye at a time, and response values integrated over the entire binocular visual cortex were collected. The ocular dominance index, computed using the formula $(C - I)/(C + I)$, in which C represents the contralateral response and I represents the ipsilateral response, indicates the degree of preference to one of the eyes (Sato and Stryker, 2008). Normally, the contralateral eye is preferred and elicits

stronger responses than the ipsilateral eye, with a baseline ODI around 0.22 (Cang et al., 2005). After 4 days of contralateral MD, optical imaging was repeated to obtain a post-MD ODI value. A decrease of ODI after MD signals plasticity as the visual cortex shifts its preference away from the deprived contralateral eye and towards the open ipsilateral eye. Recipients of freeze-thaw-killed MGE cells showed normal baseline ODI values that remained unchanged after 4 days of MD (Figure 10, left; ODI = 0.23 ± 0.006 at baseline; ODI = 0.2 ± 0.015 at 4 d MD; Mann-Whitney test, $P = 0.08$). On the other hand, recipients of *R26-DTA* MGE cells also had normal baseline ODI but showed robust plasticity after 4 d MD (Figure 10, right; ODI = 0.22 ± 0.01 at baseline; ODI = 0.08 ± 0.012 at 4 d MD; Mann-Whitney test, $P < 0.01$). These results confirmed that, without live transplanted MGE cells, 4 d MD failed to induce ODP in the P40-42 recipients, who were 12-14 days past the peak of their endogenous critical period. They also reproduced the transplant-induced ODP reported previously (Southwell et al., 2010) and demonstrated that the *R26-DTA* allele had no effect on either the baseline ODI or the induction of ODP.

MGE transplants depleted of PV⁺ cells or SST⁺ cells, but not of both, induced ODP in recipients

Next, we tested recipients of PV-depleted, SST-depleted, or PV-SST-depleted transplants for plasticity. We were not surprised to observe robust ODP in recipients of SST-depleted transplants (Figure 11, left; ODI = 0.23 ± 0.007 at baseline; ODI = 0.067 ± 0.02 at 4 d MD; Mann-Whitney test, $P < 0.01$). Given the abundance of literature supporting the notion of PV⁺ cells being crucial to critical period plasticity, we expected PV⁺ cells, which were present in normal numbers in SST-depleted transplants, to contribute to plasticity as well. The plasticity induced by SST-depleted transplants was as robust as that induced by control *R26-DTA* transplants; therefore the depletion of SST⁺ cells did not affect the induction or the strength of plasticity.

Interestingly, PV-depleted transplants also induced rapid and robust plasticity (Figure 11, middle; ODI = 0.22 ± 0.006 at baseline; ODI = 0.062 ± 0.017 at 4 d MD; Mann-Whitney test, $P < 0.0001$). On the other hand, recipients of PV-SST-depleted transplants, in which both PV⁺ and SST⁺ cells had been killed, did not show plasticity (Figure 11, right; ODI = 0.22 ± 0.007 at baseline; ODI = 0.22 ± 0.06 at 4 d MD; Mann-Whitney test, $P = 0.96$). This finding came as a surprise, as no other MGE-derived interneuron subtype has been definitively implicated in ODP. Comparing the plasticity induced by PV-depleted, SST-depleted, and control *R26-DTA* transplants, we found that all three types of transplants induced plasticity of similar magnitude (Figure 12). Therefore, MGE transplants retained their ability to induce plasticity as long as sufficient numbers of either PV⁺ or SST⁺ cells remained in the transplants.

Because the combined expression efficiency of Cre and DTA is not 100%, a few PV⁺ or SST⁺ cells were present in the selectively depleted transplants (Figure 13, middle and right, pink dots). PV⁺ cells, especially, are known to develop extensive axonal arbors with hundreds of postsynaptic targets, suggesting that a small population of PV⁺ cells might be sufficient to induce changes in circuitry. If, however, plasticity depended on PV⁺ cells alone, the required density would have to be greater than ~ 8 cells/mm² (Figure 13, middle, pink dots), the maximum density of PV⁺ cells in PV-SST-depleted transplants. The PV⁺ cell density in PV-depleted transplants (Figure 13, middle, blue dots), which induced plasticity, was always less than that of the PV-SST-depleted transplants, which did not induce plasticity. This finding makes it implausible that the small number of surviving PV⁺ cells in the was responsible for transplant-induced plasticity, though we couldn't rule out the possibility that they contributed to the plasticity induced by the normal numbers of SST⁺ cells in these PV-depleted transplants. Furthermore, when we pooled and examined all donor cell populations together, we found no correlation between the magnitudes of transplant-induced plasticity and the average densities of the surviving transplanted cells, of transplanted PV⁺ cells, or of transplanted SST⁺ cells (Figure

13, x-axis expanded logarithmically to display low cell densities). These results confirmed that MGE transplants with normal numbers of transplanted SST⁺ cells are sufficient to induce plasticity when more than 95% PV⁺ cells are depleted.

Plasticity induced by MGE transplants recapitulated key features of critical period plasticity

The maturation of GABAergic interneurons, specifically, the MGE-derived PV⁺ subtype, has been strongly implicated in critical period plasticity. It was therefore surprising that transplanted MGE interneuron precursors depleted of PV⁺ cells were still able to induce plasticity. One possible explanation is that MGE transplant-induced plasticity is not critical period plasticity, but merely an enhancement of adult ocular dominance plasticity. To test this hypothesis, we examined several features of plasticity that differentiate critical period from adult plasticity (Sato and Stryker, 2008). First, the onset of transplant-induced plasticity after only 4-5 days of deprivation is consistent with critical period plasticity and in contrast to adult plasticity, which takes 7-8 days of deprivation to produce significant ODI shifts. Second, transplant-induced plasticity was primarily driven by the loss of contralateral responsiveness, which is a key feature of critical period plasticity that is not observed in the adult form of ocular dominance plasticity (Figure 14). Finally, we examined whether these two features of transplant-induced ODP were affected by depletion of PV⁺ or SST⁺ cells. We found the degree of loss of contralateral response to be similar in recipients of PV-depleted, SST-depleted, and control *R26-DTA* transplants; it was also not influenced by the number of PV⁺ or SST⁺ cells in the transplant (Figure 15, x-axis expanded logarithmically). The plasticity induced by MGE transplants shares the rapid depression of contralateral response characteristic of critical period plasticity, and normal numbers of PV⁺ interneurons are not required for this phenomenon.

Section 3: Discussion

In experiments detailed in this chapter, we employed Cre-DTA to deplete PV⁺ or SST⁺ interneurons from cellular populations transplanted from the embryonic MGE. When MGE-derived interneuron precursors were genetically programmed to undergo apoptosis upon expression of Cre recombinase from the PV or SST locus, almost all the corresponding Cre-expressing interneurons were eliminated from the transplant population prior to the induction of plasticity. Despite the depletion of PV⁺ or SST⁺ cells, these transplants retained their ability to induce ocular dominance plasticity. Yet when both PV⁺ and SST⁺ populations were simultaneously eliminated, the remaining cells failed to induce plasticity. This suggests that either PV⁺ or SST⁺ cells must be present in normal numbers in the transplant for plasticity to occur. However, while both PV⁺ and SST⁺ cells are able to induce critical period-like ODP, other interneurons derived from the MGE appear not to be, as elimination of both PV and SST cells disrupted transplant-induced plasticity.

Studies over the last decade have suggested that PV⁺ cells play an exclusive role in initiating critical period ODP. For example, GABA_A receptors containing the $\alpha 1$ subunit, which is enriched at PV⁺ synapses, have been shown to play a particularly potent role in the opening of the critical period of ODP (Fagiolini et al., 2004). In other studies, manipulating factors that affect the maturation of PV⁺ cells also affected the opening of the critical period of ODP, including polysialylated neural cell adhesion molecule (PSA-NCAM), the homeoprotein transcription factor orthodenticle homolog 2 (Otx2), and insulin-like growth factor 1 (IGF-1) (Sugiyama et al., 2008; Ciucci et al., 2007; Di Cristo et al., 2007). Finally, depressing the activity of PV⁺ cells a few days after the critical period has been shown to increase plasticity in the primary visual cortex (Kuhlman et al., 2013). Consistent with these findings, our data support the capacity of PV⁺ cells to drive plasticity. However, our results are inconsistent with an exclusive role for PV⁺ cells in this process.

Our finding that transplants depleted of PV⁺ cells could also induce robust plasticity, but those depleted of both PV⁺ and SST⁺ cells could not, suggests that SST⁺ cells can also drive plasticity, a possibility that has largely been ignored. Although our findings are derived from the study of interneuron transplant-induced plasticity, they raise the possibility that SST⁺ cells may also regulate critical period plasticity. Indeed, in previous studies in which PV⁺ cells were manipulated to study their role in ODP, SST⁺ cells could have likewise been also affected.

Signals that are part of the immune response can affect plasticity in the visual pathway (Schafer et al., 2012; Stephan et al., 2013), including ODP (Datwani et al., 2009; Syken et al., 2006). While the diphtheria-toxin-mediated death of transplanted cells might stimulate an immune response, we did not observe plasticity following the depletion of both PV⁺ and SST⁺ cells in PV-SST-depleted transplants. Thus, the plasticity induced by PV-depleted and SST-depleted transplants was unlikely to result from the killing of transplanted cells or a nonspecific immune response from the host. Instead, plasticity appears to be a direct result of neural circuit modification induced by the integration of transplanted PV⁺ and SST⁺ cells into primary visual cortex.

By what common mechanism might transplanted PV⁺ and SST⁺ cells induce plasticity? Studies of connectivity show that transplanted MGE cells make and receive profuse connections, about 3 times as many as host inhibitory neurons at the peak of the transplant-induced critical period (Southwell et al., 2010). The intercalation of such new connections into a cortical circuit that has matured and would otherwise be stable to perturbations of visual input may be sufficient to push it out of its zone of stability. Any inhibitory neurons that made sufficiently profuse connections might then suffice to induce plasticity. Alternatively, PV⁺ and SST⁺ cells, but not the other cells of the MGE transplants, might contain factors that alter the extracellular matrix or influence peri-neuronal nets. Finally, PV⁺ and SST⁺ cells may be the only interneurons sensitive to imbalance of sensory input. There is indeed evidence that during the critical period,

PV⁺ cells rapidly reduce their activity levels following monocular deprivation, and artificial depression of PV⁺ cell activity for as little as 1 day is sufficient to recapitulate critical period-like plasticity in adult mice undergoing 3-day monocular deprivation (Kuhlman et al., 2013). Based on these observations, PV⁺ cells serve as a “sensor” of visual input imbalance by suppressing their firing rates and creating a temporary excitation-inhibition imbalance. Sustained depression of PV⁺ cell firing is not necessary, indicating that once the neural network is pushed past the threshold, other cells take over to drive plasticity. It’s possible that developing SST⁺ cells show the same rapid response to changes in visual input as PV⁺ cells but other interneurons do not. This scenario would explain several of our observations. If both PV⁺ and SST⁺ cells change activity patterns upon visual deprivation, then sufficient numbers of either “sensors” would be able to “alert” the network, hence the observation that depletion of either population does not abolish transplant-induced plasticity. If PV⁺ and SST⁺ cells only initiate plasticity and do not dictate its course or strength, then it’s logical that the density of transplanted PV⁺ and SST⁺ cells is not correlated to magnitude of plasticity. Sensitivity of endogenous PV⁺ cells to monocular deprivation seems to be a transient developmental phenomenon (Kuhlman et al., 2013), and it’s no surprise that MGE transplants lose ability to induce plasticity beyond the cellular age of 35 days (Southwell et al., 2010). Regardless of the actual mechanism, our delineation of which cell types can induce plasticity is an important step towards understanding the mechanism of transplant-induced plasticity.

Cortical plasticity plays important roles during normal development, and during recovery from disease or injury (Sharma et al., 2013; Hosp et al., 2011; Awaya et al., 1973). MGE transplantation is being developed as a promising method for modifying neural circuits in several disease states (Southwell et al., 2014). A delineation of the roles of different interneuron subtypes in transplant-induced plasticity will yield novel insights into the mechanisms

responsible for native critical period plasticity, while also guiding the therapeutic application of interneuron transplantation.

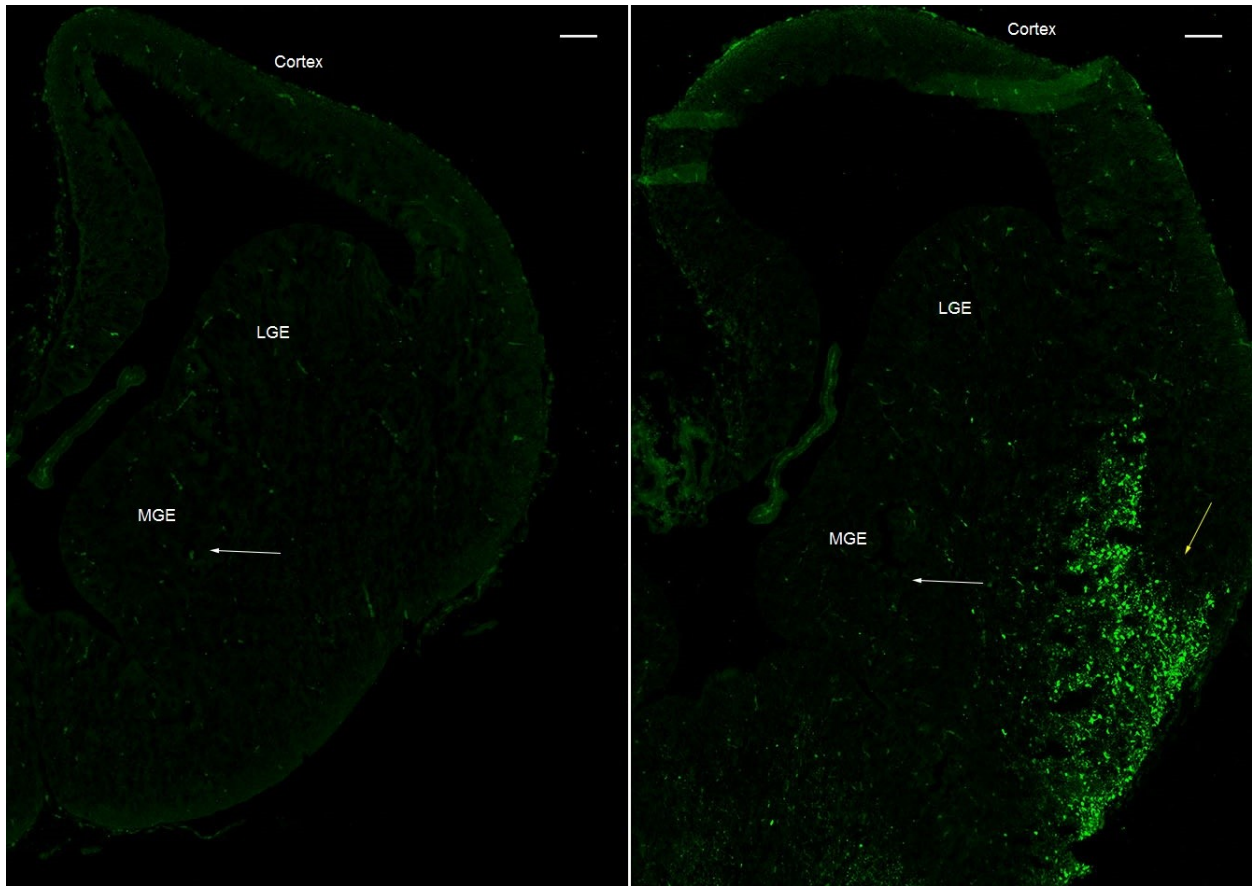


Figure 1. Lack of GFP expression in the MGE of Gin and G42 embryos at E13.5.

Coronal sections of Gin (left) and G42 (right) brains at E13.5 immunostained for GFP (green). Aside FROM scattered autofluorescence from blood vessels, the MGE (white arrows) of both strains lacked GFP signal. In the G42 brain, bright GFP+ cells were observed in the globus pallidus (yellow arrow) but none migrated towards the cortical plate. Scale bar: 100 μ m.

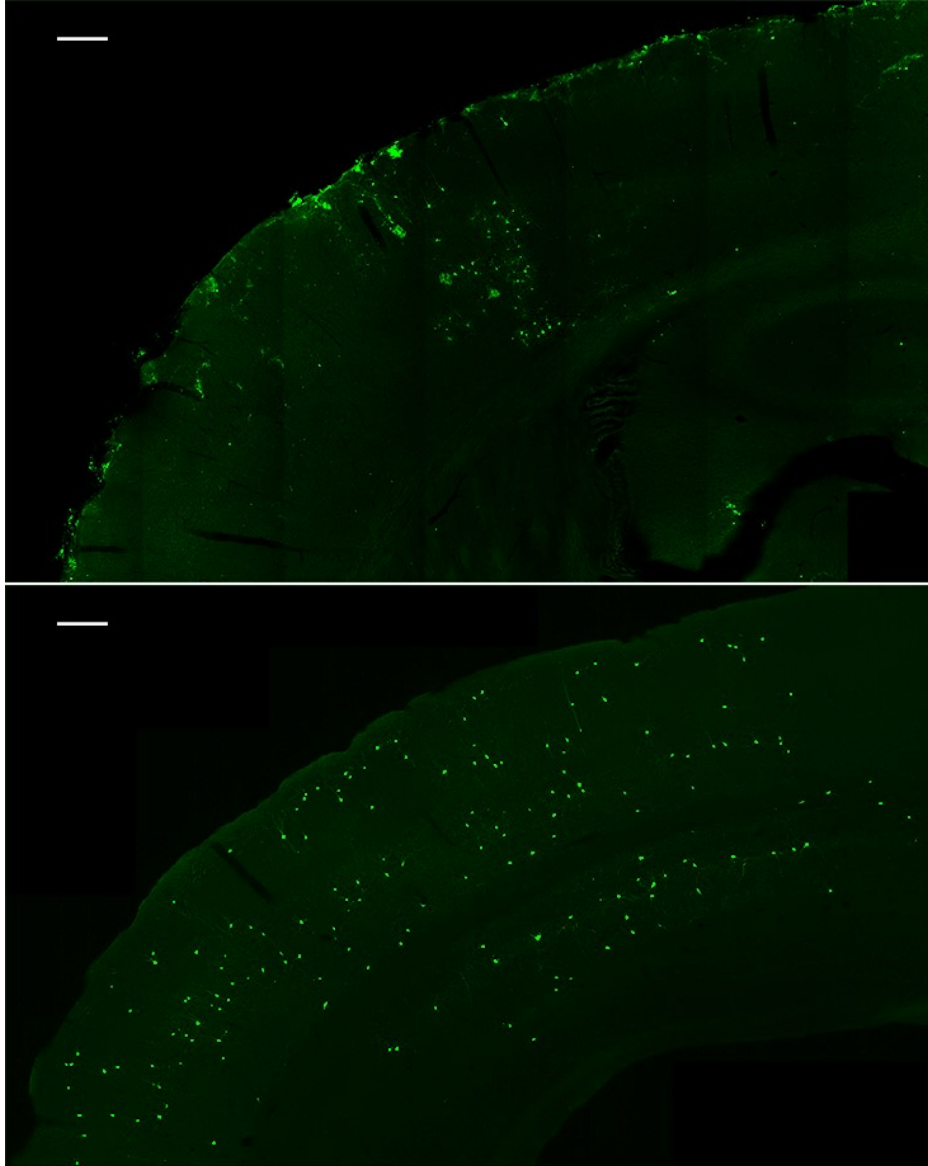


Figure 2. Transplanted P0 cortical cells have poor survival and migration.

Transplantation of dissociated P0 cortical cells (green) resulted in only a few surviving GFP⁺ cells in and around the injection site (top). In contrast, numerous GFP⁺ cells derived from transplanted MGE cells survived and dispersed widely throughout the host cortex (bottom).

Scale bar: 100 μ m.

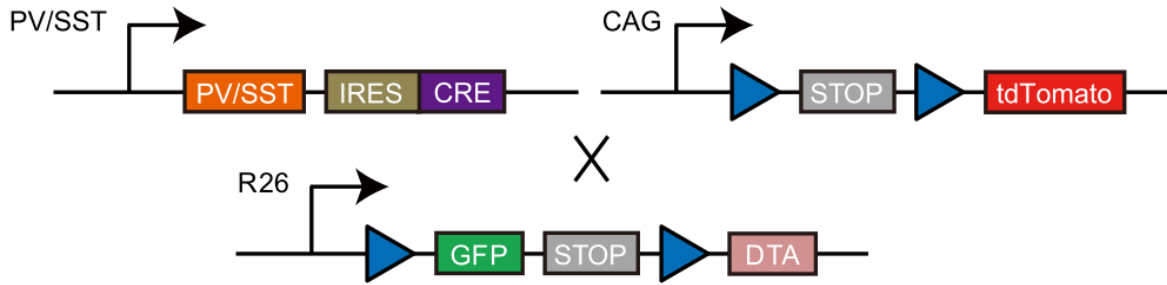
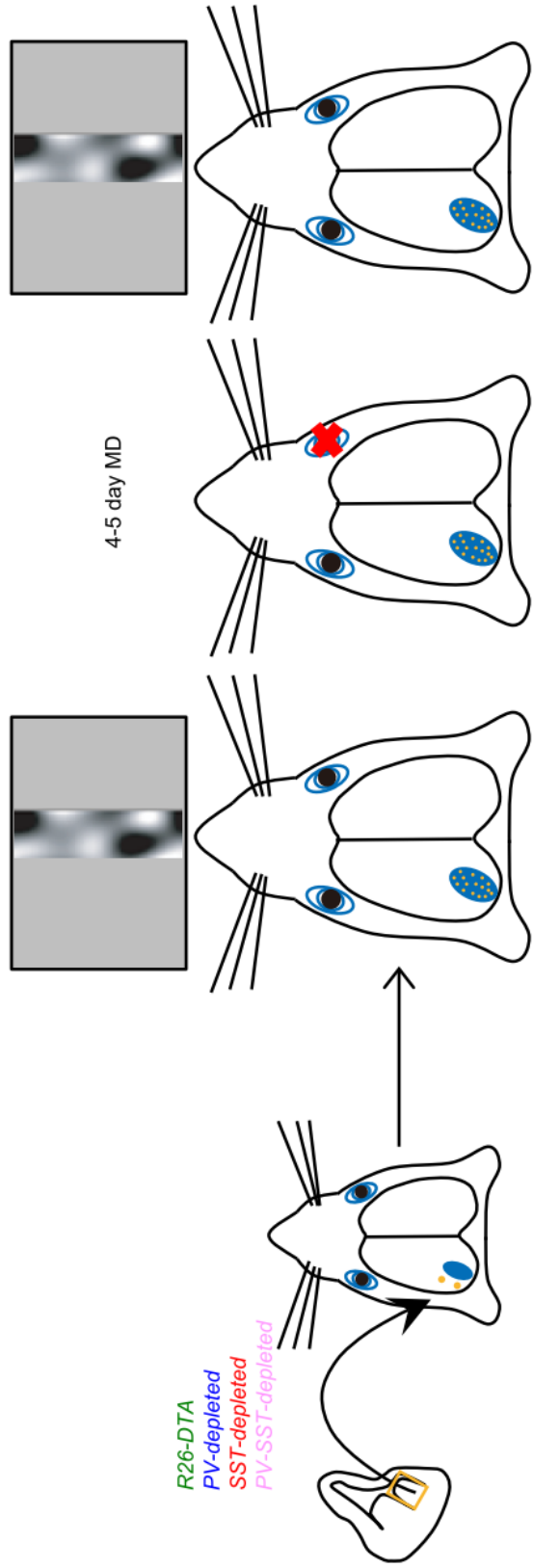


Figure 3. Genetic strategy of ablating PV⁺ and SST⁺ cells using Cre-induced expression of DTA.

Diagram of *PV-cre*, *SST-cre*, *R26-DTA*, and *Ai14* alleles. The *IRES-Cre* element is knocked into the 3' untranslated region of the endogenous *PV* or *SST* gene. The *R26-DTA* allele is a knock-in of the *Rosa26* locus with a stop cassette flanked by *loxP* sites (blue triangles). In the presence of the *Rosa26* locus with a stop cassette flanked by *loxP* sites (blue triangles). In the presence of Cre, the stop cassette is removed leading to DTA expression and cell death.. All Cre mice carry a Cre-dependent tdtomato reporter (*Ai14*) to label the few Cre-expressing cells in which *R26-DTA* failed to recombine.

Figure 4. MGE Transplantation and optical imaging of visual responses.

Interneuron precursors were dissected from MGEs of E13.5 embryos, dissociated, and transplanted into regions near the primary visual cortex of P7 postnatal mice. Recipient mice were allowed to develop for 33-35 days. They then underwent optical imaging to determine baseline ocular dominance index (ODI). Monocular deprivation (MD) was then performed on the contralateral eye for 4-5 days, after which the contralateral eye was reopened and another session of optical imaging was conducted to determine ODI post MD.



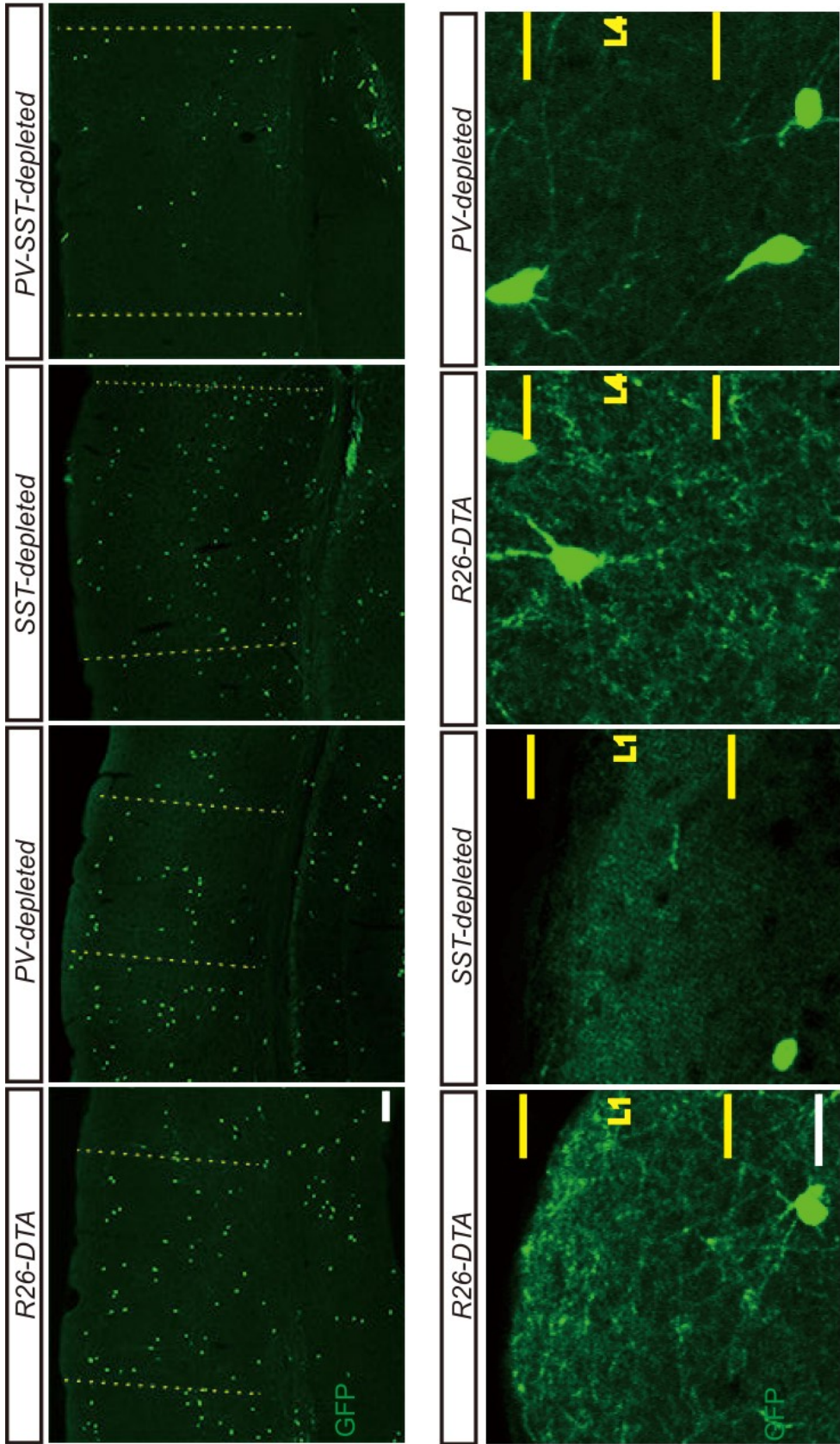
P40-42 (33-35DAT)

P7 (0DAT)

E13.5

Figure 5. Cre-induced expression of DTA ablates PV⁺ and SST⁺ cells along with their layer-specific projections.

Top panel: Cells in all transplants disperse widely in the binocular visual cortex (marked by dotted yellow lines). Bottom panel: Dense innervation of layer 1 by SST⁺ Martinotti cells and layer 4 by PV⁺ basket cells is significantly reduced upon their respective ablation. Scale bar: (top) 100 μm . (bottom) 25 μm .



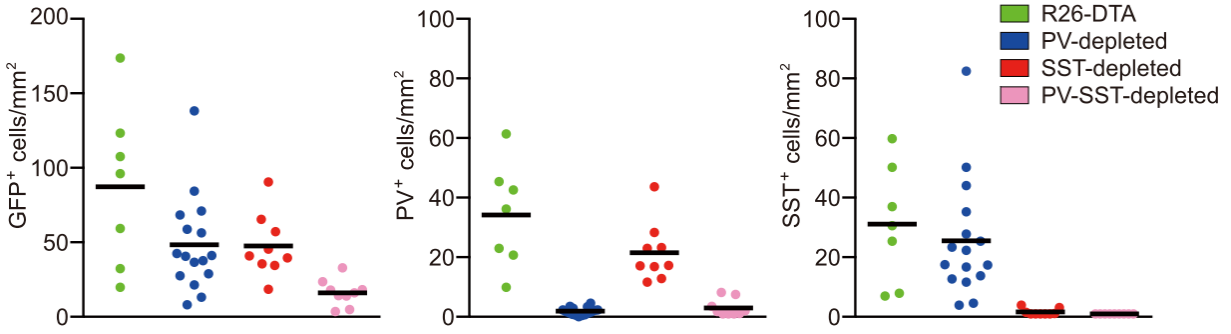


Figure 6. Depletions of PV⁺ and SST⁺ cells are efficient and do not affect the absolute population size of each other in the transplant.

Density (cells/mm²) of total GFP⁺ cells (left), PV⁺ cells (middle) and SST⁺ cells (right) in R26-DTA (green dots, $n = 7$), PV-depleted (blue dots, $n = 16$), SST-depleted (red dots, $n = 9$) and PV-SST-depleted (pink dots, $n = 9$) transplants. The densities of PV⁺ cells in R26-DTA and SST-depleted transplants are comparable (middle, green dots vs. red dots; Mann-Whitney, $P = 0.38$). Likewise, the densities of SST⁺ cells in R26-DTA and PV-depleted transplants are similar as well (right, green dots vs. blue dots; Mann-Whitney, $P = 0.21$). Horizontal bars indicate mean.

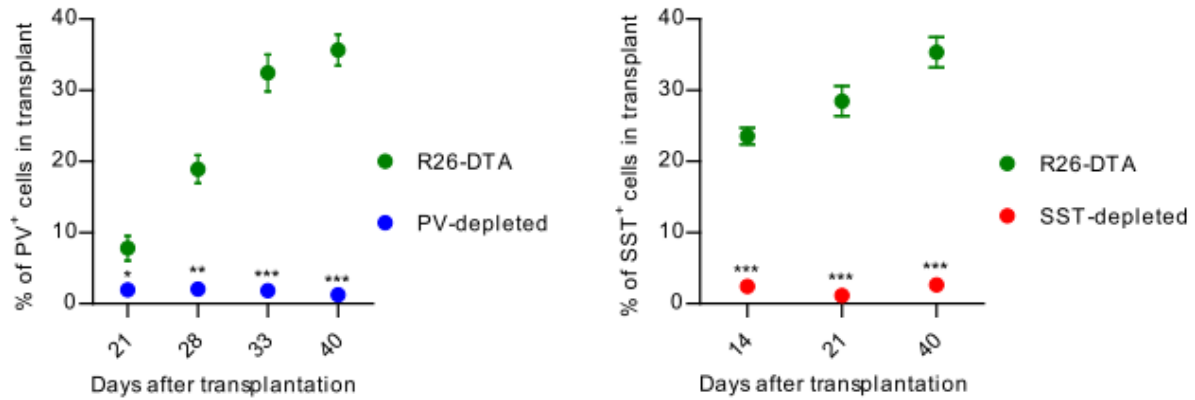


Figure 7. PV-depleted and SST-depleted transplants consist of low percentages of PV⁺ and SST⁺ cells, respectively, throughout development.

(Left) PV-depleted transplants (blue dots) contained few PV⁺ cells compared to *R26-DTA* control transplants (green dots) at 21 days after transplantation (DAT), the earliest time point when PV expression is detectable by immunofluorescence. (Right) Likewise, the percentage of SST⁺ cells in SST-depleted transplants (red dots) was significantly lowered compared to that of *R26-DTA* transplants (green dots) as early as 14 DAT, and remained consistently low throughout development. In both panels, error bars represent SEM. $n = 3$ per time point per transplant type. * $P < 0.05$, ** $P < 0.01$, *** $P < 0.001$, unpaired two-tailed t test.

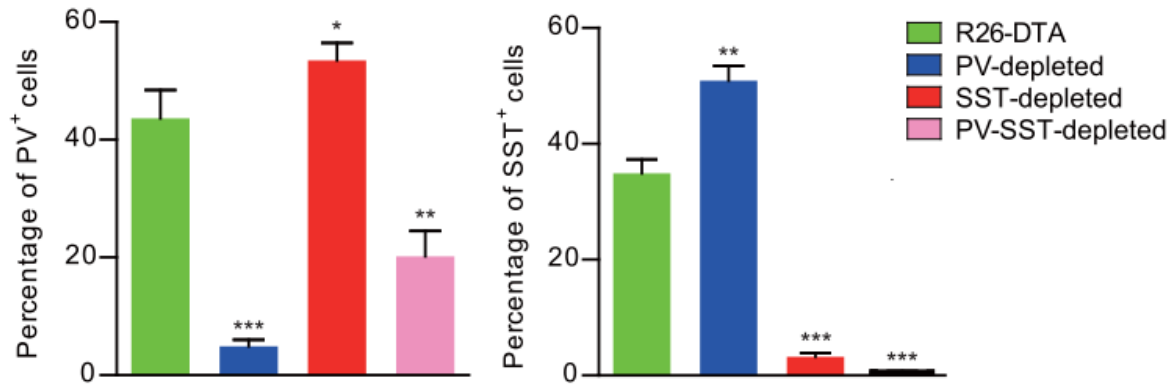


Figure 8. Efficient depletions of PV⁺ and SST⁺ cells cause reciprocal increase in the percentage of each other in the transplant.

(Left) Compare to *R26-DTA* transplants (green bar), the proportion of PV⁺ cells is extremely low in PV-depleted (blue bar), and relatively enriched in SST-depleted transplants (red bar). A few PV⁺ cells remain in PV-SST-depleted transplants (pink bar), but the absolute PV⁺ cell density is very low and comparable to that found in PV-depleted transplants (see Figure 6). (Right) Similarly, SST⁺ cells have been largely eliminated from SST-depleted transplants (red bar), but account for the majority of cells in PV-depleted transplants (blue bar). In both panels, $n = 7$ for R26-DTA, $n = 16$ for PV-depleted, $n = 9$ for SST-depleted, and $n = 9$ for PV-SST-depleted.

* $P < 0.05$, ** $P < 0.01$, *** $P < 0.001$, unpaired two-tailed t test.

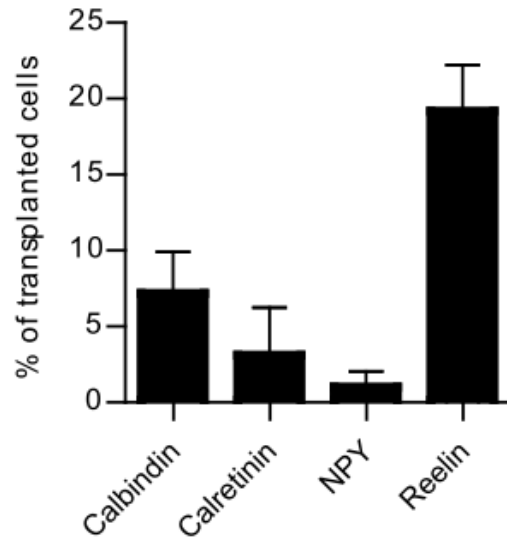


Figure 9. Marker expression of the surviving cells in PV-SST-depleted transplants.

Quantification of interneuron markers calbindin, calretinin, neuropeptide Y (NPY) and reelin expression in PV-SST-depleted transplants at 40 DAT. Error bars represent SEM. *n* = 4 animals.

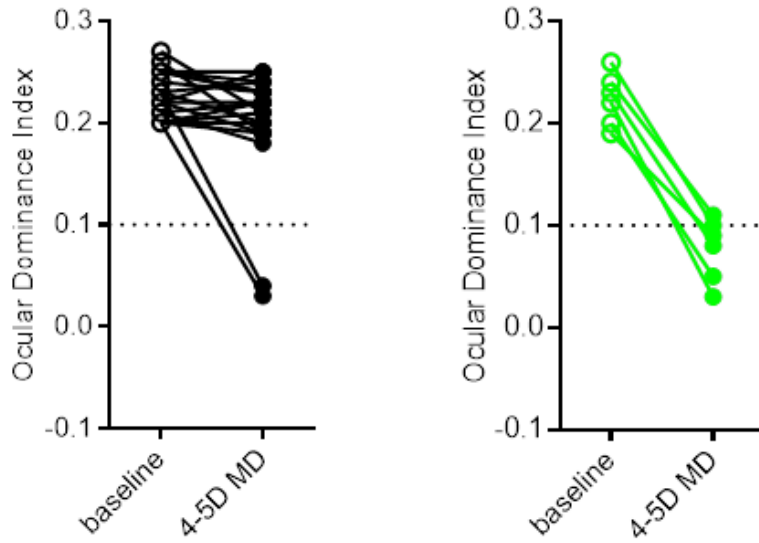


Figure 10. Ocular dominance plasticity is induced by *R26-DTA* transplants, but not dead MGE cells.

Ocular dominance index (ODI) at baseline and after 4-5 days of monocular deprivation (MD) of the contralateral eye in recipients of dead cells (left, $n = 9$) and *R26-DTA* (right, $n = 7$) transplants. Lower values of ODI after deprivation indicate greater plasticity. Dotted line at 0.1 indicates threshold for plasticity.

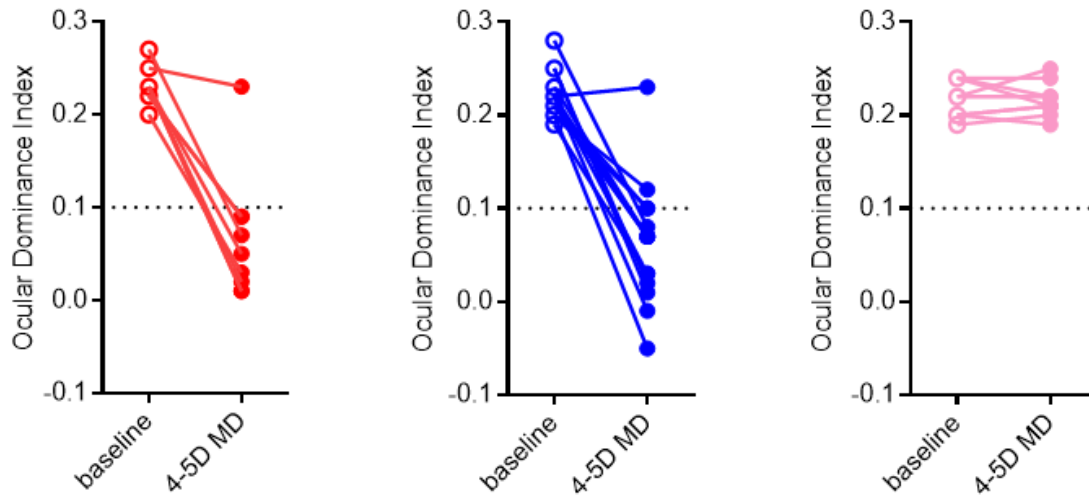


Figure 11. MGE transplants depleted in PV⁺ or SST⁺ cells, both not both, are capable of inducing plasticity.

Ocular dominance index (ODI) at baseline and after 4-5 days of monocular deprivation (MD) of the contralateral eye in recipients of SST-depleted (left, $n = 9$), PV-depleted (middle, $n = 16$) and PV-SST-depleted (right, $n = 9$) transplants. Lower values of ODI after deprivation indicate greater plasticity. Dotted line at 0.1 indicates threshold for plasticity.

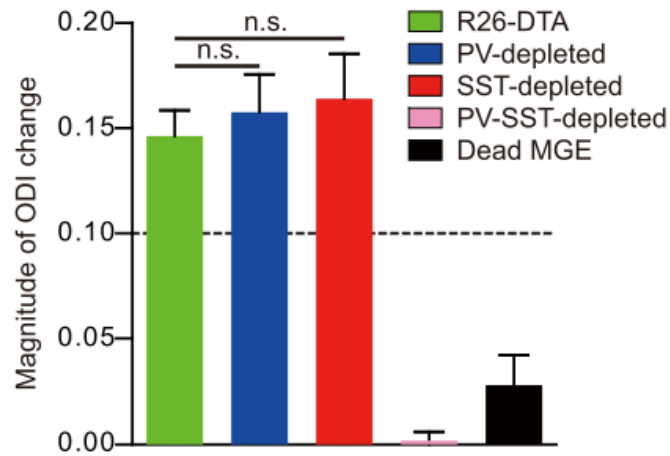


Figure 12. Change in ODI is similar among *R26-DTA*, PV-depleted, and SST-depleted transplants.

The magnitude of plasticity (baseline ODI – post-MD ODI) induced by *R26-DTA* (green bar, $n = 7$), PV-depleted (blue bar, $n = 16$), and SST-depleted (red bar, $n = 9$) transplants is statistically indistinguishable from each other. Error bars represent SEM. Line at 0.1 indicates threshold for plasticity. n.s., not significant (one-way ANOVA and Bonferroni post hoc test).

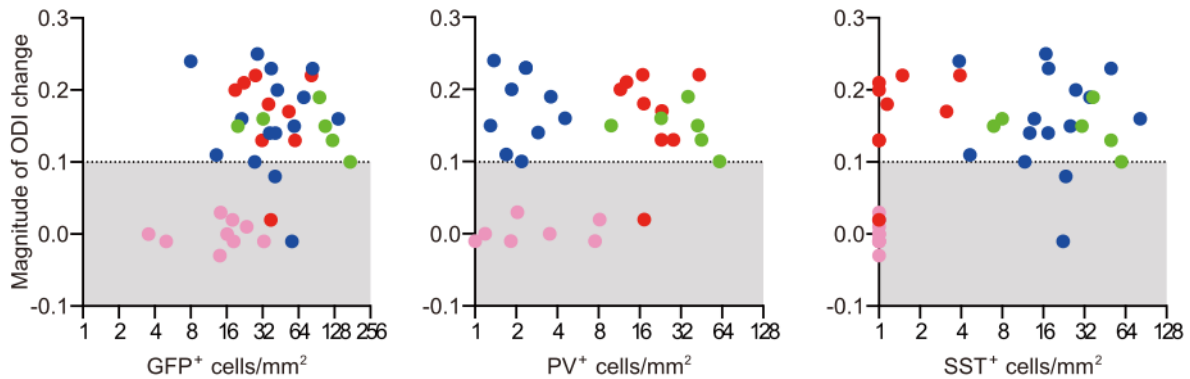


Figure 13. Magnitude of plasticity induced by MGE transplants is not related to the density of total GFP⁺ cells, PV⁺ cells, or SST⁺ cells.

Magnitude of ODI change (baseline - MD) plotted against cell density revealed that the plasticity induced is consistent (between 0.1-0.2) throughout the range of transplant cell densities. The strength of plasticity is not related to the density of total GFP⁺ cells (left, $n = 39$, slope = 0.0006, $r^2 = 0.07$, n.s.), PV⁺ cells (middle, $n = 39$, slope = 0.0012, $r^2 = 0.05$, n.s.), or SST⁺ cells (right, $n = 39$, slope = 0.0013, $r^2 = 0.08$, n.s., linear regression analysis). x-axis expanded logarithmically. Shaded region indicates little or no plasticity.

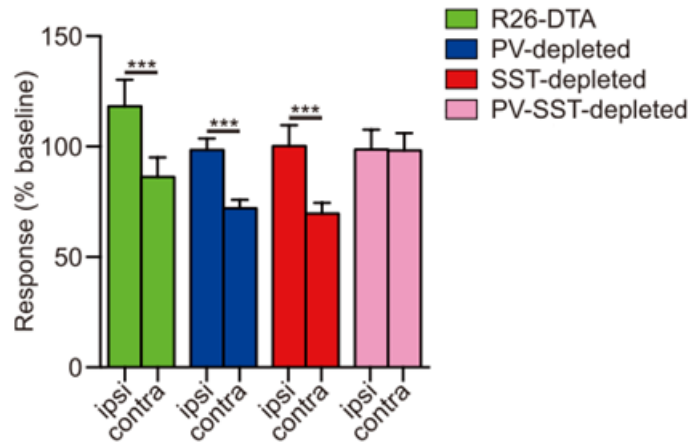


Figure 14. Critical period-like characteristics of transplant-induced plasticity.

Changes in magnitude of ipsilateral and contralateral responses after MD deprivation, expressed as percentage of pre-MD baseline values, in *R26-DTA* (green bars, $n = 7$), PV-depleted (blue bars, $n = 14$), SST-depleted (red bars, $n = 9$) and PV-SST-depleted (pink bars, $n = 9$) transplants. Recipients of the three types of transplants that induced plasticity show marked depression of contralateral responses with moderate to no change in ipsilateral responses (green, blue, and red bars). Error bars represent SEM *** $P < 0.001$ (Mann-Whitney-Wilcoxon rank-sum test).

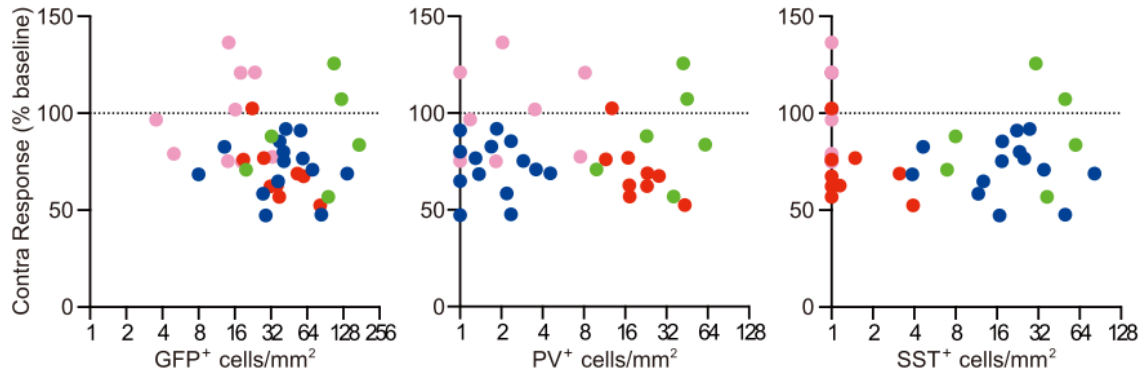


Figure 15. Depression of contralateral responses is not correlated with the density of total GFP⁺ cells, PV⁺ cells, or SST⁺ cells.

Change in magnitude of contralateral response is unrelated to density of total GFP⁺ cells (left, $n = 39$, slope = -0.045, $r^2 = 0.0066$, n.s.), PV⁺ cells (middle, $n = 39$, slope = 0.011, $r^2 = 0.00006$, n.s.), or SST⁺ cells (right, $n = 39$, slope = -0.1085, $r^2 = 0.01$, n.s., linear regression analysis).

Dotted line indicates 100% of baseline.

Migration, Differentiation, and Induction of Cortical Plasticity by Transplanted CGE Cells

Section 1: Introduction

In the previous chapter, I described the finding that both PV⁺ and SST⁺ subtypes of interneurons derived from the MGE are capable of inducing plasticity. This is surprising—most previous studies of ocular dominance plasticity (ODP) only identified PV⁺ interneurons as a vital component of critical period ODP (Hensch et al., 1998; Di Cristo et al. 2007; Sugiyama et al., 2008; Miyata et al., 2012). It has been proposed that PV⁺ cells gate plasticity through their powerful and widespread perisomatic innervation that control large populations of pyramidal cells (Fagiolini et al., 2004). Indeed, the maturation of perisomatic innervation coincides with the beginning of the critical period, and brief decreases in PV⁺ cells activity are sufficient to reintroduce a second period of heightened ODP in post-critical period mice (Chattopadhyaya et al., 2004; Sugiyama et al., 2008). However, we have determined in Chapter 3 that critical-period-like ODP can be induced by transplantation of either PV⁺ cells, which innervate the soma of target cells, or SST⁺ cells, which target the distal dendrites (Chapter 3, Figure 11; Makram et al., 2004). Thus, the notion that PV⁺ cells and their perisomatic innervation possess the unique ability to induce ODP is called into question. Furthermore, this finding raises the possibility that other non-perisomatic innervating, PV-negative interneurons can induce plasticity as well.

In the forebrain, PV⁺ and SST⁺ cells are not the only subtypes of interneuron that populate the cortex; nor is MGE the only germinal zone from which cortical interneurons are derived. CGE, another major embryonic germinal zone in the ventral telencephalon that is caudal to the LGE and the MGE, gives rise to about 30% of the interneurons in the cortex (Butt et al., 2007; Miyoshi et al., 2010). Most CGE-derived interneurons do not express PV or SST; rather, they are positive for a wide array of cellular marker proteins such as reelin, calretinin, calbindin, neuropeptide Y (NPY), and vasoactive intestinal peptide (VIP) (Nery et al., 2002; Miyoshi et al., 2010; Lodato et al., 2011). These cells contribute to the inhibitory control of neural networks in the forebrain, and their loss has been shown to induce epilepsy in mice (Cobos et al., 2005). Nevertheless, a more in-depth understanding of the function of CGE-derived cortical interneurons has been largely lacking. Specifically, we do not know if CGE-derived interneurons can remodel existing neural networks and induce cortical plasticity like MGE-derived cells do. Given that CGE-derived interneurons are distinct from their MGE-derived counterparts in origin, expression of cellular markers, and patterns of innervation, I set out to test their ability to induce plasticity. The results will help define the characteristics of cortical interneurons that can induce plasticity. For example, are plasticity-inducing interneurons only generated from a certain germinal zone (MGE vs. CGE)? Is subtype identity defined by cellular marker expression predictive of the cells' ability to induce plasticity? Besides SST⁺ cells, can other non-perisomatic-innervating interneurons induce plasticity? This work was done again in collaboration with Sebastian Espinosa from the Stryker Lab. Here we present the finding that transplanted CGE-derived cells migrate extensively in the cortex, occupying all layers of the cortex including layer 1, which MGE-derived cells generally avoid. CGE transplants differentiate into reelin⁺, calretinin⁺, calbindin⁺, NPY⁺, and VIP⁺ cells, all of which are known to derive from the CGE during normal inhibitory neurogenesis. Finally, we found that CGE transplants contain a small population of PV⁺ and SST⁺ cells, and these cells are required for CGE transplants to induce plasticity.

Section 2: Results

Dissection and transplantation of the dorsal CGE

Being the second largest source of cortical GABAergic interneurons, CGE cells have rarely been transplanted and the transplants have not been thoroughly characterized. One reason might be the difficulty in performing consistent and efficient dissection of CGE. The tails of LGE and MGE extend caudally and merge to form the rostral region of CGE, and there are no clear anatomical distinctions that allow for a clean separation of the three germinal structures (Wonders and Anderson, 2006). The caudal CGE gradually transits into the developing caudal cortical plate that is, again, difficult to precisely identify and avoid. Dissections that went too caudal in an effort to minimize MGE contamination resulted in mostly cortical tissue and very poor engraftment (Figure 1B, top panel). For all subsequent experiments we dissected the dorsal part of the ganglionic eminences caudal to the LGE-MGE sulcus to minimize contamination by the caudal MGE while ensuring that the majority of tissues harvested were from regions within the ganglionic eminences corresponding to the presumed dorsal CGE (Figure 1B, bottom panel). Some of the tissues in these dissections may be from the caudal extension of the dorsal LGE, but LGE cells neither migrate effectively in the cortex post transplantation nor induce plasticity (Wichterle et al., 1999; Southwell et al., 2010). Therefore possible contaminating LGE cells would not influence either the composition of dispersed transplanted cells or the assessment of plasticity.

Transplanted CGE cells migrate extensively in the cortex and show a specific pattern of layer occupation

Transplantation of cells dissected from the dorsal CGE resulted in successful engraftment and extensive migration of cells throughout the host visual cortex. Rostral-caudally, transplanted CGE cells and MGE cells can both disperse through the entire length of the mouse cortex (about 4.5mm collected in coronal sections). The dorsal-ventral dispersion of transplanted CGE cells is also similar to that observed in transplanted MGE cells (Figure 2, $n = 5$, Mann-Whitney test, $P = 0.94$). However, we did notice several differences between CGE and MGE cells. One was that CGE cells occupy all layers of the cortex, including layer 1, which MGE cells usually stay clear of (Figure 3). To determine the precise layer distribution of CGE and MGE cells, we performed immunostaining of *satb2* and *ctip2* on coronal sections of host cortex engrafted with CGE or MGE cells. *Satb2* is a homeobox gene expressed preferentially in neurons in the cortical layers 2/3 and 4, and *Ctip2* is a zinc finger protein expressed in layers 5 and 6 (Molyneaux et al., 2007; Britanova et al., 2008; McKenna et al., 2011). Co-staining for these proteins and *GFP* allowed for visualization of the layer position of transplanted cells (Figure 4A). Comparing MGE transplants to CGE transplants, we found no difference in percentages of cells that end up in the deep layers (4 to 6) (Figure 4B, $n = 3$, Mann-Whitney test, $P = 0.99$ for layer 4, $P = 0.99$ for layer 5, $P = 0.67$ for layer 6). In contrast, there was a trend towards more transplanted CGE cells in layer 1, with a compensatory decrease of CGE cells in layer 2/3 (Figure 4B, $n = 3$, Mann-Whitney test, $P = 0.05$ for layer 1, $P = 0.3$ for layer 2/3). Immunostaining showed that many transplanted CGE cells in layer 1 were *reelin*⁺ (Figure 4C). This is consistent with what has been reported on cortical interneuron development, that CGE is the source of interneurons in layer 1 (Miyoshi et al., 2010; Rudy et al., 2011).

Transplanted CGE cells differentiate into interneurons expressing diverse cellular markers

Using immunohistochemistry, we determined that CGE transplants contained 40% of *reelin*⁺ cells, 20% each of *VIP*⁺ and *calretinin*⁺ cells, and around 10% each of *NPY*⁺ and

calbindin⁺ cells (Figure 5 & 6). These subtypes of interneurons are known to derive from the CGE during development (Nery et al., 2002; Butt et al., 2005; Lee et al., 2010; Lodato et al., 2011). However we also detected 8-10% each of PV⁺ and SST⁺ cells. The presence of these cells could be due to contamination by MGE cells during dissection, but could also be the result of MGE-derived neuroblasts migrating through CGE to reach caudal cortex. A common cellular marker expressed by virtually all CGE-derived interneurons but not by MGE-derived cells is 5-hydroxytryptamine receptor 3A (5-HT_{3A}R), a serotonergic ionotropic receptor (Férezou et al., 2002; Inta et al., 2008; Lee et al., 2010). However, no reliable antibody exists for this receptor, and we could not use this CGE marker to determine if the PV⁺ and SST⁺ cells were derived from the CGE. Instead we decided to identify the cells in our CGE transplants that were derived from the MGE. We dissected and transplanted CGE cells from Nkx2.1-cre;Ai14;actin-GFP embryos. Nkx2.1 is a transcription factor expressed in the MGE but not the CGE (Corbin et al., 2003; Xu et al., 2004; Du et al., 2008; Gelman and Marin, 2010), therefore all MGE-derived cells in these transplants would express red tdTomato protein from the Ai14 locus, but CGE-derived cells would only be labeled green with the ubiquitous actin-GFP allele. Co-staining of GFP, tdTomato, PV and SST revealed that 100% of PV⁺ cells and 95% of SST⁺ cells in these CGE transplants were tdTomato⁺ and therefore MGE in origin (Figure 7). These results support the most recent literature indicating that CGE is not a source of cortical PV⁺ or SST⁺ cells. Overall, the subtype profile of CGE transplants is distinct from what is observed following MGE transplantation (Figure 6), confirming that these cells indeed derived from separate neurogenic regions.

Reelin⁺ cells are found in both MGE and CGE transplants, but differ in marker co-expression and layer distribution

Upon staining for reelin, it became apparent that reelin⁺ cells represent a significant percentage of both MGE and CGE transplants (Figure 6). To determine if MGE-derived and CGE-derived reelin⁺ cells belong to the same subtype, we characterized their marker co-

expression and layer distribution. While PV⁺ cells do not readily express other common interneuron markers, SST⁺ cells are known to co-express a wide variety of cellular markers (Wonders and Anderson, 2006; Rudy et al., 2011). Indeed, over 85% of the reelin⁺ cells in MGE transplants co-expressed SST. In contrast, only about 10% of CGE-derived reelin⁺ cells were SST⁺ (Figure 8). Another distinction was the layer distribution of MGE and CGE derived reelin⁺ cells. Numerous CGE-derived reelin⁺ cells were found in layer 1, but MGE-derived reelin⁺ cells only occupied layers 2 to 6 (Figure 9). Therefore, reelin⁺ cells in MGE and CGE transplants likely represent two subclasses of reelin⁺ interneurons that are different in biochemical profiles and form networks with neurons that reside in different cortical layers.

CGE transplants induce ocular dominance plasticity only in the presence of MGE-derived PV⁺ and SST⁺ cells

To determine whether CGE transplants induce plasticity, we subjected recipients of transplanted CGE cells to the same intrinsic signal imaging and monocular deprivation experiments described for MGE transplant recipients in Chapter 3. After transplantation of dissected CGE precursors into the visual cortex of P7 recipients, we let the cells mature for 33-35 days before assessing their ocular dominance, both at baseline and after 4-5 days of contralateral deprivation. We found that recipients of CGE transplants demonstrated robust ocular dominance plasticity that was indistinguishable in magnitude or time of onset from plasticity induced by MGE transplants (Figure 10B, $n = 9$ for CGE, $n = 6$ for MGE, Mann-Whitney, $P = 0.71$). When we probed the changes of cortical responses to each of the eyes, we found that, similar to MGE-induced ODP, ODP induced by CGE transplants was also driven by depression of the response to visual stimulation of the contralateral eye (Figure 10C, $n = 9$, Mann-Whitney, $P = 0.33$ for ipsilateral responses, $P < 0.0001$ for contralateral responses). These findings strongly suggest that CGE transplants are able to induce critical period-like plasticity, but we cannot rule out the possibility that the PV⁺ and SST⁺ cells introduced by MGE

contamination were solely responsible for driving plasticity. We showed in Chapter 3 that a few PV⁺ and SST⁺ cells were left in PV-cre;SST-cre;R26-DTA (PV-SST-depleted) MGE transplants depleted of PV⁺ and SST⁺ cells, but they did not induce plasticity. However, the densities of both PV⁺ and SST⁺ populations were several folds higher in CGE transplants than in PV-SST-depleted MGE transplants (Figure 11, mean PV⁺ cell density is 8.14/mm² for *R26-DTA* CGE and 3.00/mm² for PV-SST-depleted MGE; mean SST⁺ cell density is 7.29/mm² for *R26-DTA* CGE and 0.004/mm² for PV-SST-depleted MGE). To assess the true plasticity-inducing potential of CGE cells, these contaminants that are known to induce plasticity need to be depleted to levels at or below those found in PV-SST-depleted MGE transplants, which do not induce plasticity.

To remove the small but potentially influential population of MGE-derived cells from CGE transplants, we transplanted dissections of dorsal CGE from PV-cre;SST-cre;R26-DTA (PV-SST-depleted) embryos, and assessed their ability to induce plasticity. The small population of PV⁺ and SST⁺ cells would be ablated by Cre-mediated DTA expression, but the majority of the CGE cells should survive. We found that in PV-SST-depleted CGE transplants, the densities of PV⁺ and SST⁺ cells in PV-SST-depleted CGE transplants were comparable to those found in PV-SST-depleted MGE transplants (Figure 11). Despite excellent engraftment and dispersion, PV-SST-depleted CGE transplants failed to induce plasticity (Figure 12). Therefore, it's the density of PV⁺ and SST⁺ cells, not the total density of transplanted cells that dictates whether transplants are competent at inducing plasticity. These findings indicate that CGE-derived interneurons do not contain PV⁺ or SST⁺ cells and do not possess the ability to induce plasticity.

Section 3: Discussion

The CGE is the second largest source of cortical GABAergic interneurons in mice, but CGE inhibitory progenitors have not been transplanted or characterized as extensively as their

MGE counterparts have been. We transplanted micro-dissected dorsal CGE cells and determined that similar to transplanted MGE cells, CGE-derived inhibitory progenitors survive, migrate, and differentiate into interneurons in the postnatal mouse cortex. The extensive dispersion of CGE cells into all six cortical layers was particularly impressive, considering that MGE cells usually only reside in layers 2 to 6. Because MGE and CGE together produce the overwhelming majority of cortical interneuron population and subtypes (Nery et al., 2002; Xu et al., 2004; Rudy et al., 2011), our findings indicate that most inhibitory neuroblasts destined for the cortex have the potential to survive in a heterochronic host brain, penetrate the host brain parenchyma, and disperse over long distances.

After migration was complete, cells from CGE transplants displayed morphologies and cellular markers of mature interneurons. Unlike MGE transplants, the majority of these cells did not stain positive for PV or SST. Instead, they expressed reelin, VIP, NPY, calretinin, and calbindin, all of which are cellular markers known to be expressed by cortical interneurons derived from the CGE (Nery et al., 2002; Miyoshi et al., 2010). Among these subtypes, reelin⁺ cells represented the biggest population, comprising approximately 40% of cells in CGE transplants. Interestingly, we also found that 24% of cells in MGE transplants expressed reelin, which makes reelin the third most highly expressed marker by MGE cells, after PV and SST. However, MGE- and CGE-born reelin⁺ cells do not seem to be identical. It has been reported that MGE-derived reelin⁺ cells are actually a subset of SST⁺ cells, and indeed we found 80% of reelin⁺ cells in MGE transplants to co-express SST (Lee et al., 2010). In contrast, only about 10% of reelin⁺ cells in CGE transplants expressed SST, and many of these CGE-derived reelin⁺/SST⁻ cells migrated to layer 1, a region that MGE cells do not usually occupy. Together, these findings indicate that CGE- and MGE-derived reelin⁺ cells do not share the same biochemical or positional profile and likely belong to different subclasses of reelin⁺ cortical interneurons. Calretinin⁺, Calbindin⁺, and NPY⁺ cells were also found in both MGE and CGE transplants,

although those derived from the MGE are thought to be subclasses of SST⁺ cells (Wonders and Anderson, 2006; Lodato et al., 2011). Finally, VIP⁺ cells, which are generated almost exclusively from the CGE during development (Lee et al., 2010; Miyoshi et al., 2010; Vucurovic et al., 2010), were found to be 20% of CGE transplants but were hardly present in MGE transplants.

Curiously, we found around 10% each of PV⁺ and SST⁺ cells in CGE transplants. Because *Nkx2.1* specifies MGE identity and is required for the proper development of PV⁺ and SST⁺ cells (Sussel et al., 1999; Butt et al., 2008; Du et al., 2011), we used a reporter driven by *Nkx2.1-cre* to label any MGE cell in CGE transplants. We found that almost all PV⁺ and SST⁺ cells in our CGE transplants were Nkx2.1⁺, and thus not derived from the dorsal CGE. These PV⁺ and SST⁺ cells probably made their way into the CGE transplants via two routes: as Nkx2.1⁺ ventral CGE tissue attached to the dorsal CGE dissections, and/or as individual MGE interneurons migrating through the CGE to reach the caudal cortex (Butt et al., 2007). Overall, CGE transplants are comprised of a diverse panel of interneurons subtypes, with reelin⁺ cells being the most numerous. Most of these interneuron populations, including the VIP⁺ cells, are expected from this germinal zone (Miyoshi et al., 2010).

Given the drastically different subtype profiles of MGE and CGE transplants, testing CGE transplants for plasticity could yield valuable information regarding how broadly applicable the plasticity-inducing ability of PV⁺ and SST⁺ cells is to other interneuron subtypes generated from a different germinal region. Initially, our results indicated that CGE transplants are capable of inducing plasticity. Further scrutiny revealed that the speed and magnitude of plasticity induced by CGE transplants were identical to those observed in MGE-transplant-induced plasticity. Finally, plasticity induced by CGE transplants is entirely explained by the depression of response to the contralateral eye, similar to the plasticity induced by MGE transplants. However, up to 20% of these CGE transplants expressed PV or SST, which correlated to an average of about 8 PV⁺ or SST⁺ cells per mm² of host binocular visual cortex. These cell

densities fell within the range of PV⁺ and SST⁺ cell densities in MGE transplants that induced plasticity (Chapter 3, Figure 13). When we transplanted PV-SST-depleted CGE, these transplants failed to induce plasticity. Because plasticity is eliminated following the depletion of PV⁺ and SST⁺ cells, we conclude that PV- SST-negative interneurons, even in large numbers, do not induce plasticity (see Figure 12). The plasticity observed in recipients of non-depleted CGE transplants is in fact due to the presence of PV⁺ and SST⁺ cells from the MGE.

Our study of transplanted CGE cells has provided several key pieces of information regarding transplant-induced plasticity and interneuron transplantation in general. Our data have established that transplanted interneuron precursors from both MGE and CGE migrate vigorously in the postnatal cortex. In the mouse brain, these two germinal regions give rise to greater than 90% of cortical interneurons and almost all the cortical interneuron subtypes (Sussel et al., 1999; Butt et al., 2007; Fogarty et al., 2007; Miyoshi et al., 2010; Rudy et al., 2011). In addition to MGE-derived PV⁺ and SST⁺ cells, CGE-derived interneuron subtypes can now be explored for their functional contribution to the neural network of a heterochronic recipient brain. Transplanted MGE cells has been shown to effectively increase inhibition and suppress seizure activity in models of both genetic and injury-induced epilepsy (Alvarez-Dolado et al., 2006; Baraban et al., 2009; Hunt et al., 2013). If transplanted CGE cells can generate inhibitory output and therapeutic outcome similar to MGE cells, it would significantly expand the candidate interneuron subtypes suitable for cell therapy. In some instances, CGE may actually be the preferred source of cells for transplantation. For example, CGE transplants contain more calretinin⁺ cells (19%) than MGE transplants (4%, see Figure 6), a cell type that has been shown to be particularly vulnerable in Alzheimer's disease and epilepsy (Baglietto-Vargas et al., 2010; Barinka and Druga, 2010; Tóth and Maglóczy, 2014). Therefore, CGE transplants will be better suited to investigating the role of calretinin⁺ cells in these diseases or replenishing calretinin⁺ cells via cell therapy. VIP⁺ cells, generated solely from the CGE, can regulate local

cerebral blood flow (Itakura et al., 1987; Magistretti, 1990, Cauli et al., 2004). Altered cerebral blood flow and local perfusion deficits have been observed in Alzheimer's disease and Huntington's disease (Firbank et al., 2003; Gao et al., 2013; Hasselbalch et al., 1992). CGE transplants may be uniquely positioned to supply VIP⁺ cells that increase local blood flow to improve neuronal health and even curb neuronal loss.

Given that CGE transplants migrate extensively in the host cortex and differentiate into mature interneurons, it is perhaps surprising that transplanted CGE cells do not induce plasticity. Nonetheless, this result is extremely informative. From the myriad of interneuron subtypes found in the mouse cortex, we have identified PV⁺ and SST⁺ cells as the only two populations that induce plasticity when transplanted. Having multiple, but not all, interneuron subtypes induce plasticity poses a rather intriguing dilemma. On one hand, properties unique to PV⁺ cells, such as perisomatic innervating, fast-spiking firing, or formation of perineuronal nets, cannot explain the plasticity induced by SST⁺ cells. But on the other hand, properties common to all GABAergic cortical interneurons, such as inhibition of post-synaptic neurons or release of GABA, also cannot explain the inability of CGE-derived interneurons to induce plasticity. It is possible that PV⁺ and SST⁺ cells release diffusible factors that affect the gene expression or dendritic pruning of host pyramidal cells. They may also recapitulate the inhibitory connectivity of the critical period and revert the pyramidal cells to a more juvenile state.

Alternatively, some cells in CGE transplants may be capable of inducing plasticity, but are actively suppressed by other cells within the transplant. For instance, VIP⁺ cells primarily inhibit other GABAergic interneurons, and silencing them has been shown to enhance the adult form of plasticity (Pi et al., 2013; Pfeffer et al., 2013; Fu et al., 2015). Perhaps VIP⁺ cells can exert the same inhibitory control during transplant-induced, critical period-like plasticity and mask the plasticity-inducing potential of other interneuron populations in the transplant. In this scenario, depletion of VIP⁺ cells would induce, rather than eliminate, plasticity. Because PV⁺

and SST⁺ cells contaminating CGE transplants were not impeded by the suppressants among the CGE cells, the proposed suppression by VIP⁺ cells is specific to CGE cells. If plasticity can be successfully “unmasked” by eliminating the suppressors, then CGE cells must induce plasticity via an entirely different mechanism than MGE cells.

Finally, the inability of CGE transplants lacking PV⁺ and SST⁺ cells to induce plasticity may be attributed to non-PV-non-SST interneurons’ insensitivity to sensory deprivation. We have proposed in Chapter 3 that PV⁺ and SST⁺ cells may induce plasticity by serving as early sensors of visual deprivation, altering their activity levels to initiate a cascade of events that lead to plasticity (see Chapter 3, discussion). If CGE-derived interneurons are not able to adjust their activity levels to reflect imbalances in visual input, plasticity will not ensue. This scenario also explains how PV⁺ and SST⁺ cells mediated plasticity even when non-plasticity-inducing CGE cells were present in much higher density, as the ambient inhibition provided by CGE cells would not offset the transient excitation-inhibition imbalance created when PV⁺ and SST⁺ cells respond to visual deprivation.

Cortical plasticity plays important roles in normal development as well as diseases, and identification of cell types pertinent to the induction of plasticity will provide crucial information to the understanding and therapeutic application of cortical plasticity. Although CGE-derived interneurons do not mediate ocular dominance plasticity, it has been shown that the human CGE produces a higher proportion of cortical interneurons than the mouse CGE does (Hansen et al., 2013). As such, CGE cells likely play a bigger role in human cortical inhibitory networks than they do in rodents, and transplantation of CGE cells may be very effective in providing a general increase in inhibition or replenishing CGE-derived cell types in a diseased brain.

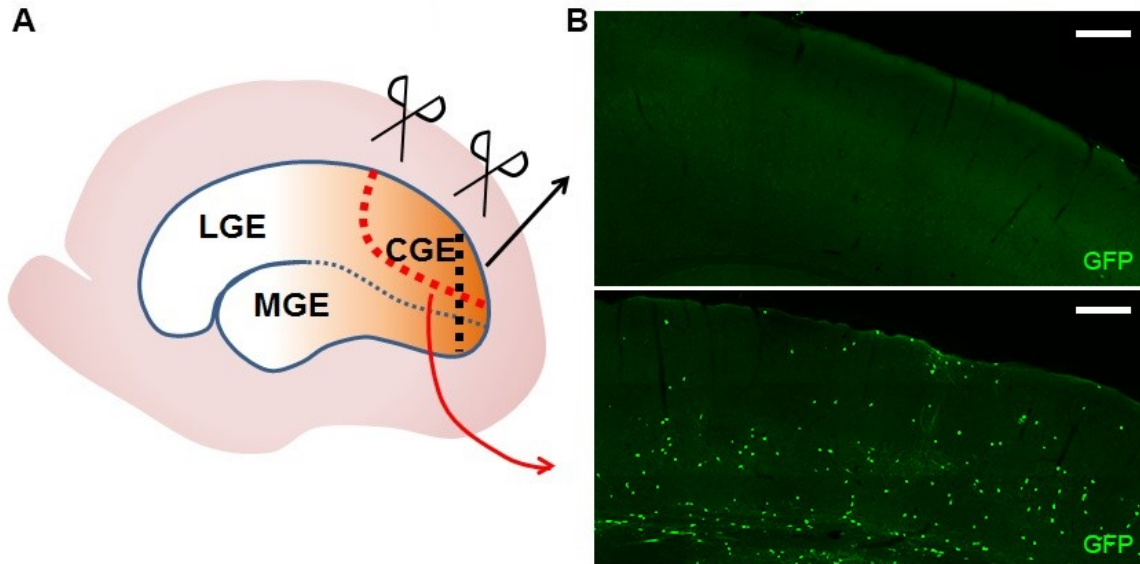


Figure 1. Dissection and transplantation of dorsal CGE.

A. A schematic drawing of the embryonic mouse brain in a sagittal view, showing the three germinal zones. While a sulcus separates LGE and MGE (blue solid line), the Nkx2.1-expressing germinal zone extends into the ventral CGE without any anatomical separation from the Nkx2.1-negative dorsal CGE (blue dashed line). Likewise, the dorsal CGE is anatomically continuous with LGE. The black vertical dashed line indicates the initial attempt to isolate only the caudal CGE (deep orange) and avoid MGE/LGE contamination. The red dashed lines represent rostral-dorsal dissections with ventral CGE discarded. **B.** At 40 days after transplantation, the caudal CGE dissection resulted in poor engraftment (top panel), but the rostral-dorsal CGE dissection survived and migrated in the postnatal cortex (bottom panel, green cells). Scale bar: 200 μ m.

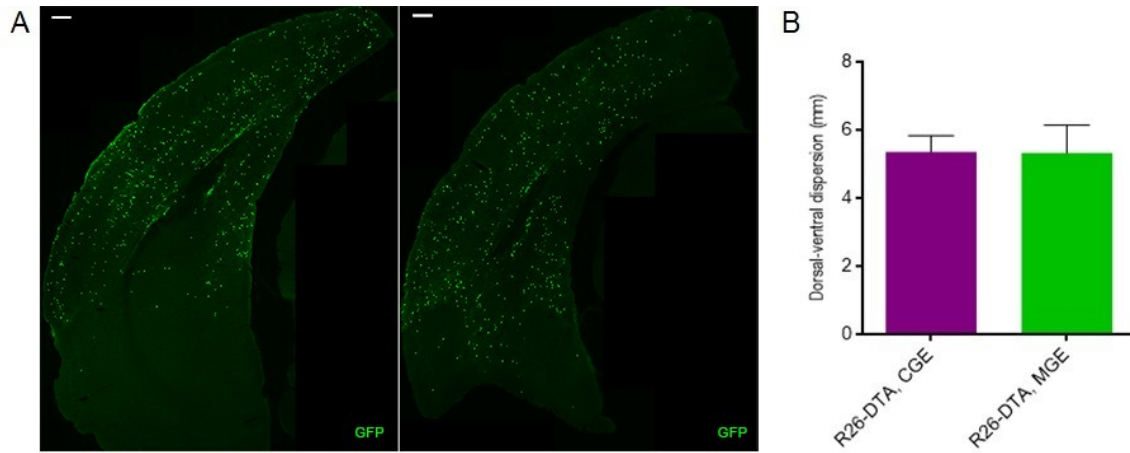


Figure 2. Extensive migration of transplanted CGE cells.

A. At 40 days after transplantation, CGE transplants (left) demonstrated wide dispersion throughout the host cortex, which was mostly indistinguishable in extent of spread and number of successfully grafted cells from that achieved by MGE transplants at the same cellular age (right). Scale bar: 200 μ m. **B.** The extent of dorsal-ventral migration is similar between CGE and MGE transplants. $n = 5$ for each type of transplant, Mann-Whitney test, $P = 0.94$.

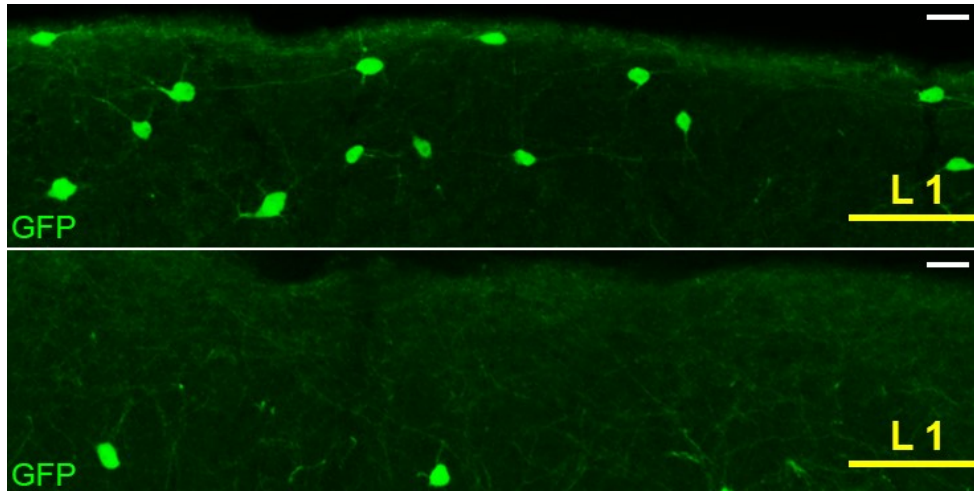


Figure 3. Occupation of layer 1 by cell bodies of CGE but not MGE cells.

Top: many transplanted *R26-DTA* CGE cells (green) migrated to and resided within layer 1 of the host cortex. Bottom: in contrast, *R26-DTA* MGE cell bodies (green) generally avoided layer 1, even though they project vigorously into layer 1. Scale bar: 25 μ m.

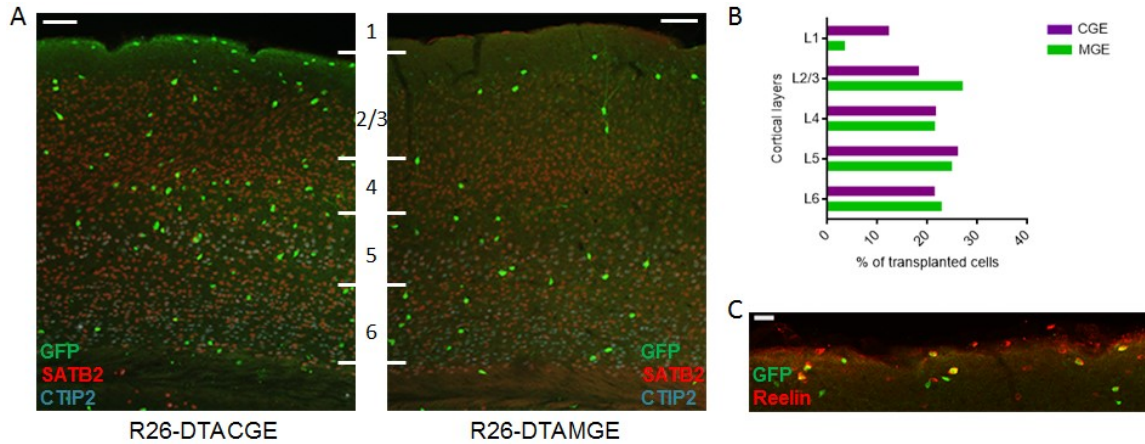
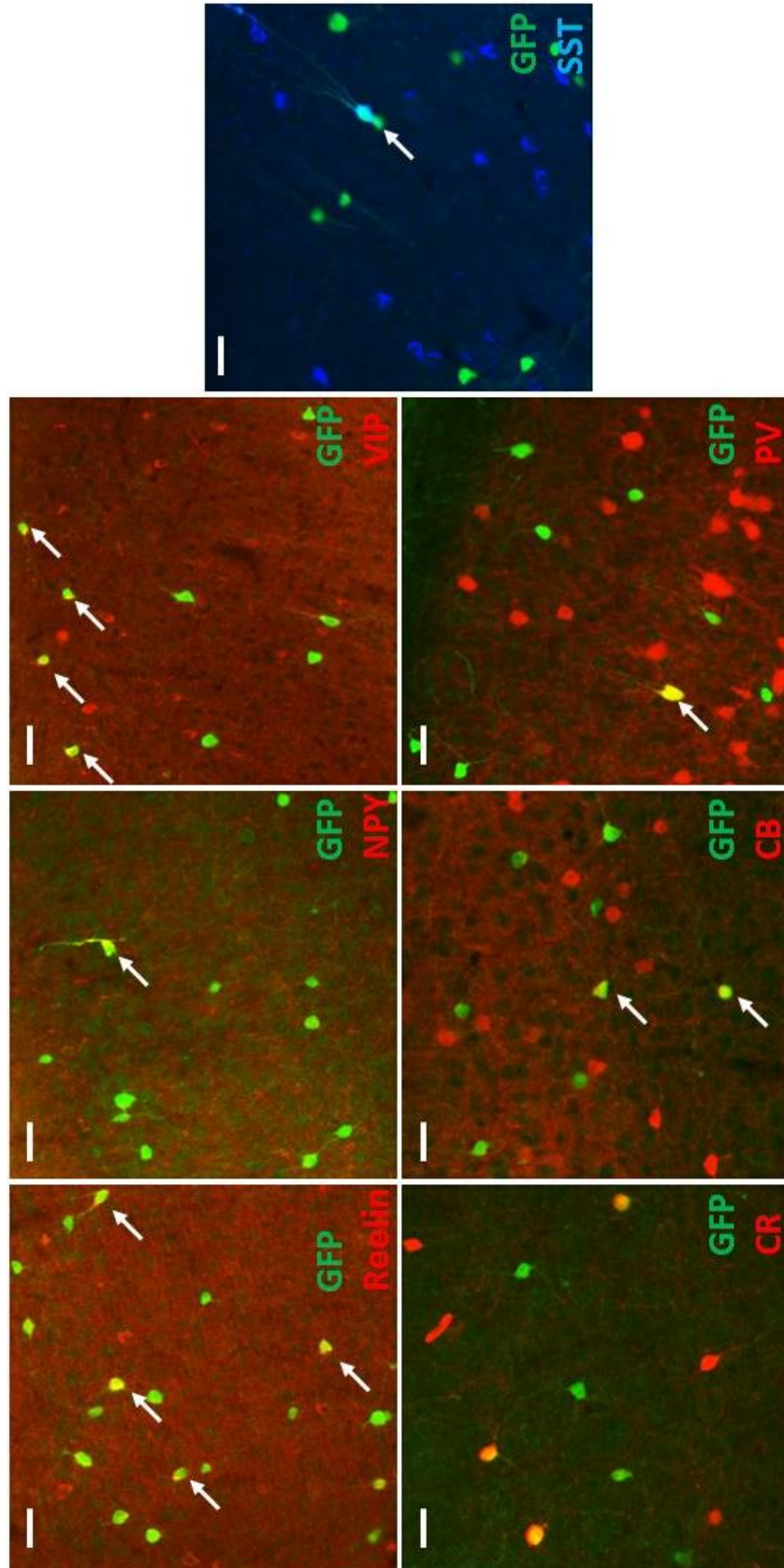


Figure 4. Population of superficial layers by transplanted CGE and MGE cells.

A. staining of satb2 (red) labeled neurons in the upper cortical layers, and ctip2 (blue) staining labeled deep layer cells (5 and 6). Compared to MGE transplants (green, left panel), CGE transplants (green, right panel) were better able to migrate to layer 1 of the host cortex. **B.** percentage of transplanted CGE and MGE cells in each cortical layer. $n = 3$ for each transplant type. **C.** many transplanted CGE cells (green) that migrated into layer 1 co-label with reelin (yellow cells). Scale bar: A, 100 μm ; C, 25 μm .

Figure 5. Transplanted CGE cells differentiate into multiple classes of interneurons.

Immunohistochemistry of transplanted *R26-DTA* CGE cells (green) and neurochemical markers of mature interneurons, including reelin, neuropeptide Y (NPY), vasoactive intestinal peptide (VIP), calretinin (CR), calbindin (CB), parvalbumin (PV), and somatostatin (SST). Scale bar: 50 μm .



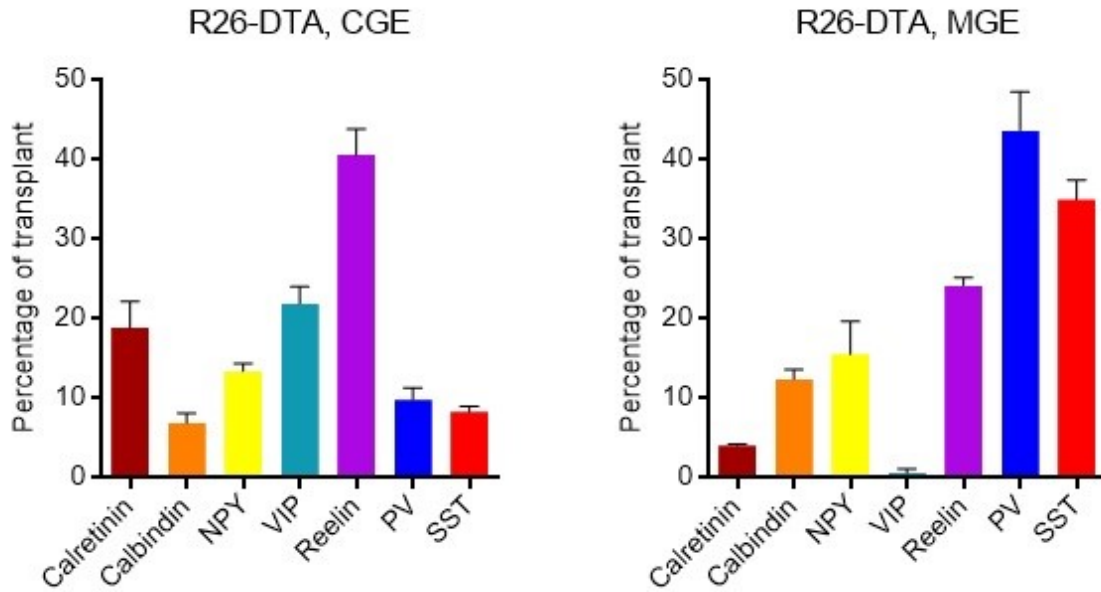


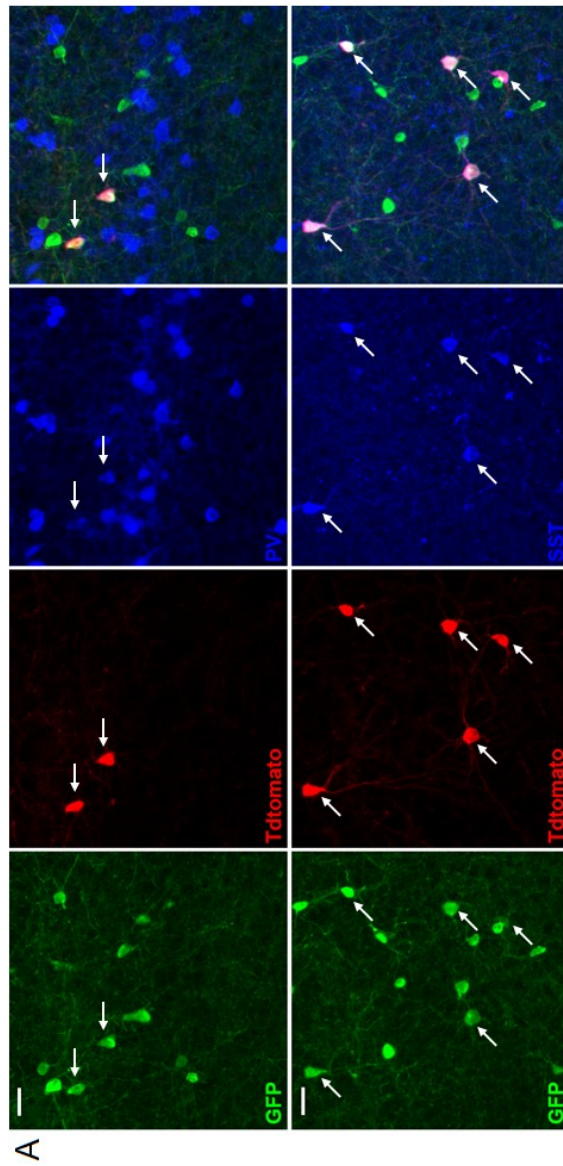
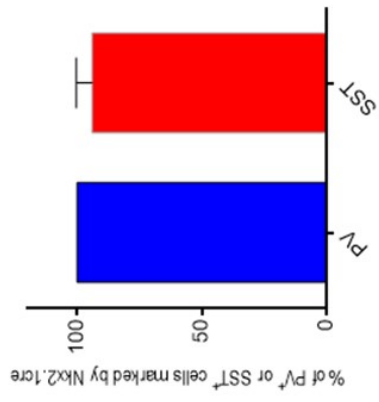
Figure 6. Quantification of interneuron marker expression in transplanted CGE and MGE cells.

Percentage of transplanted R26-DTA CGE cells (left) and MGE cells (right) that expressed calretinin, calbindin, neuropeptide Y (NPY), vasoactive intestinal peptide (VIP), reelin, parvalbumin (PV), and somatostatin (SST). Transplants were assessed at 40 days after transplantation. $n = 3$ per panel.

Figure 7. Almost all PV⁺ and SST⁺ cells in CGE transplants are Nkx2.1⁺ and likely MGE in origin.

A. Transplants of dorsal CGE tissues from Nkx2.1-cre;Ai14;actin-GFP embryos. All transplanted cells express GFP (green), while transplanted cells that derived from *nkx2.1*-expressing germinal domains are also labeled with tdTomato (red). The GFP⁺/tdTomato⁺ cells likely derived from the MGE, since the preoptic area is ventral-medial to the MGE and was not included in the dorsal CGE dissections. Immunostaining with parvalbumin (top panel, blue) revealed many GFP⁺/tdTomato⁺/PV⁺ cells (pink), but GFP⁺/tdTomato⁻ cells (green) do not express PV. Similarly, immunostaining with somatostatin (bottom panel, blue) identified numerous GFP⁺/tdTomato⁺/SST⁺ cells (pink), but none of the GFP⁺/tdTomato⁻ cells (green) co-label with SST. Scale bar: 25 μm. **B.** Quantification of the percentage of PV⁺ and SST⁺ cells in Nkx2.1-cre;Ai14;actin-GFP transplants that expressed tdTomato. *n* = 3, mean = 100% for PV⁺ cells, mean = 94.1% for SST⁺ cells.

B



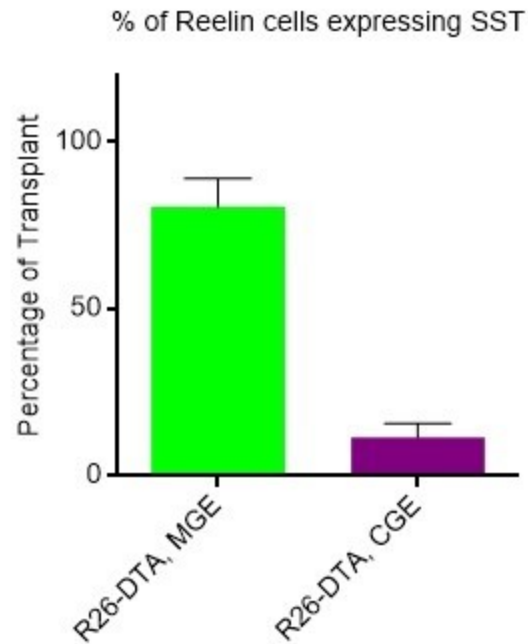


Figure 8. MGE- and CGE-derived reelin⁺ cells have distinct neurochemical marker profiles.

Quantification of reelin⁺/SST⁺ cells in *R26-DTA* MGE and *R26-DTA* CGE transplants. The majority of MGE-derived reelin⁺ cells co-stained with SST, but the proportion of CGE-derived reelin⁺ cells expressing SST was very small. $n = 3$, mean = 85.5% for MGE transplants. $n = 3$, mean = 11.3% for CGE transplants. Mann-Whitney, $P = 0.05$.

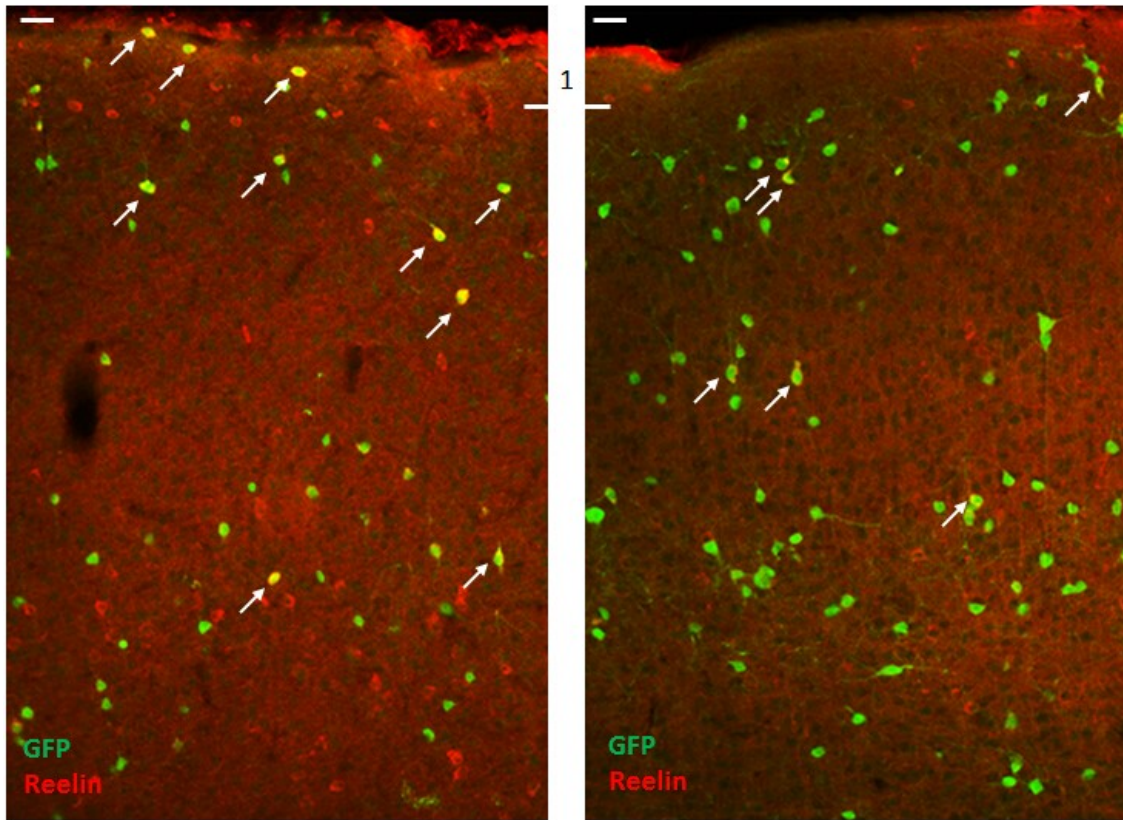


Figure 9. CGE-derived reelin⁺ cells migrate into layer 1 of the cortex of transplant recipients.

Immunostaining of GFP (green) and reelin (red) revealed many reelin⁺ cells (arrows) in both CGE (left) and MGE (right) transplants derived from *R26-DTA* embryos. Only CGE-derived reelin⁺ cells migrate into layer 1 of the recipient cortex. Scale bar: 50 μ m.

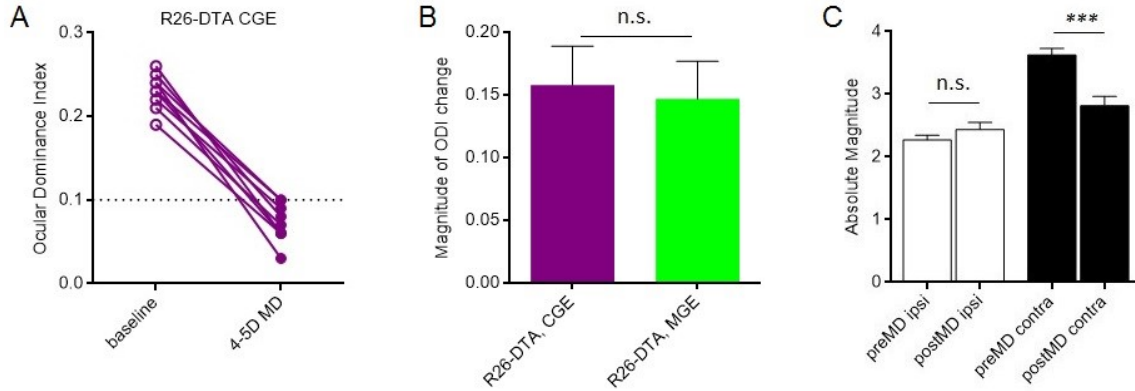


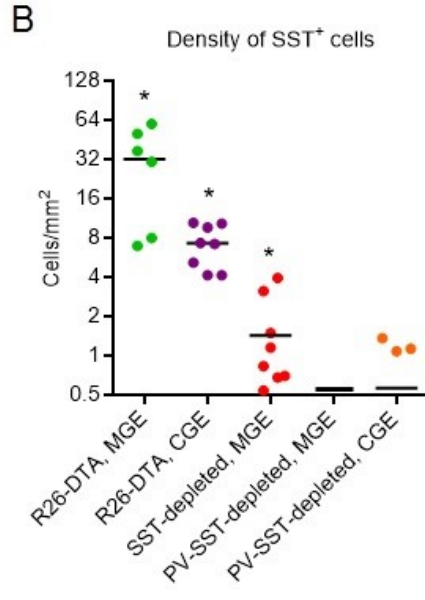
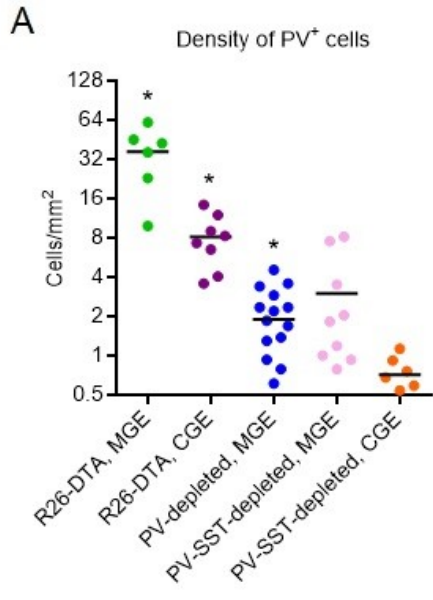
Figure 10. Indistinguishable ocular dominance plasticity mediated by transplanted CGE and MGE cells.

A. After 4-5 days of monocular deprivation, R26-DTA CGE transplants induced robust ocular dominance plasticity. $n = 9$, Mann-Whitney, $P < 0.0001$, dotted line at 0.1 indicates threshold for plasticity. **B.** Transplanted R26-DTA MGE (green bar) and R26-DTA CGE (purple bar) transplants induced ocular dominance plasticity with similar magnitude. $n = 6$, mean = 0.15 for MGE. $n = 9$, mean = 0.16 for CGE. n.s., not significant. **C.** Plasticity induced by transplanted CGE cells demonstrated prominent contralateral depression as seen in MGE-induced plasticity (Chapter 3, Figure 14). $n = 9$, n.s., not significant. ***, $P < 0.0001$.

Figure 11. Density of PV⁺ and SST⁺ cells in R26-DTA CGE and PV-SST-depleted CGE transplants.

A. Density of PV⁺ cells (cells/mm²) in R26-DTA CGE transplants (purple dots) is similar to PV⁺ cell density in R26-DTA MGE (green dots, $P = 0.99$), but higher than PV⁺ cell density in PV-depleted MGE (blue dots, $P < 0.01$) and PV-SST-depleted MGE transplants (pink dots, $P < 0.05$). However, PV⁺ cell density in PV-SST-depleted CGE transplants (orange dots) is lower than both PV-depleted MGE ($P < 0.05$) and PV-SST-depleted MGE transplants ($P < 0.01$).

B. R26-DTA CGE transplants (purple dots) contain similar numbers of SST⁺ cells when compared to R26-DTA MGE transplants (green dots, $P = 0.99$) and SST-depleted MGE (red dots, $P = 0.11$), but more SST⁺ cells than in PV-SST-depleted MGE transplants (pink dots, $P < 0.0001$). On the other hand, PV-SST-depleted CGE transplants (orange dots) contained comparable numbers of SST⁺ cells when compared to SST-depleted MGE ($P = 0.2$) and PV-SST-depleted MGE ($P = 0.12$) transplants. In **A** and **B**, $n = 6$ for R26-DTA MGE, $n = 8$ for R26-DTA CGE, $n = 16$ for PV-depleted MGE, $n = 9$ for SST-depleted MGE, $n = 9$ for PV-SST-depleted MGE, $n = 7$ for PV-SST-depleted CGE. Asterisks mark transplant types that induced plasticity. P values calculated using Kruskal-Wallis test with correction for multiple comparisons.



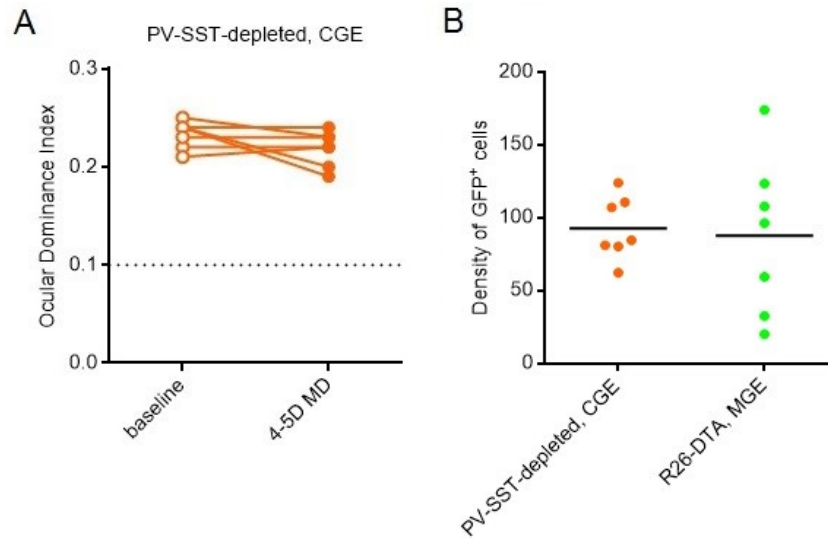


Figure 12. CGE transplants depleted of PV⁺ and SST⁺ cells fail to induce plasticity.

A. PV-SST-depleted CGE transplants did not induce ocular dominance plasticity after monocular deprivation ($n = 7$, Mann-Whitney, $P = 0.12$, dotted line at 0.1 indicates threshold for plasticity). **B.** R26-DTA CGE transplants (orange dots) have similar transplant density (cells/mm²) as R26-DTA MGE transplants (green dots) that did induce plasticity ($n = 7$ for each transplant type, Mann-Whitney, $P = 0.78$).

Conclusions

My thesis research evolved around the identification of interneuron subpopulations that possess the unique ability to remodel neural networks and mediate critical-period-like ocular dominance plasticity in the adult mouse brain. In the late 1990s, our laboratory developed the techniques of interneuron transplantation, and has since used heterochronic transplantation of interneuron precursors to investigate the development and therapeutic potential of interneurons derived from the medial ganglionic eminence (MGE). To date we have established that transplanted interneuron precursors migrate, integrate, undergo population adjustment through programmed cell death, and mature into functional interneurons in the recipient brain, where they increase inhibition, ameliorate seizures, and induce cortical plasticity (Wichterle et al., 1999; Wichterle et al., 2001; Alvarez-Dolado et al., 2003; Baraban et al., 2009; Southwell et al., 2010; Southwell et al., 2012).

The goal of my thesis research was to elucidate the contribution of distinct interneuron subtypes in ocular dominance plasticity induced by interneuron transplantation. The normal critical period for ocular dominance plasticity closes after P32 in mice (Gordon and Stryker, 1996). Previous collaborative work with the Stryker Lab demonstrated that transplanting MGE-derived interneuron precursors into the primary visual cortex can open a new period of heightened plasticity in mice after their endogenous critical period has closed (Southwell et al., 2010). MGE gives rise to a mixture of interneurons, with the majority of them being parvalbumin-expressing (PV⁺) and somatostatin-expressing (SST⁺) cells. My initial attempts to purify individual interneuron subpopulations via fluorescence activated cell sorting were unsuccessful:

interneuron precursors express very low levels of subtype markers. To counter this problem, I devised a strategy to selectively deplete interneuron subtypes through Cre-mediated expression of diphtheria toxin alpha subunit (DTA). The Cre-DTA combination successfully removed over 90% of Cre-expressing cells without affecting the survival or maturation of the Cre-negative cells. In collaboration with the Stryker laboratory, I tested whether the removal of PV⁺ or SST⁺ interneurons could affect the ability of the transplant to induce ocular dominance plasticity in post-critical-period recipient mice. We first transplanted MGE cells depleted of PV⁺ cells, expecting plasticity to be affected due to the prominent role PV⁺ cells are known to play in critical period plasticity (Sugiyama et al., 2008; Miyata et al., 2012; Kuhlman et al., 2013). We were surprised to find that the MGE transplants' ability to induce plasticity was preserved despite the efficient depletion of over 90% of PV⁺ cells. As expected based on previous studies, depletion of SST⁺ cells didn't affect plasticity, either. However, when we removed both PV⁺ and SST⁺ cells simultaneously, the transplants failed to induce plasticity. When we further examined the characteristics of plasticity induced by non-depleted, PV-depleted, and SST-depleted MGE transplants, we were able to determine that the plasticity mediated by all three types of transplants resembled plasticity seen in the normal critical period in their magnitude, sensitivity to brief monocular deprivation, and the significant weakening of response to the deprived eye. These results indicate that PV⁺ interneurons are not the only interneuron subtype capable of initiating ocular dominance plasticity. MGE-derived SST⁺ cells, whose function in cortical plasticity has not been previously described, can also effectively modify neural circuits and facilitate plasticity. Last but not least, we established that plasticity mediated by PV⁺ and SST⁺ cells recapitulates key features of critical period plasticity, such as the rapid onset of plasticity and the weakening of cortical response to the deprived eye.

Following the discovery that SST⁺ cells are important players in ocular dominance plasticity, I continued to investigate whether other interneuron subtypes also hold potential for

inducing ocular dominance plasticity. Because MGE transplants are dominated by PV⁺ and SST⁺ cells, I turned to interneurons derived from the caudal ganglionic eminence (CGE). Transplantation of interneuron precursors from the CGE has not been systematically examined before. As I performed histological characterization of transplanted CGE cells, it became apparent that they parallel MGE transplants in their ability to disperse throughout the host cortex and differentiate into mature interneurons. However, immunohistochemistry with neurochemical markers revealed a drastically different subtype profile of CGE-derived interneurons. Instead of PV⁺ and SST⁺ cells, transplanted interneuron precursors from the CGE gave rise to cells expressing reelin, vasoactive intestinal peptide (VIP), calretinin, calbindin, and neuropeptide Y (NPY). Interestingly, when we examined the recipients of CGE transplants, we found robust ocular dominance plasticity upon monocular deprivation. However, we determined that a minor population of MGE-derived PV⁺ and SST⁺ cells was present among CGE cells. Removal of these contaminating MGE cells from CGE transplants abolished transplant-induced plasticity, despite plenty of successfully grafted CGE-derived interneurons in the host cortex. Together, these findings paint an intriguing picture of cortical interneuron subtypes: on the one hand, the ability to survive, migrate, and mature in a heterochronic brain environment seems to be shared by almost all interneurons, regardless of their subtype identity or place of origin. Yet on the other hand, only a small set of interneurons subtypes derived from a specific subcortical germinal zone (MGE) are uniquely positioned to reshape cortical neural circuits and recapitulate juvenile-like plasticity in an adult brain that normally is not conducive to such plasticity.

MGE transplantation offers a unique opportunity to study the mechanism of critical period plasticity. By transplanting MGE cells, we can isolate the effect of juvenile interneurons on a mature visual cortex, and how these effects lead to plasticity. But how might we proceed to elucidate the mechanism of plasticity induction by PV⁺ and SST⁺ cells? First, electrophysiological studies should be conducted on transplanted CGE cells to determine their

firing properties and the synapses they receive and form. It's known that transplanted MGE cells form functional synapses and integrate into the host neural circuitry (Baraban et al., 2009; Southwell et al., 2010). Although the extensive neuronal processes formed by transplanted CGE cells suggest that they integrate into the host cortex, we need to prove it using electrophysiology. Knowing whether transplanted CGE cells functionally integrate is important, because if CGE cells do not integrate after transplantation, then the observed specificity of PV⁺ and SST⁺ interneurons in facilitating plasticity might simply be explained by their ability to integrate and provide synaptic output in the host cortex. Knowing the inhibitory output of CGE cells is also essential in evaluating their potential application in cell therapy. If CGE cells do increase inhibition in the host cortex, the next step will be assessing whether they have a different level of sensitivity to monocular deprivation than PV⁺ and SST⁺ cells do. As I proposed in Chapter 3 and 4, PV⁺ and SST⁺ cells may be unique in their ability to rapidly respond to sensory deprivation (see discussions in Chapter 3 and 4). Calcium imaging of visually evoked interneuron activity like that done on PV⁺ cells will demonstrate whether all or only some interneurons respond to visual deprivation (Kuhlman et al., 2014). At the same time, we cannot exclude the possibility that mechanisms other than synaptic GABA release mediate transplant-induced plasticity. Comparing the gene expression profile of interneuron subtypes may yield clues to subtype-specific expression of secreted factors or surface signal molecules that may induce plasticity. To accomplish this, we need to be aware that there are multiple methods to define interneuron subtypes. While neurochemical markers are commonly used to identify interneuron subtypes due to the reproducibility and efficiency of this method, many interneurons express multiple neurochemical markers, and interneurons sharing the same set of markers can display different firing patterns or connectivity (Butt et al., 2005; Wonders and Anderson, 2006; Rudy et al., 2011). With recent advances in algorithms of microarray analysis, it may be possible to identify functionally meaningful co-expression of genes from those not salient to plasticity (Oldham et al., 2012). Finally, we may want to probe the impact of transplanted interneurons on existing

connections in the host cortex. Some subtypes of interneurons may compete with host inhibitory interneurons for synaptic targets and eliminate a subset of their synapses. Doing so may destabilize the otherwise mature and inflexible host neural circuits, making them more juvenile and receptive to plasticity.

Overall, my thesis research helps to further the characterization of the behaviors and functional diversity of transplanted cortical interneurons. Identification of interneuron subtypes implicated in juvenile plasticity is the first step in elucidating mechanisms of developmental plasticity. Manipulations of these cells prior to transplantation can isolate cellular mechanisms that are essential in inducing plasticity. Such information will provide insights into cortical neural development and discovery of pharmacological agents that induce plasticity. Interneurons and/or molecules capable of mediating juvenile-like plasticity will be good therapeutic agents for the treatment of stroke, amblyopia, and PTSD. Cell replacement therapy using MGE- and CGE-derived interneurons may hold promise for treating epilepsy, Parkinson's disease, Alzheimer's disease, and Huntington's disease (Richardson et al., 2008; Southwell et al., 2014). Understanding the functional application of each subtype will be crucial in devising safe and effective strategies of transplant therapy.

References

- Allen Developing Mouse Brain Atlas. Website: ©2013 Allen Institute for Brain Science. Allen Developing Mouse Brain Atlas [Internet]. Available from: <http://developingmouse.brain-map.org>.
- Alvarez-Dolado M, Calcagnotto ME, Karkar KM, Southwell DG, Jones-Davis DM, Estrada RC, Rubenstein JL, Alvarez-Buylla A, Baraban SC. (2006). Cortical inhibition modified by embryonic neural precursors grafted into the postnatal brain. *J Neurosci* 26, 7380-7389.
- Anderson SA, Eisenstat DD, Shi L, Rubenstein JL. (1997). Interneuron migration from basal forebrain to neocortex: dependence on Dlx genes. *Science* 278(5337):474-6.
- Anderson SA, Marín O, Horn C, Jennings K, Rubenstein JL. (2001). Distinct cortical migrations from the medial and lateral ganglionic eminences. *Development* 128(3):353-63.
- Awaya S, Miyake Y, Imaizumi Y, Shiose Y, Kanda T, Komuro K. (1973). Amblyopia in man, suggestive of stimulus deprivation amblyopia. *Japanese Journal of Ophthalmology* 17:69-82.
- Baglietto-Vargas D, Moreno-Gonzalez I, Sanchez-Varo R, Jimenez S, Trujillo-Estrada L, Sanchez-Mejias E, Torres M, Romero-Acebal M, Ruano D, Vizuete M, Vitorica J, Gutierrez A. (2010). Calretinin interneurons are early targets of extracellular amyloid-beta pathology in PS1/AbetaPP Alzheimer mice hippocampus. *J Alzheimers Dis* 21(1):119-32.
- Baraban SC, Southwell DG, Estrada RC, Jones DL, Sebe JY, Alfaro-Cervello C, García-Verdugo JM, Rubenstein JL, Alvarez-Buylla A. (2009). Reduction of seizures by transplantation of cortical GABAergic interneuron precursors into Kv1.1 mutant mice. *Proc Natl Acad Sci U S A* 106(36):15472-7.
- Barinka F, Druga R, Marusic P, Krsek P, Zamecnik J. (2010). Calretinin immunoreactivity in focal cortical dysplasias and in non-malformed epileptic cortex. *Epilepsy Res* 88(1):76-86.

Batista-Brito R, Rossignol E, Hjerling-Leffler J, Denaxa M, Wegner M, Lefebvre V, Pachnis V, Fishell G. (2009). The cell-intrinsic requirement of Sox6 for cortical interneuron development. *Neuron* 63(4):466-81.

Bland BH, Oddie SD. (2001). Theta band oscillation and synchrony in the hippocampal formation and associated structures: the case for its role in sensorimotor integration. *Behav Brain Res* 127(1-2):119-36.

Behar TN, Li YX, Tran HT, Ma W, Dunlap V, Scott C, Barker JL. (1996). GABA stimulates chemotaxis and chemokinesis of embryonic cortical neurons via calcium-dependent mechanisms. *J Neurosci* 16(5):1808-18.

Ben-Ari Y. Basic developmental rules and their implications for epilepsy in the immature brain. *Epileptic Disord* 8(2):91-102.

Bender AC, Morse RP, Scott RC, Holmes GL, Lenck-Santini PP. (2012). SCN1A mutations in Dravet syndrome: impact of interneuron dysfunction on neural networks and cognitive outcome. *Epilepsy Behav* 23(3):177-86.

Bhalla D, Godet B, Druet-Cabanac M, Preux PM. (2011). Etiologies of epilepsy: a comprehensive review. *Expert Rev Neurother* 11(6):861-76.

Blatow M, Rozov A, Katona I, Hormuzdi SG, Meyer AH, Whittington MA, Caputi A, Monyer H. (2003). A novel network of multipolar bursting interneurons generates theta frequency oscillations in neocortex. *Neuron* 38(5):805-17.

Blatt GJ, Fitzgerald CM, Guptill JT, Booker AB, Kemper TL, Bauman ML. (2001). Density and distribution of hippocampal neurotransmitter receptors in autism: an autoradiographic study. *J Autism Dev Disord* 31(6):537-43.

Britanova O, de Juan Romero C, Cheung A, Kwan KY, Schwark M, Gyorgy A, Vogel T, Akopov S, Mitkovski M, Agoston D, Sestan N, Molnár Z, Tarabykin V. *Satb2* is a postmitotic determinant for upper-layer neuron specification in the neocortex. (2008). *Neuron* 57(3):378-92.

Bráz JM, Sharif-Naeini R, Vogt D, Kriegstein A, Alvarez-Buylla A, Rubenstein JL, Basbaum AI. (2012). Forebrain GABAergic neuron precursors integrate into adult spinal cord and reduce injury-induced neuropathic pain. *Neuron* 74(4):663-75.

Burgos-Ramos E, Hervás-Aguilar A, Aguado-Llera D, Puebla-Jiménez L, Hernández-Pinto AM, Barrios V, Arilla-Ferreiro E. (2008). Somatostatin and Alzheimer's disease. *Mol Cell Endocrinol* 286(1-2):104-11.

Butt SJ, Fuccillo M, Nery S, Noctor S, Kriegstein A, Corbin JG, Fishell G. (2005). The temporal and spatial origins of cortical interneurons predict their physiological subtype. *Neuron* 48(4):591-604.

Butt SJ, Cobos I, Golden J, Kessar N, Pachnis V, Anderson S. (2007). Transcriptional regulation of cortical interneuron development. *J Neurosci* 27(44):11847–11850.

Butt SJ, Sousa VH, Fuccillo MV, Hjerling-Leffler J, Miyoshi G, Kimura S, Fishell G. (2008). The requirement of *Nkx2-1* in the temporal specification of cortical interneuron subtypes. *Neuron* 59(5):722-32

Buzsáki G, Wang XJ. (2012). Mechanisms of gamma oscillations. *Annu Rev Neurosci* 35:203-25.

Cai Y, Zhang Q, Wang C, Zhang Y, Ma T, Zhou X, Tian M, Rubenstein JL, Yang Z. (2013). Nuclear receptor COUP-TFII-expressing neocortical interneurons are derived from the medial and lateral/caudal ganglionic eminence and define specific subsets of mature interneurons. *J Comp Neurol* 521(2):479-97.

Cancedda L, Fiumelli H, Chen K, Poo MM. (2007). Excitatory GABA action is essential for morphological maturation of cortical neurons in vivo. *J Neurosci* 27(19):5224-35.

Cang J, Kalatsky VA, Löwel S, Stryker MP. (2005). Optical imaging of the intrinsic signal as a measure of cortical plasticity in the mouse. *Vis Neurosci* 22(5):685-91.

Cauli B, Tong XK, Rancillac A, Serluca N, Lambolez B, Rossier J, Hamel E. (2004). Cortical GABA interneurons in neurovascular coupling: relays for subcortical vasoactive pathways. *J Neurosci* 24(41):8940-9.

Chakrabarti L, Best TK, Cramer NP, Carney RS, Isaac JT, Galdzicki Z, Haydar TF. (2010). Olig1 and Olig2 triplication causes developmental brain defects in Down syndrome. *Nat Neurosci* 13(8):927-34.

Chattopadhyaya B, Di Cristo G, Higashiyama H, Knott GW, Kuhlman SJ, Welker E, Huang ZJ. (2004). Experience and activity-dependent maturation of perisomatic GABAergic innervation in primary visual cortex during a postnatal critical period. *J Neurosci* 24(43):9598-611.

Choe S, Bennett MJ, Fujii G, Curmi PM, Kantardjieff KA, Collier RJ, Eisenberg D. (1992). The crystal structure of diphtheria toxin. *Nature* 357(6375):216-222.

Ciucci F, Putignano E, Baroncelli L, Landi S, Berardi N, Maffei L. (2007). Insulin-like growth factor 1 (IGF-1) mediates the effects of enriched environment (EE) on visual cortical development. *PloS one* 2(5):e475.

Cobos I, Calcagnotto ME, Vilaythong AJ, Thwin MT, Noebels JL, Baraban SC, Rubenstein JL. (2005). Mice lacking Dlx1 show subtype-specific loss of interneurons, reduced inhibition and epilepsy. *Nat Neurosci* 8(8):1059-68.

- Coppola G, Schoenen J. (2012). Cortical excitability in chronic migraine. *Curr Pain Headache Rep* 16(1):93-100.
- Corbin JG, Rutlin M, Gaiano N, Fishell G. (2003). Combinatorial function of the homeodomain proteins Nkx2.1 and Gsh2 in ventral telencephalic patterning. *Development* 130(20):4895-906.
- Datwani A, McConnell MJ, Kanold PO, Micheva KD, Busse B, Shamloo M, Smith SJ, Shatz CJ. (2009). Classical MHCI molecules regulate retinogeniculate refinement and limit ocular dominance plasticity. *Neuron* 64(4):463-470.
- Di Cristo G, Chattopadhyaya B, Kuhlman SJ, Fu Y, Bélanger MC, Wu CZ, Rutishauser U, Maffei L, Huang ZJ. (2007). Activity-dependent PSA expression regulates inhibitory maturation and onset of critical period plasticity. *Nature neuroscience* 10(12):1569-1577.
- Du T, Xu Q, Ocbina PJ, Anderson SA. (2008). NKX2.1 specifies cortical interneuron fate by activating Lhx6. *Development* 135(8):1559-67.
- Elias LA, Wang DD, Kriegstein AR. (2007). Gap junction adhesion is necessary for radial migration in the neocortex. *Nature* 448(7156):901-7.
- Elias LA, Turmaine M, Parnavelas JG, Kriegstein AR. (2010). Connexin 43 mediates the tangential to radial migratory switch in ventrally derived cortical interneurons. *J Neurosci* 30(20):7072-7.
- Fagiolini M, Hensch TK. (2000). Inhibitory threshold for critical-period activation in primary visual cortex. *Nature* 404(6774):183-6.
- Fagiolini M, Fritschy JM, Löw K, Möhler H, Rudolph U, Hensch TK. (2004). Specific GABA_A circuits for visual cortical plasticity. *Science* 303(5664):1681-1683.

Férézou I, Cauli B, Hill EL, Rossier J, Hamel E, Lambolez B. (2002). 5-HT₃ receptors mediate serotonergic fast synaptic excitation of neocortical vasoactive intestinal peptide/cholecystokinin interneurons. *J Neurosci* 22(17):7389–7397

Firbank MJ, Colloby SJ, Burn DJ, McKeith IG, O'Brien JT. (2003). Regional cerebral blood flow in Parkinson's disease with and without dementia. *Neuroimage* 20(2):1309-19.

Flames N, Long JE, Garratt AN, Fischer TM, Gassmann M, Birchmeier C, Lai C, Rubenstein JL, Marín O. (2004). Short- and long-range attraction of cortical GABAergic interneurons by neuregulin-1. *Neuron* 44(2):251-61.

Flandin P, Zhao Y, Vogt D, Jeong J, Long J, Potter G, Westphal H, Rubenstein JL. (2011). Lhx6 and Lhx8 coordinately induce neuronal expression of Shh that controls the generation of interneuron progenitors. *Neuron* 70(5):939-50.

Fogarty M, Grist M, Gelman D, Marín O, Pachnis V, Kessaris N. (2007). Spatial genetic patterning of the embryonic neuroepithelium generates GABAergic interneuron diversity in the adult cortex. *J Neurosci* 27(41):10935-46.

Freund TF, Katona I. (2007). Perisomatic inhibition. *Neuron* 56(1):33-42.

Fries P, Reynolds JH, Rorie AE, Desimone R. (2001). Modulation of oscillatory neuronal synchronization by selective visual attention. *Science* 291(5508):1560-3.

Fu Y, Kaneko M, Tang Y, Stryker MP. (2015). A cortical disinhibitory circuit for enhancing adult plasticity. *eLife* 4, e05558.

Gandhi SP, Yanagawa Y, Stryker MP. (2008). Delayed plasticity of inhibitory neurons in developing visual cortex. *Proc Natl Acad Sci U S A* 105(43):16797-802.

- Gao YZ, Zhang JJ, Liu H, Wu GY, Xiong L, Shu M. (2013). Regional cerebral blood flow and cerebrovascular reactivity in Alzheimer's disease and vascular dementia assessed by arterial spinlabeling magnetic resonance imaging. *Curr Neurovasc Res* 10(1):49-53.
- Gelman DM, Marín O. (2010). Generation of interneuron diversity in the mouse cerebral cortex. *Eur J Neurosci* 31(12):2136-41.
- Gelman D, Griveau A, Dehorter N, Teissier A, Varela C, Pla R, Pierani A, Marín O. (2011). A wide diversity of cortical GABAergic interneurons derives from the embryonic preoptic area. *J Neurosci* 31(46):16570-80.
- Gonchar Y, Wang Q, Burkhalter A. (2007). Multiple distinct subtypes of GABAergic neurons in mouse visual cortex identified by triple immunostaining. *Frontiers in neuroanatomy* 1:3.
- Gonzalez-Burgos G, Lewis DA. (2008). GABA neurons and the mechanisms of network oscillations: implications for understanding cortical dysfunction in schizophrenia. *Schizophr Bull* 34(5):944–961.
- Gordon JA, Stryker MP. (1996). Experience-dependent plasticity of binocular responses in the primary visual cortex of the mouse. *J Neurosci* 15;16(10):3274-86.
- Hanover JL1, Huang ZJ, Tonegawa S, Stryker MP. (1999). Brain-derived neurotrophic factor overexpression induces precocious critical period in mouse visual cortex. *J Neurosci* 19(22):RC40.
- Hansen DV, Lui JH, Flandin P, Yoshikawa K, Rubenstein JL, Alvarez-Buylla A, Kriegstein AR. (2013). Non-epithelial stem cells and cortical interneuron production in the human ganglionic eminences. *Nat Neurosci* 16(11):1576-87.

Hasselbalch SG, Oberg G, Sørensen SA, Andersen AR, Waldemar G, Schmidt JF, Fenger K, Paulson OB. (1992). Reduced regional cerebral blood flow in Huntington's disease studied by SPECT. *J Neurol Neurosurg Psychiatry* 55(11): 1018–1023.

Hensch TK, Fagiolini M, Mataga N, Stryker MP, Baekkeskov S, Kash SF. (1998). Local GABA circuit control of experience-dependent plasticity in developing visual cortex. *Science* 282(5393):1504-8.

Hippenmeyer S, Vrieseling E, Sigrist M, Portmann T, Laengle C, Ladle DR, Arber S. (2005). A developmental switch in the response of DRG neurons to ETS transcription factor signaling. *PLoS Biol* 3(5):e159.

Hosp JA, Luft AR. (2011). Cortical plasticity during motor learning and recovery after ischemic stroke. *Neural plasticity* 2011:871296.

Huang ZJ, Kirkwood A, Pizzorusso T, Porciatti V, Morales B, Bear MF, Maffei L, Tonegawa S. (1999). BDNF regulates the maturation of inhibition and the critical period of plasticity in mouse visual cortex. *Cell* 98(6):739-55.

Hubel DH, Wiesel TN, Stryker MP. (1977). Orientation columns in macaque monkey visual cortex demonstrated by the 2-deoxyglucose autoradiographic technique. *Nature* 269(5626):328-30.

Hunt RF, Girskis KM, Rubenstein JL, Alvarez-Buylla A, Baraban SC. (2013). GABA progenitors grafted into the adult epileptic brain control seizures and abnormal behavior. *Nat Neurosci* 16(6): 692-697.

Inada H, Watanabe M, Uchida T, Ishibashi H, Wake H, Nemoto T, Yanagawa Y, Fukuda A, Nabekura J. (2011). GABA regulates the multidirectional tangential migration of GABAergic interneurons in living neonatal mice. *PLoS One* 6(12):e27048.

Inta D, Alfonso J, von Engelhardt J, Kreuzberg MM, Meyer AH, van Hooft JA, Monyer H. (2008). Neurogenesis and widespread forebrain migration of distinct GABAergic neurons from the postnatal subventricular zone. *Proc Natl Acad Sci U S A* 105(52):20994–20999.

Itakura T, Yokote H, Okuno T, Naka Y, Nakakita K, Kamei I, Nakai K, Imai H, Komai N. (1987). Regulation of rCBF by intracortical vasoactive intestinal polypeptide-containing neurons. Immunohistochemical and hydrogen clearance study in rats. *J Neurosurg* 67(1):93-6.

Ivanova A, Signore M, Caro N, Greene ND, Copp AJ, Martinez-Barbera JP. (2005). In vivo genetic ablation by Cre-mediated expression of diphtheria toxin fragment A. *Genesis* 43(3):129-35.

Kalatsky VA, Stryker MP. (2003). New paradigm for optical imaging: temporally encoded maps of intrinsic signal. *Neuron* 38(4):529-45.

Kanatani S, Yozu M, Tabata H, Nakajima K. (2008). COUP-TFII is preferentially expressed in the caudal ganglionic eminence and is involved in the caudal migratory stream. *J Neurosci* 28(50):13582-91.

Kaneko M, Stryker MP. (2014). Sensory experience during locomotion promotes recovery of function in adult visual cortex. *Elife* 3, e02798.

Klausberger T, Roberts JD, Somogyi P. (2002). Cell type- and input-specific differences in the number and subtypes of synaptic GABA(A) receptors in the hippocampus. *J Neurosci* 22(7):2513-21.

Koliatsos VE, Kecojevic A, Troncoso JC, Gastard MC, Bennett DA, Schneider JA. (2006). Early involvement of small inhibitory cortical interneurons in Alzheimer's disease. *Acta Neuropathol* 112(2):147-62.

Kuhlman SJ, Olivas ND, Tring E, Ikrar T, Xu X, Trachtenberg JT. (2013). A disinhibitory microcircuit initiates critical-period plasticity in the visual cortex. *Nature* 501(7468):543-546.

Lanoue AC, Blatt GJ, Soghomonian JJ. (2013). Decreased parvalbumin mRNA expression in dorsolateral prefrontal cortex in Parkinson's disease. *Brain Res* 1531:37-47.

Lee S, Hjerling-Leffler J, Zagha E, Fishell G, Rudy B. (2010). The Largest Group of Superficial Neocortical GABAergic Interneurons Expresses Ionotropic Serotonin Receptors. *J Neurosci* 30(50):16796-808.

Li G, Adesnik H, Li J, Long J, Nicoll RA, Rubenstein JL, Pleasure SJ. (2008). Regional distribution of cortical interneurons and development of inhibitory tone are regulated by Cxcl12/Cxcr4 signaling. *J Neurosci* 28(5):1085-98.

Li H, Tornberg J, Kaila K, Airaksinen MS, Rivera C. (2002). Patterns of cation-chloride cotransporter expression during embryonic rodent CNS development. *Eur J Neurosci* 16(12):2358-70.

Li X, Morita K, Robinson HP, Small M. (2013). Control of layer 5 pyramidal cell spiking by oscillatory inhibition in the distal apical dendrites: a computational modeling study. *J Neurophysiol* 109(11):2739-56.

Liu X, Novosedlik N, Wang A, Hudson ML, Cohen IL, Chudley AE, Forster-Gibson CJ, Lewis SM, Holden JJ. (2009). The DLX1 and DLX2 genes and susceptibility to autism spectrum disorders. *Eur J Hum Genet* 17(2):228-35.

Liu Y, Liu H, Sauvey C, Yao L, Zarnowska ED, Zhang SC. (2013). Directed differentiation of forebrain GABA interneurons from human pluripotent stem cells. *Nat Protoc* 8(9):1670-9.

Lodato S, Tomassy GS, De Leonibus E, Uzcategui YG, Andolfi G, Armentano M, Touzot A, Gaztelu JM, Arlotta P, Menendez de la Prida L, Studer M. (2011). Loss of COUP-TFI alters the balance between caudal ganglionic eminence- and medial ganglionic eminence-derived cortical interneurons and results in resistance to epilepsy. *J Neurosci* 31(12):4650-62.

LoTurco JJ, Owens DF, Heath MJ, Davis MB, Kriegstein AR. (1995). GABA and glutamate depolarize cortical progenitor cells and inhibit DNA synthesis. *Neuron* 15(6):1287-98.

Madisen L, Zwingman TA, Sunkin SM, Oh SW, Zariwala HA, Gu H, Ng LL, Palmiter RD, Hawrylycz MJ, Jones AR, Lein ES, Zeng H. (2010). A robust and high-throughput Cre reporting and characterization system for the whole mouse brain. *Nat Neurosci* 13(1):133-40.

Magistretti PJ. (1990). VIP neurons in the cerebral cortex. *Trends Pharmacol Sci* 11(6):250-4.

Manent JB, Demarque M, Jorquera I, Pellegrino C, Ben-Ari Y, Aniksztejn L, Represa A. (2005). A noncanonical release of GABA and glutamate modulates neuronal migration. *J Neurosci* 25(19):4755-65.

Marín O, Yaron A, Bagri A, Tessier-Lavigne M, Rubenstein JL. (2001). Sorting of striatal and cortical interneurons regulated by semaphorin-neuropilin interactions. *Science* 293(5531):872-5.

Markram H, Toledo-Rodriguez M, Wang Y, Gupta A, Silberberg G, Wu C. (2004). Interneurons of the neocortical inhibitory system. *Nat Rev Neurosci* 5(10):793-807.

Martínez-Cerdeño V, Noctor SC, Espinosa A, Ariza J, Parker P, Orasji S, Daadi MM, Bankiewicz K, Alvarez-Buylla A, Kriegstein AR. (2010). Embryonic MGE precursor cells grafted into adult rat striatum integrate and ameliorate motor symptoms in 6-OHDA-lesioned rats. *Cell Stem Cell* 6(3):238-50.

Martini FJ, Valiente M, Lopez Bendito G, Szabo G, Moya F, Valdeolmillos M, Marín O. (2009). Biased selection of leading process branches mediates chemotaxis during tangential neuronal migration. *Development* 136(1):41-50.

Martinowich K, Schloesser RJ, Jimenez DV, Weinberger DR, Lu B. (2011). Activity-dependent brain-derived neurotrophic factor expression regulates cortistatin-interneurons and sleep behavior. *Mol Brain* 4:11.

Maya Vetencourt JF, Sale A, Viegi A, Baroncelli L, De Pasquale R, O'Leary OF, Castren E, Maffei L. (2008). The antidepressant fluoxetine restores plasticity in the adult visual cortex. *Science* 320(5874):385-8.

McCauley JL, Olson LM, Delahanty R, Amin T, Nurmi EL, Organ EL, Jacobs MM, Folstein SE, Haines JL, Sutcliffe JS. (2004). A linkage disequilibrium map of the 1-Mb 15q12 GABA(A) receptor subunit cluster and association to autism. *Am J Med Genet B Neuropsychiatr Genet* 131B(1):51-9.

McKenna WL, Betancourt J, Larkin KA, Abrams B, Guo C, Rubenstein JL, Chen B. (2011). Tbr1 and Fezf2 regulate alternate corticofugal neuronal identities during neocortical development. *J Neurosci* 31(2):549-64.

Mitra A, Blank M, Madison DV. (2012). Developmentally altered inhibition in Ts65Dn, a mouse model of Down syndrome. *Brain Res* 1440, 1–8.

Miyata S, Komatsu Y, Yoshimura Y, Taya C, Kitagawa H. (2012). Persistent cortical plasticity by upregulation of chondroitin 6-sulfation. *Nat. Neurosci* 15(3):414-22.

Miyoshi G, Hjerling-Leffler J, Karayannis T, Sousa VH, Butt SJ, Battiste J, Johnson JE, Machold RP, Fishell G. (2010). Genetic fate mapping reveals that the caudal ganglionic eminence

produces a large and diverse population of superficial cortical interneurons. *J Neurosci* 30(5):1582-94.

Möhler H. (2012). The GABA system in anxiety and depression and its therapeutic potential. *Neuropharmacology* 62(1):42-53.

Molyneaux BJ, Arlotta P, Menezes JR, Macklis JD. (2007). Neuronal subtype specification in the cerebral cortex. *Nat Rev Neurosci* 8(6):427-37.

Nery S, Fishell G, Corbin JG. (2002). The caudal ganglionic eminence is a source of distinct cortical and subcortical cell populations. *Nat Neurosci* 5(12):1279-87.

Okabe M, Ikawa M, Kominami K, Nakanishi T, Nishimune Y. (1997). 'Green mice' as a source of ubiquitous green cells. *FEBS Lett* 407(3):313-9.

Oldham MC, Langfelder P, Horvath S. (2012). Network methods for describing sample relationships in genomic datasets: application to Huntington's disease. *BMC Syst Biol* 6:63.

Oliva AA Jr, Jiang M, Lam T, Smith KL, Swann JW. (2000). Novel hippocampal interneuronal subtypes identified using transgenic mice that express green fluorescent protein in GABAergic interneurons. *J. Neurosci* 20(9):3354-68.

Owens DF, Kriegstein AR. (2002). Is there more to GABA than synaptic inhibition? *Nat Rev Neurosci* 3(9):715-27.

Palop JJ, Mucke L. (2010). Amyloid-beta-induced neuronal dysfunction in Alzheimer's disease: from synapses toward neural networks. *Nat Neurosci* 13(7):812-8.

Pfeffer CK, Xue M, He M, Huang ZJ, Scanziani M. (2013). Inhibition of inhibition in visual cortex: the logic of connections between molecularly distinct interneurons. *Nat Neurosci* 16(8):1068-76.

- Pi HJ, Hangya B, Kvitsiani D, Sanders JI, Huang ZJ, Kepecs A. (2013). Cortical interneurons that specialize in disinhibitory control. *Nature* 503(7477):521-4.
- Pleasure SJ, Anderson S, Hevner R, Bagri A, Marin O, Lowenstein DH, Rubenstein JL. (2000). Cell migration from the ganglionic eminences is required for the development of hippocampal GABAergic interneurons. *Neuron* 28(3):727-40.
- Polleux F, Whitford KL, Dijkhuizen PA, Vitalis T, Ghosh A. (2002). Control of cortical interneuron migration by neurotrophins and PI3-kinase signaling. *Development* 129(13):3147-60.
- Powell EM, Mars WM, Levitt P. (2001). Hepatocyte growth factor/scatter factor is a motogen for interneurons migrating from the ventral to dorsal telencephalon. *Neuron* 30(1):79-89.
- Pozas E, Ibáñez CF. (2005). GDNF and GFRalpha1 promote differentiation and tangential migration of cortical GABAergic neurons. *Neuron* 45(5):701-13.
- Ramón y Cajal, S. (1894). The Croonian Lecture. La fine structure des centres nerveux. *Proc R Soc Lond B* 55, 444–468.
- Ramón y Cajal, S. (1901). Significación probable de las células de axon corto. *Trab Lab Invest Biol Univ Madrid* 1, 151–157.
- Richardson RM1, Barbaro NM, Alvarez-Buylla A, Baraban SC. (2008). Developing cell transplantation for temporal lobe epilepsy. *Neurosurgical Focus* 24(3-4):E17.
- Roux L, Buzsáki G. (2015). Tasks for inhibitory interneurons in intact brain circuits. *Neuropharmacology* 88:10-23.
- Rudy B, Fishell G, Lee S, Hjerling-Leffler J. (2011). Three groups of interneurons account for nearly 100% of neocortical GABAergic neurons. *Dev Neurobiol* 71(1):45-61.

Saiz-Sanchez D, De la Rosa-Prieto C, Ubeda-Banon I, Martinez-Marcos A. (2014). Interneurons, tau and amyloid- β in the piriform cortex in Alzheimer's disease. *Brain Struct Funct* 2014 Apr 19.

Sale A, Maya Vetencourt JF, Medini P, Cenni MC, Baroncelli L, De Pasquale R, Maffei L. (2007). Environmental enrichment in adulthood promotes amblyopia recovery through a reduction of intracortical inhibition. *Nat Neurosci* 10(6):679-81.

Sato M, Stryker MP. (2008). Distinctive features of adult ocular dominance plasticity. *J Neurosci* 28(41):10278-10286.

Schafer DP, Lehrman EK, Kautzman AG, Koyama R, Mardinly AR, Yamasaki R, Ransohoff RM, Greenberg ME, Barres BA, Stevens B. (2012). Microglia sculpt postnatal neural circuits in an activity and complement-dependent manner. *Neuron* 74(4):691-705.

Sharma N, Classen J, Cohen LG. (2013). Neural plasticity and its contribution to functional recovery. *Handbook of clinical neurology* 110:3-12.

Shipp S. (2007). Structure and function of the cerebral cortex. *Curr Biol* 17(12):R443-9.

Spencer KM. (2009). The functional consequences of cortical circuit abnormalities on gamma oscillations in schizophrenia: insights from computational modeling. *Front Hum Neurosci* 3:33

Spratling MW, Johnson MH. (2003). Exploring the functional significance of dendritic inhibition in cortical pyramidal cells. *Neurocomputing* 52-54:389-395.

Southwell DG, Froemke RC, Alvarez-Buylla A, Stryker MP, Gandhi SP. (2010). Cortical plasticity induced by inhibitory neuron transplantation. *Science* 327(5969):1145-1148.

Southwell DG, Paredes MF, Galvao RP, Jones DL, Froemke RC, Sebe JY, Alfaro-Cervello C, Tang Y, Garcia-Verdugo JM, Rubenstein JL, Baraban SC, Alvarez-Buylla A. (2012). Intrinsically determined cell death of developing cortical interneurons. *Nature* 491(7422):109-13.

Southwell DG, Nicholas CR, Basbaum AI, Stryker MP, Kriegstein AR, Rubenstein JL, Alvarez-Buylla A. (2014). Interneurons from embryonic development to cell-based therapy. *Science* 344(6180):1240622.

Stephan AH, Madison DV, Mateos JM, Fraser DA, Lovelett EA, Coutellier L, Kim L, Tsai HH, Huang EJ, Rowitch DH, Berns DS, Tenner AJ, Shamloo M, Barres BA. (2013). A dramatic increase of C1q protein in the CNS during normal aging. *J Neurosci* 33(33):13460-13474.

Sugiyama S, Di Nardo AA, Aizawa S, Matsuo I, Volovitch M, Prochiantz A, Hensch TK. (2008). Experience-dependent transfer of Otx2 homeoprotein into the visual cortex activates postnatal plasticity. *Cell* 134(3):508-520.

Sussel L, Marin O, Kimura S, Rubenstein JL. (1999). Loss of Nkx2.1 homeobox gene function results in a ventral to dorsal molecular respecification within the basal telencephalon: evidence for a transformation of the pallidum into the striatum. *Development* 126(15): 3359–3370.

Syken J, Grandpre T, Kanold PO, Shatz CJ. (2006). PirB restricts ocular-dominance plasticity in visual cortex. *Science* 313(5794):1795-1800.

Tai C, Abe Y, Westenbroek RE, Scheuer T, Catterall WA. (2014). Impaired excitability of somatostatin- and parvalbumin-expressing cortical interneurons in a mouse model of Dravet syndrome. *Proc Natl Acad Sci U S A* 111(30):E3139-48.

Tallon-Baudry C, Bertrand O. (1999). Oscillatory gamma activity in humans and its role in object representation. *Trends Cogn Sci* 3(4):151-162.

Tamanaki N, Yanagawa Y, Tomioka R, Miyazaki J, Obata K, Kaneko T. (2003). Green fluorescent protein expression and colocalization with calretinin, parvalbumin, and somatostatin in the GAD67-GFP knock-in mouse. *J Comp Neurol* 467(1):60–79.

Taniguchi H, He M, Wu P, Kim S, Paik R, Sugino K, Kvitsani D, Fu Y, Lu J, Lin Y, Miyoshi G, Shima Y, Fishell G, Nelson SB, Huang ZJ. (2011). A resource of cre driver lines for genetic targeting of GABAergic neurons in cerebral cortex. *Neuron* 71(6):995-1013.

Taniguchi H, Lu J, Huang ZJ. (2013). The spatial and temporal origin of chandelier cells in mouse neocortex. *Science* 339(6115):70-4.

Tong LM, Djukic B, Arnold C, Gillespie AK, Yoon SY, Wang MM, Zhang O, Knoferle J, Rubenstein JL, Alvarez-Buylla A, Huang Y. (2014). Inhibitory interneuron progenitor transplantation restores normal learning and memory in ApoE4 knock-in mice without or with A β accumulation. *J Neurosci* 34(29):9506-15.

Tóth K, Maglóczy Z. (2014). The vulnerability of calretinin-containing hippocampal interneurons to temporal lobe epilepsy. *Front Neuroanat* 8:100.

van Versendaal D, Rajendran R, Saiepour MH, Klooster J, Smit-Rigter L, Sommeijer JP, De Zeeuw CI, Hofer SB, Heimel JA, Levelt CN. (2012). Elimination of inhibitory synapses is a major component of adult ocular dominance plasticity. *Neuron* 74(2):374-83.

Verret L, Mann EO, Hang GB, Barth AM, Cobos I, Ho K, Devidze N, Masliah E, Kreitzer AC, Mody I, Mucke L, Palop JJ. (2012). Inhibitory interneuron deficit links altered network activity and cognitive dysfunction in Alzheimer model. *Cell* 149(3):708-21.

Voehringer D, Liang HE, Locksley RM. (2008). Homeostasis and effector function of lymphopenia-induced 'memory-like' T cells in constitutively T cell-depleted mice. *J Immunol* 180(7):4742-53.

Volk DW, Matsubara T, Li S, Sengupta EJ, Georgiev D, Minabe Y, Sampson A, Hashimoto T, Lewis DA. (2012). Deficits in transcriptional regulators of cortical parvalbumin neurons in schizophrenia. *Am J Psychiatry* 169(10):1082-91.

Vucurovic K, Gallopin T, Ferezou I, Rancillac A, Chameau P, van Hooft JA, Geoffroy H, Monyer H, Rossier J, Vitalis T. (2010). Serotonin 3A receptor subtype as an early and protracted marker of cortical interneuron subpopulations. *Cereb Cortex* 20(10):2333-47.

Wang DD, Kriegstein AR. (2008). GABA regulates excitatory synapse formation in the neocortex via NMDA receptor activation. *J Neurosci* 28(21):5547-58.

Wang Y, Dye CA, Sohal V, Long JE, Estrada RC, Roztocil T, Lufkin T, Deisseroth K, Baraban SC, Rubenstein JL. (2010). Dlx5 and Dlx6 regulate the development of parvalbumin-expressing cortical interneurons. *J Neurosci* 30(15):5334-45.

Wang Y, Li G, Stanco A, Long JE, Crawford D, Potter GB, Pleasure SJ, Behrens T, Rubenstein JL. (2011). CXCR4 and CXCR7 have distinct functions in regulating interneuron migration. *Neuron* 69(1):61-76.

Whittington MA, Traub RD. (2003). Interneuron diversity series: inhibitory interneurons and network oscillations in vitro. *Trends Neurosci* 26(12):676-82.

Wichterle H, Garcia-Verdugo JM, Herrera DG, Alvarez-Buylla A. (1999). Young neurons from medial ganglionic eminence disperse in adult and embryonic brain. *Nat Neurosci* 2(5):461-6.

Wichterle H, Turnbull DH, Nery S, Fishell G, Alvarez-Buylla A. (2001). In utero fate mapping reveals distinct migratory pathways and fates of neurons born in the mammalian basal forebrain. *Development* 128(19):3759-71.

Wichterle H, Alvarez-Dolado M, Erskine L, Alvarez-Buylla A. (2003). Permissive corridor and diffusible gradients direct medial ganglionic eminence cell migration to the neocortex. *Proc Natl Acad Sci U S A* 100(2):727-32.

Wiesel TN, Hubel DH. (1963). Single-cell responses in striate cortex of kittens deprived of vision in one eye. *J Neurophysiol* 26:1003-17.

Wonders CP, Anderson SA. (2006). The origin and specification of cortical interneurons. *Nat Rev Neurosci* 7(9):687-96.

Wu X, Fu Y, Knott G, Lu J, Di Cristo G, Huang ZJ. (2012). GABA signaling promotes synapse elimination and axon pruning in developing cortical inhibitory interneurons. *J Neurosci* 32(1):331-43.

Wu S, Wu Y, Capecchi MR. (2006). Motoneurons and oligodendrocytes are sequentially generated from neural stem cells but do not appear to share common lineage-restricted progenitors in vivo. *Development* 133(4):581-90.

Xu Q, Cobos I, De La Cruz E, Rubenstein JL, Anderson SA. (2004). Origins of Cortical Interneuron Subtypes. *J Neurosci* 24(11):2612-22.

Xu Q, Tam M, Anderson SA. (2008). Fate mapping Nkx2.1-lineage cells in the mouse telencephalon. *J Comp Neurol* 506(1):16-29.

Xu Q, Wonders CP, Anderson SA. (2005). Sonic hedgehog maintains the identity of cortical interneuron progenitors in the ventral telencephalon. *Development* 132(22):4987-98.

Yokota Y, Gashghaei HT, Han C, Watson H, Campbell KJ, Anton ES. (2007). Radial glial dependent and independent dynamics of interneuronal migration in the developing cerebral cortex. *PLoS One* 2(8):e794.

Yozu M, Tabata H, Nakajima K. (2005). The caudal migratory stream: a novel migratory stream of interneurons derived from the caudal ganglionic eminence in the developing mouse forebrain. *J Neurosci* 25(31):7268-77.

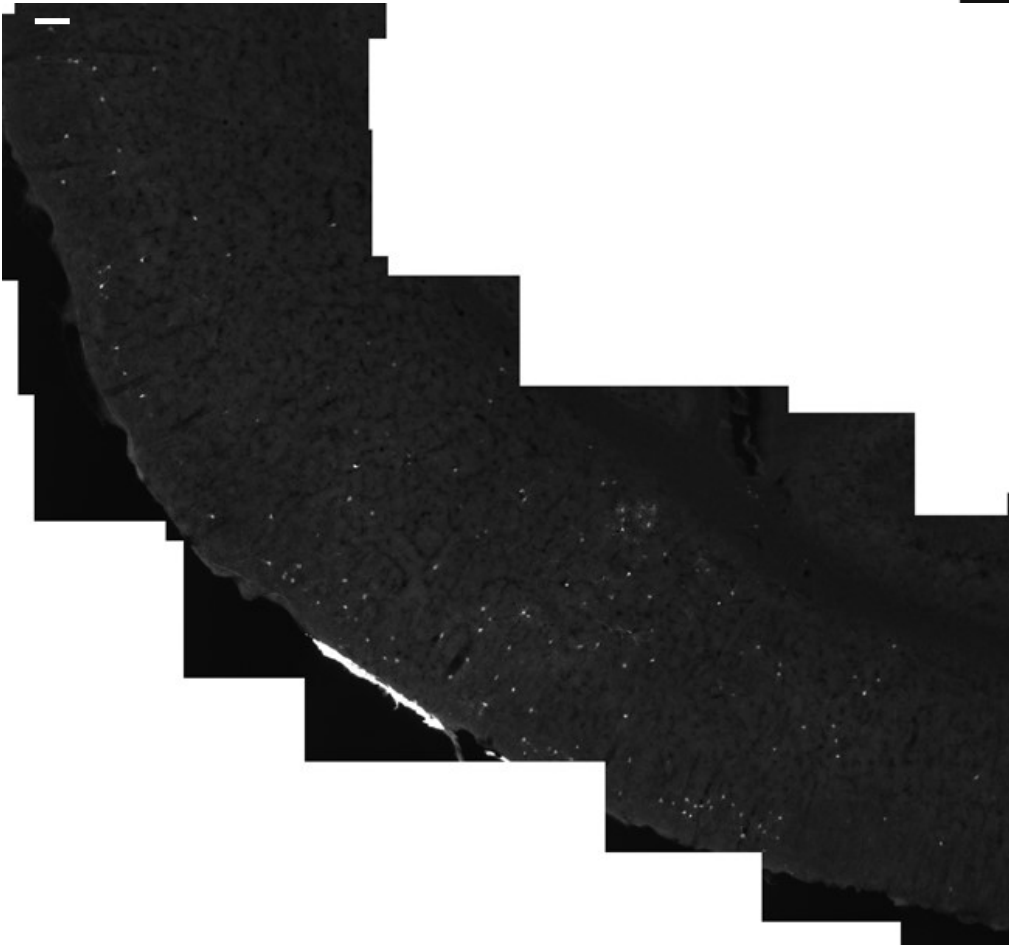
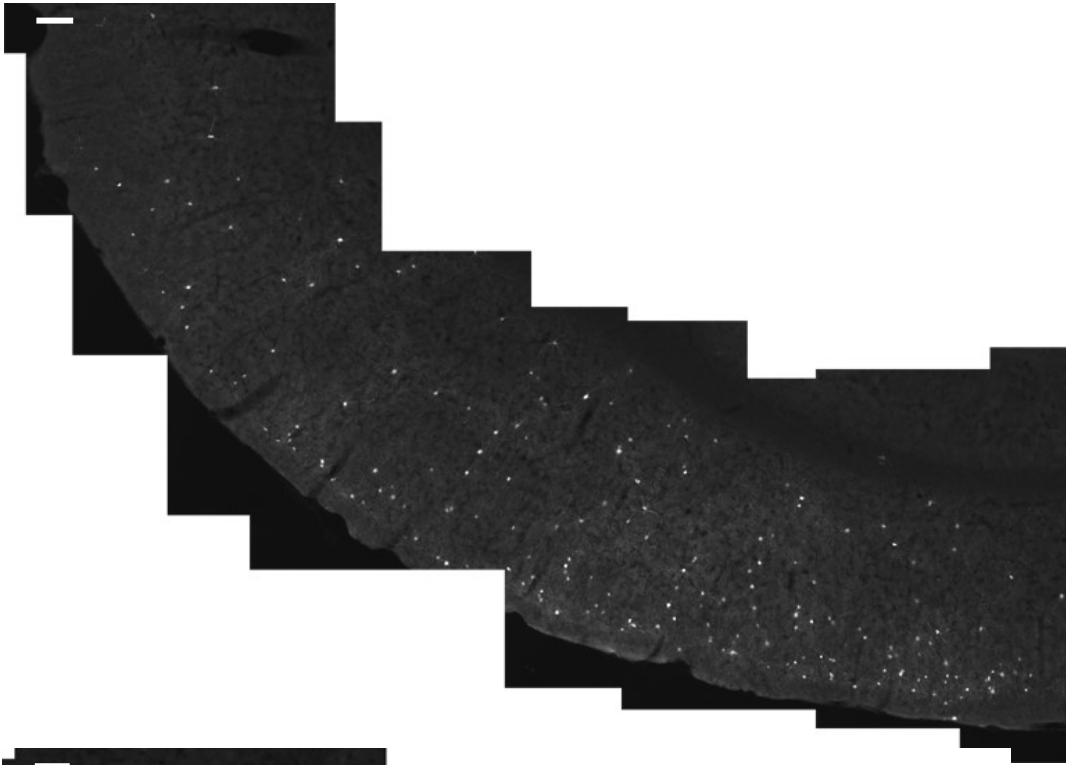
Zimmer G, Garcez P, Rudolph J, Niehage R, Weth F, Lent R, Bolz J. (2008). Ephrin-A5 acts as a repulsive cue for migrating cortical interneurons. *Eur J Neurosci* 28(1):62-73.

Appendix

Figure A1. Transplantation of previously frozen MGE cells.

50 days after transplantation (DAT), transplants of freshly dissected MGE cells (**top**) and frozen MGE cells (**bottom**) both migrate in the host cortex. Scale bars: 200 μ m.

MGE tissue was dissected from E13.5 actin-GFP embryos and frozen as whole MGE chunks in freezing medium (50% L-15, 40% fetal bovine serum, 10% DMSO) at -80°C for 24-48 hours, before transferring to liquid nitrogen storage tanks. Frozen MGE tissue was thawed in 37 °C water bath, triturated using a P-200 pipette, centrifuged at 600 *g* for 3 minutes, and washed twice with L-15 medium. After the final centrifugation, medium was removed and the concentrated cell pellets were transplanted as described in Chapter 2. Counting on a hemocytometer with trypan blue revealed that more than half of MGE cells were dead after thawing, in contrast to the < 10% dead cells typically observed in freshly dissected MGE cells. Using glycerol in place of DMSO in freezing medium resulted in more death upon thawing.



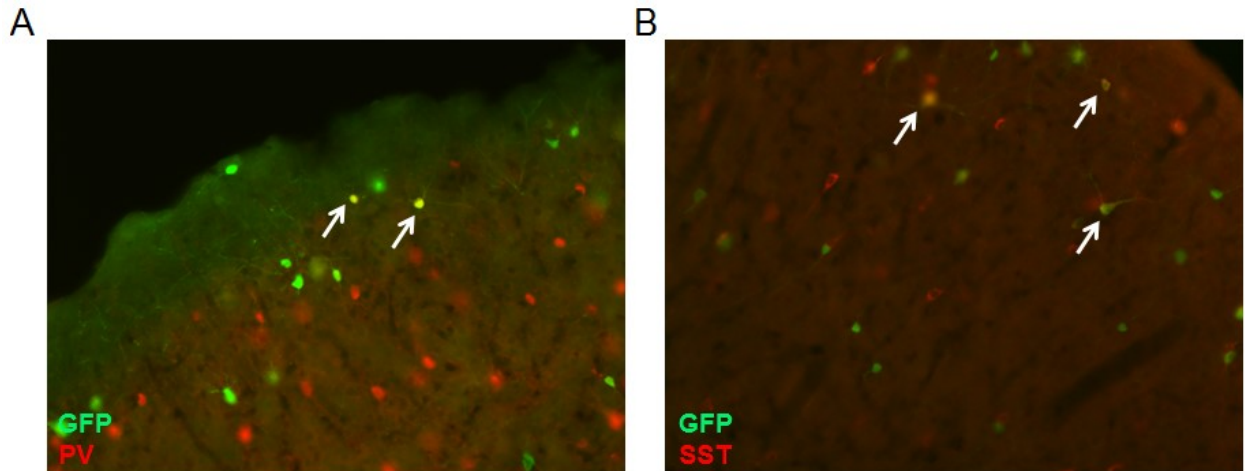


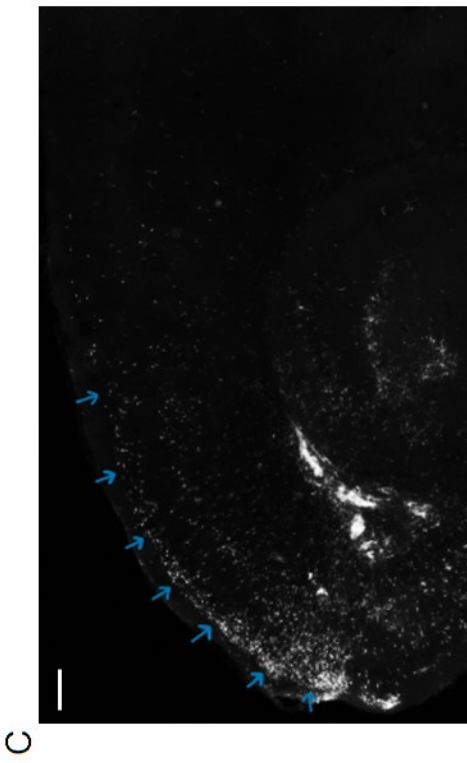
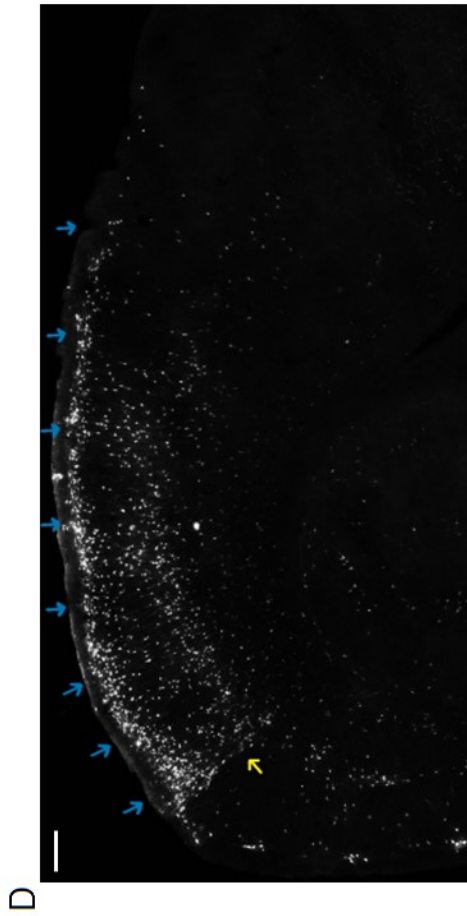
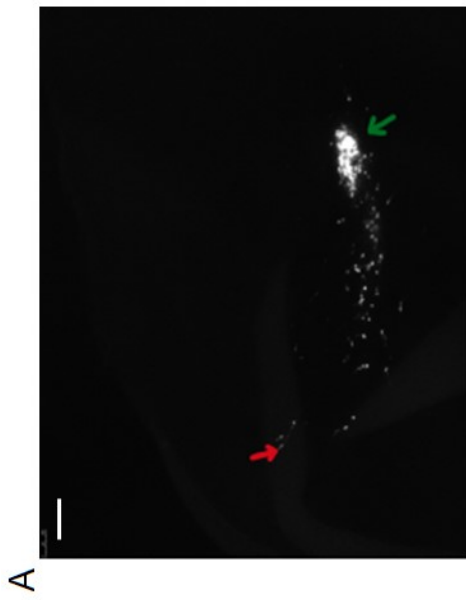
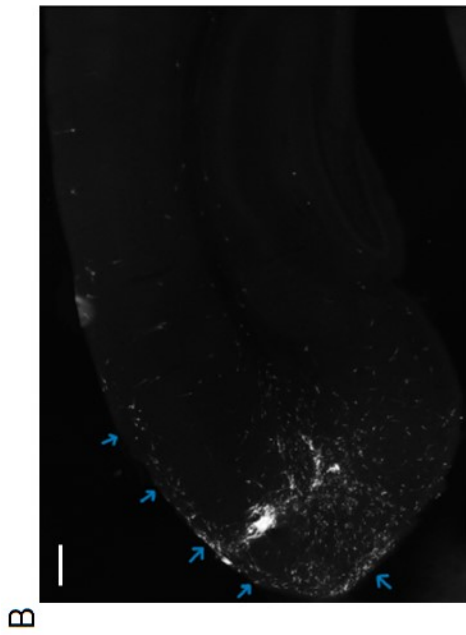
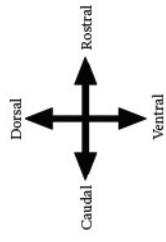
Figure A2. Transplanted frozen MGE cells express markers of mature interneurons.

At 50 DAT, transplanted MGE cells that were previously frozen expressed markers of MGE-derived interneurons, including PV (21%, **A**, arrows), SST (46%, **B**, arrows), and NPY (8%).

Figure A3. Migration of transplanted tdtomato⁺ MGE cells in the host cortex.

A. At 1 day after transplantation (DAT), a migrating stream of transplanted tdtomato⁺ cells has already formed. The leading edge (red arrow) is about 1mm away from the injection site (green arrow). **B.** At 3 DAT, transplanted cells migrate preferentially through layer 1 (blue arrows). **C.** At 5 DAT, transplanted cells have descended from layer 1 to line the upper boundary of layers 2/3 (blue arrows). Some cells have penetrated into deeper layers. **D.** At 10 DAT, transplanted cells continue to aggregate at the boundary of layer 1 and layers 2/3 (blue arrows), but a significant proportion of cells are now in the deeper layers (yellow arrow). Scale bars: 250µm.

MGE cells were micro-dissected from E13.5 tdtomato⁺ embryos and transplanted into the cortex of P7 recipients as described in Chapter 2. Recipients were perfused at 1, 2, 3, 5, 7, and 10 DAT and sectioned sagittally and coronally at 50µm. Images were acquired using the Zeiss Axiovert-200 microscope (Zeiss), AxioCam Mrm (Zeiss), and Neurolucida (MBF).



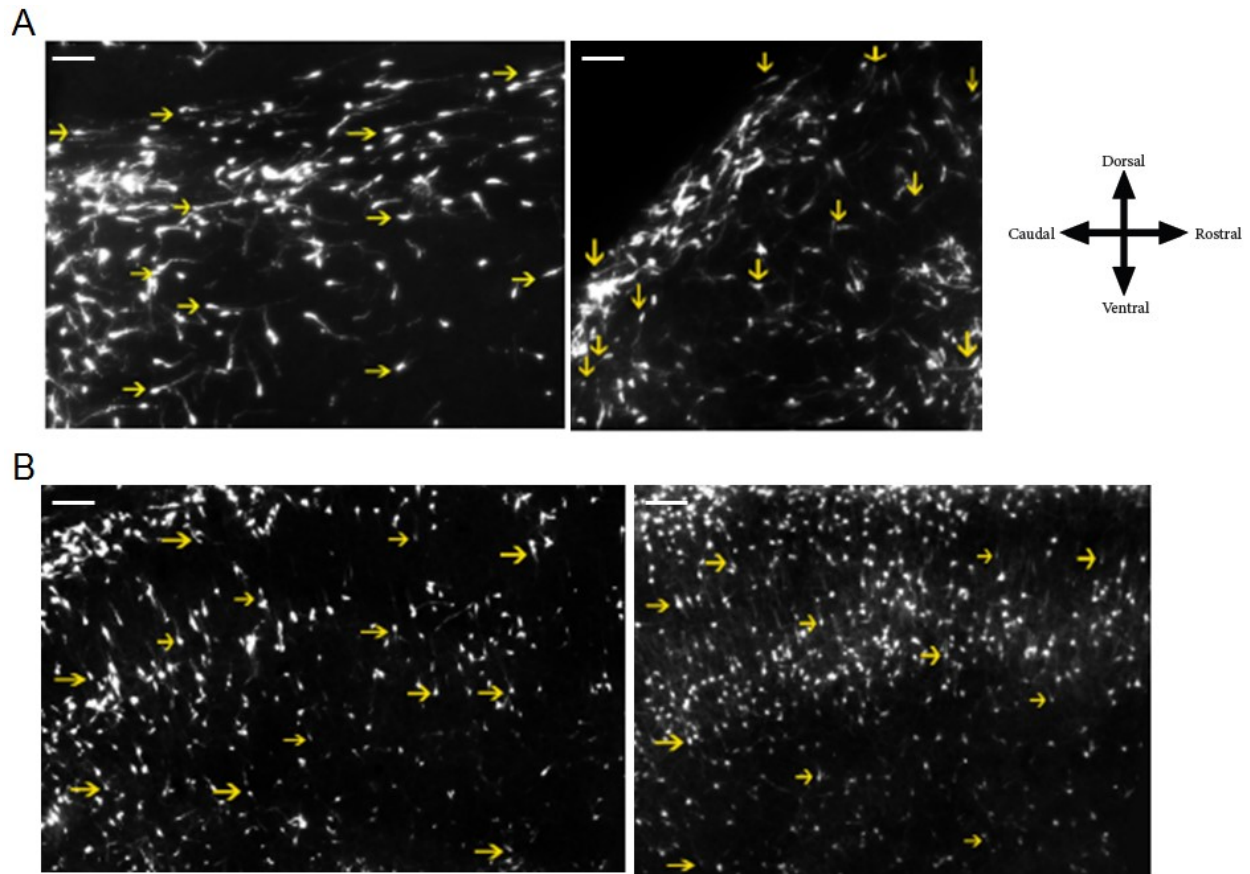


Figure A4. Tangential and radial migration of transplanted MGE cells.

A. At 3 DAT (left panel) and 5 DAT (right panel), transplanted *tdtomato*⁺ cells migrate tangentially (arrows) through the superficial layers of host cortex. **B.** At 7 DAT (left panel) and 10 DAT (right panel), many transplanted cells are migrating radially (arrows) to reach the different cortical layers. Scale bars: 200 μ m.

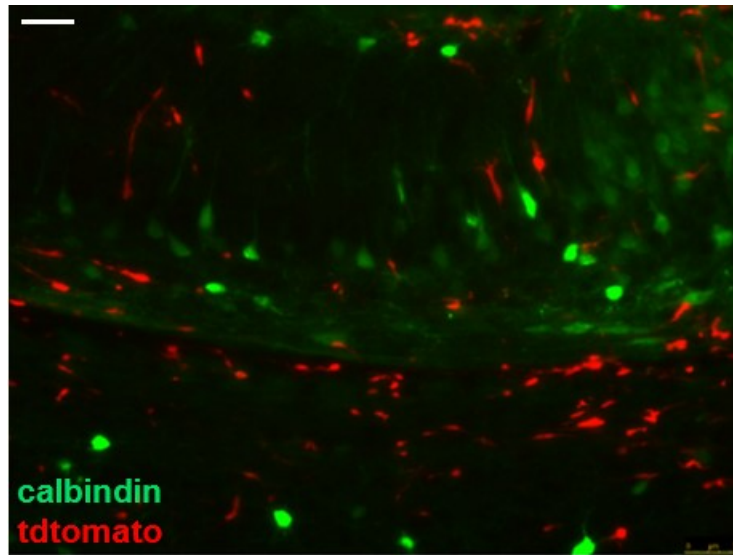


Figure A5. Transplanted interneurons do not express calbindin.

Many interneurons express calbindin while migrating to the cortex (Anderson et al., 2001). However, at 2 DAT, transplanted $tdtomato^+$ MGE cells (red) do not co-label with calbindin (green). Scale bar: 25 μ m.

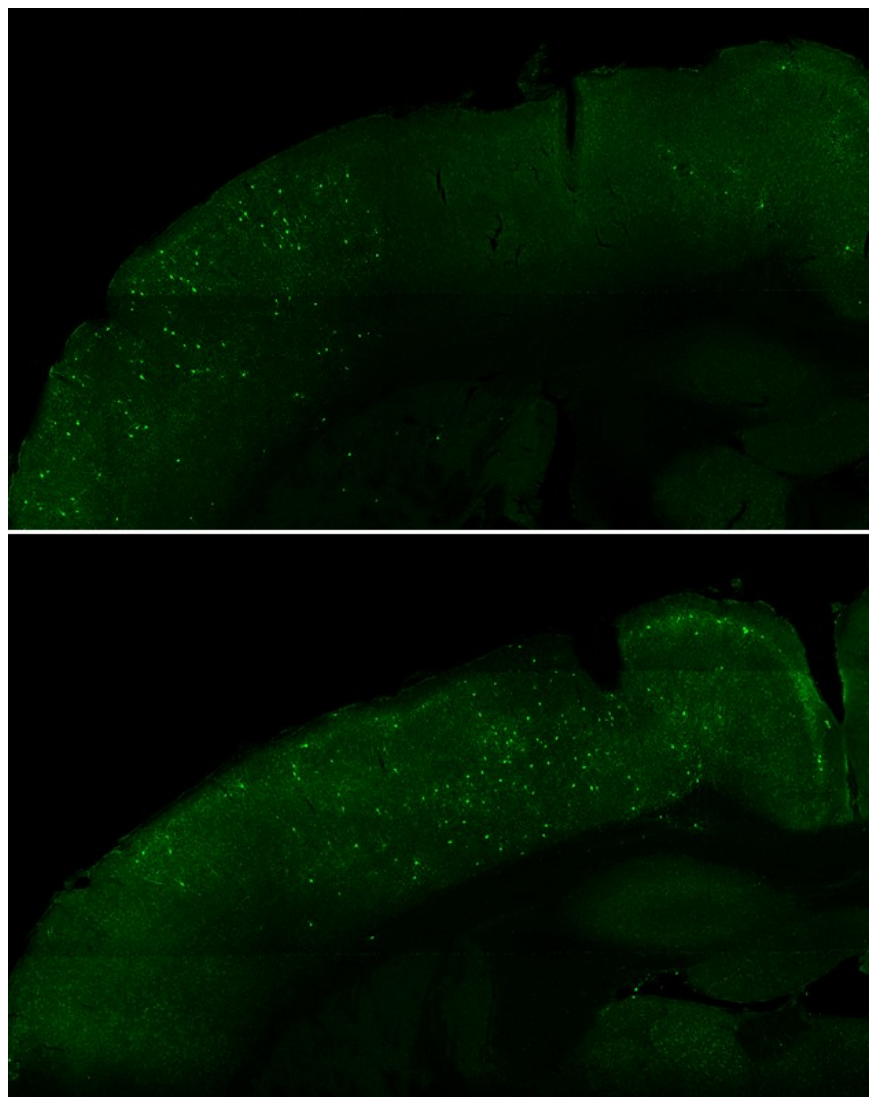


Figure A6. Transplantation of MGE cells cultured for 4 days in vitro.

At 42 DAT, transplants of freshly dissected GFP⁺ MGE cells (top) and GFP⁺ MGE cells cultured in vitro for 4 days (bottom) both survive and disperse in the host cortex. MGE cells were cultured on laminin and polylysine-coated plates with DMEM medium, N2 and B27 supplements.

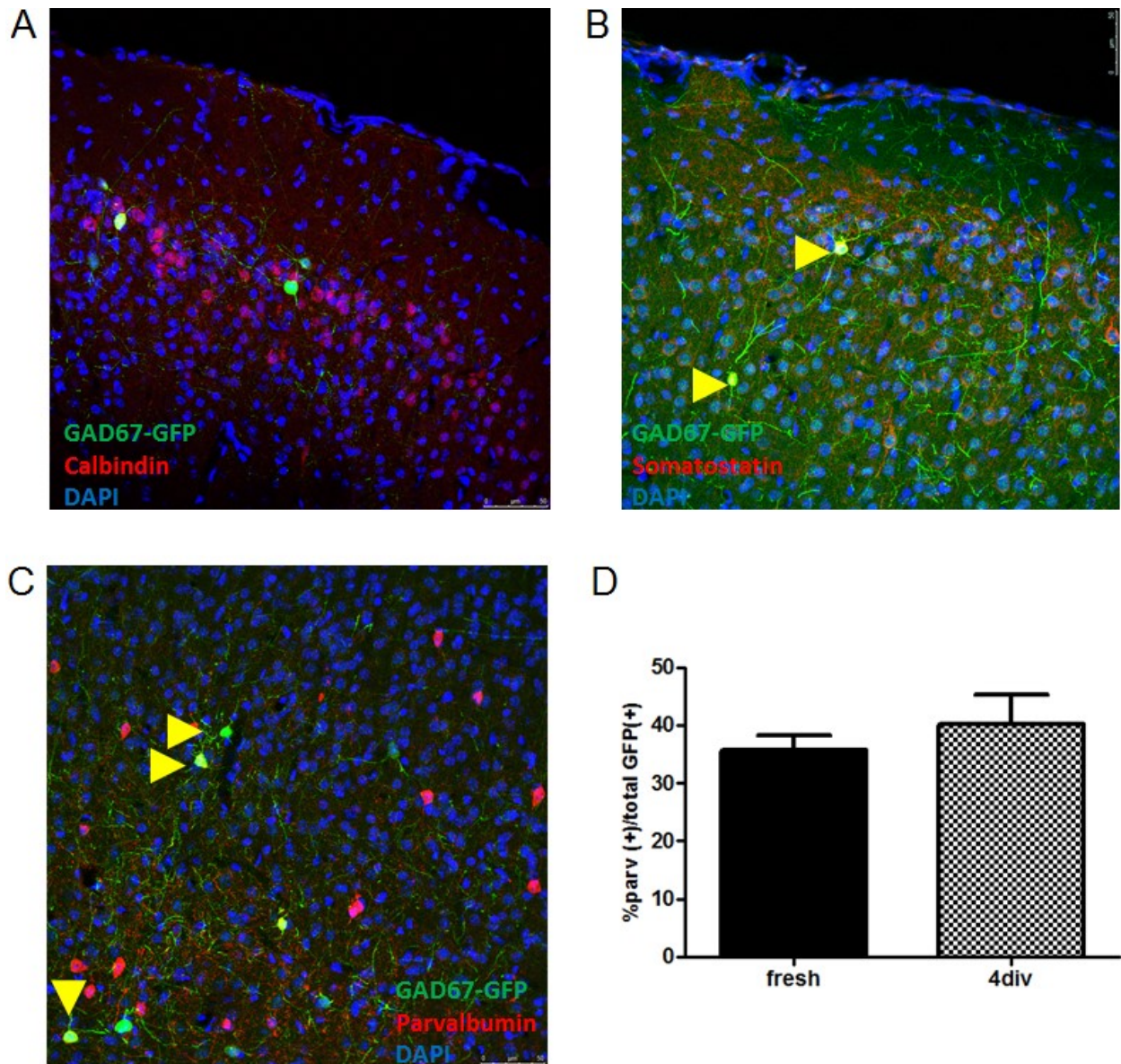


Figure A7. Expression of subtype markers by MGE cells cultured for 4 days in vitro.

At 42 DAT, transplanted MGE cells that have been cultured for 4 days in vitro express interneuron subtype markers such as calbindin (**A**, arrowhead), somatostatin (**B**, arrowheads), and parvalbumin (**C**, arrowheads). **D**. PV⁺ interneurons make up equivalent proportion of interneurons in both fresh and cultured MGE transplants.

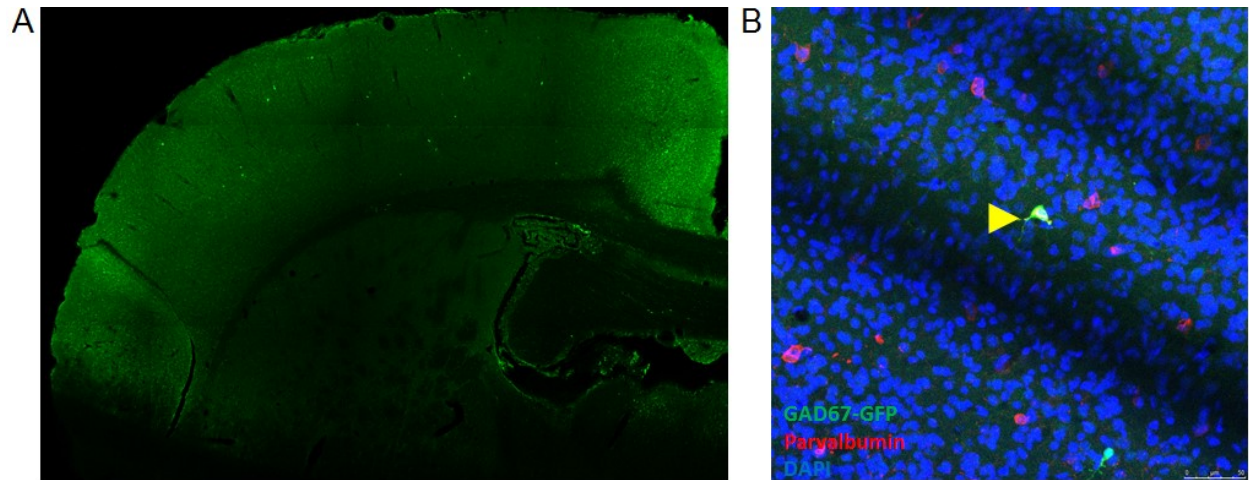


Figure A8. Transplantation of MGE cells cultured for 6 days in vitro shows poor survival.

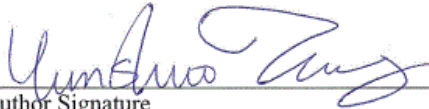
A. After being cultured in vitro for 6 days, only a few GFP⁺ MGE cells survived in the host cortex at 42 DAT. **B.** Despite poor survival, MGE cells cultured for 6 days differentiate into PV⁺ cells (arrowhead) at 42 DAT.

Publishing Agreement

It is the policy of the University to encourage the distribution of all theses, dissertations, and manuscripts. Copies of all UCSF theses, dissertations, and manuscripts will be routed to the library via the Graduate Division. The library will make all theses, dissertations, and manuscripts accessible to the public and will preserve these to the best of their abilities, in perpetuity.

Please sign the following statement:

I hereby grant permission to the Graduate Division of the University of California, San Francisco to release copies of my thesis, dissertation, or manuscript to the Campus Library to provide access and preservation, in whole or in part, in perpetuity.


Author Signature

3/5/2015
Date